

THE UNIVERSITY OF CALGARY

Geophysical Study of
Precambrian Basement Fault Structure and Related
Cretaceous Stratigraphic Variation in
Southern Alberta

by

Gary W. Paukert

A THESIS

SUBMITTED TO THE FACULTY OF GRADUATE STUDIES
IN PARTIAL FULFILLMENT OF THE REQUIREMENTS FOR THE
DEGREE OF MASTER OF SCIENCE

DEPARTMENT OF GEOLOGY AND GEOPHYSICS

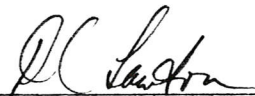
CALGARY, ALBERTA

September 1982

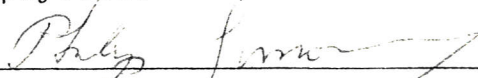
© Gary W. Paukert 1982

THE UNIVERSITY OF CALGARY
FACULTY OF GRADUATE STUDIES

The undersigned certify that they have read, and recommend to the Faculty of Graduate Studies for acceptance, a thesis entitled, "Geophysical Study of Precambrian Basement Fault Structure and Related Cretaceous Stratigraphic Variation in Southern Alberta" submitted by Gary W. Paukert in partial fulfillment of the requirements for the degree of Master of Science.



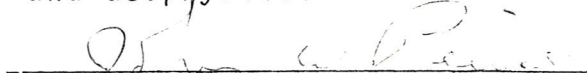
Supervisor, Dr. D.C. Lawton,
Department of Geology and Geophysics.



Dr. P.S. Simony, Department of
Geology and Geophysics.



Dr. F. Cook, Department of Geology
and Geophysics.



Dr. J. Pierce, Petro-Canada Inc.

Date: September 21, 1982

ABSTRACT

An integrated interpretation of gravity and seismic data was undertaken for an area of southern Alberta to determine the feasibility of using integrated data to model the density and structure of the Precambrian basement and overlying sedimentary sequence. A gravity survey was conducted along three 60-kilometre long profiles in an area east of Claresholm, Alberta. The survey indicates Bouguer anomalies of up to 50 gravity units. Seismic profiles were obtained for the survey lines for use as control data in an integrated interpretation. These data show basement fault-block structure and faults of up to 300 metres throw. The average depth of these basement features is 3000 metres.

Gravity modelling was undertaken with initial models constructed from the seismic time sections and well velocity data. However, these simple models proved to generate gravitational responses which did not agree with the observed anomalies. It was found necessary to vary the density of the upper and lower Cretaceous layers laterally across the sections in order to match model response and observed anomalies.

Interpretation of the final models shows that rapid changes in Bouguer anomaly value occur across faults with throws of more than 150 metres, however the density variation of the Cretaceous sequence obscures the gravitational effects of the smaller faults. Relative elevation changes in the basement are reflected in the overlying strata and cause variations in the observed Bouguer

anomalies by creating relative mass excesses and deficiencies.

Structural and stratigraphic interpretations indicate recurrent motion along pre-existing parallel basement faults, vertically oriented with an average strike of 330 degrees. This fault activity is interpreted to be late Paleozoic and late Cretaceous in age, based upon comparison of fault throws within the sections and thickness variations in the upper Cretaceous sequence. These thickness variations were found to be directly related to the relative motion of basement fault blocks; e.g., thickness increases over downthrown blocks and thinning over upthrown blocks. A general relationship between basement structure and sediment density was also found and was attributed to compaction in response to varying depth of burial within the clastic wedge caused by vertical motion of the fault blocks. The study illustrates that basement tectonics have affected overlying stratigraphy and that the gravity method is capable of delineating larger faults and regional structural trends of the basement in southern Alberta.

ACKNOWLEDGEMENTS

My most sincere thanks to Dr. Don Lawton for his time, effort, and infinite patience in supervising this project. Thanks are also due Dr. Lawton for supplying and familiarising me with computer programs, for his invaluable directions on project development, and for his criticism of the text.

Dr. Tom L. Davis initiated the project, and funding was provided by grant number A-7370 from Natural Sciences and Engineering Research Council Canada. Seismic control data were generously provided by Sefel Geophysical, Ltd., of Calgary, and thanks are due to Corinne Verkely, Ken Johnson, and Ron Carmichael for their assistance in the gravity survey at Claresholm.

Finally, I wish to express my thanks to my parents, to Miss Barb Penner, and to the First Alliance Church College and Career group for their constant support during my time in Calgary.

TABLE OF CONTENTS

Title Page.....	i
Approval Page.....	ii
Abstract.....	iii
Acknowledgements.....	v
Table of Contents.....	vi
List of Figures.....	ix
 CHAPTER ONE: Introduction.....	 1
1.1 Introduction.....	1
1.2 Purpose of Study.....	1
 CHAPTER TWO: Background.....	 3
2.1 Gravitational Theory.....	3
2.2 Anomalies and Their Sources.....	4
2.3 Gravitational Effects of Basement Structures.....	6
2.4 Previous Related Work.....	8
 CHAPTER THREE: General Information.....	 10
3.1 Study Location.....	10
3.2 Geology of the Study Area.....	13
 CHAPTER FOUR: Acquisition and Reduction of Data.....	 19
4.1 Description of Seismic Data.....	19
4.2 Description of Well Data.....	19
4.3 Description and Treatment of Gravity Data.....	21
(4.3.1) The Gravity Survey.....	21

(4.3.2)	The Elevation Survey.....	22
(4.3.3)	Reduction to Bouguer Anomalies.....	23
(4.3.4)	Regional Gravity Gradients.....	29
CHAPTER FIVE:	Data Analysis.....	37
5.1	Analysis of Seismic Data.....	37
(5.1.1)	Initial Model Construction.....	37
(5.1.2)	Features of the Seismic Data and Initial Model.....	38
(5.1.3)	Time-thickness Profiles and Iso- chron Maps.....	46
(5.1.4)	Error Limits on the Structure Section..	56
5.2	Analysis of Gravity Data.....	57
(5.2.1)	Density Data for Model Construction....	57
(5.2.2)	Gravitational Response of the Initial Model.....	57
(5.2.3)	The Gravity Modelling Process.....	58
(5.2.4)	Description of the Final Models.....	68
(5.2.5)	Error Limits on the Density Interp'n...	78
CHAPTER SIX:	Data Interpretation.....	80
6.1	Stratigraphic Interpretation.....	80
(6.1.1)	General Stratigraphic Description.....	80
(6.1.2)	Effect of Faulting on Sediment Thickness.....	80
6.2	Structural Interpretation.....	82
(6.2.1)	Vertical Extent and History of Faulting.....	82

(6.2.2) Active Length and Orientation of Faulting.....	84
6.3 Density Variation Interpretation.....	87
(6.3.1) Description of Density Structure.....	87
(6.3.2) Effect of Faulting on Sediment Density Variations.....	89
CHAPTER SEVEN: Conclusions.....	93
7.1 Summary.....	93
7.2 Significance of the Gravity Study.....	93
7.3 Significance and Application of Integrated Studies.....	96
7.4 Implications of the Study to the Tectonic History of Western Canada.....	97
7.5 Recommendations for Further Study.....	100
BIBLIOGRAPHY.....	101
APPENDIX: Field and Theoretical Gravity Data.....	104

LIST OF FIGURES

(2.1)	Block Faulting Diagram.....	7
(3.1)	Study Area Map.....	11
(3.2)	Well Control and Profile Location Map.....	12
(3.3)	Generalised Southern Alberta Stratigraphic Column.....	14
(3.4)	Basement Feature Map of Southern Alberta.....	17
(4.1)	General Seismic Data Example.....	20
(4.2a)	Carmangay Observed Bouguer Anomaly Profile.....	26
b)	Claresholm Observed Bouguer Anomaly Profile.....	27
c)	Barons Observed Bouguer Anomaly Profile.....	28
(4.3a)	Observed Bouguer Anomaly Map.....	30
b)	Published Bouguer Anomaly Map of Study Area.....	31
(4.4a)	Carmangay Anomaly Profile with Regional.....	34
b)	Claresholm Anomaly Profile with Regional.....	35
c)	Barons Anomaly Profile with Regional.....	36
(5.1)	Example of Basement Fault in Seismic Section.....	40
(5.2)	Example of Listric Normal Fault in Seismic Section.....	41
(5.3)	Example of Stratigraphic Termination in Section.....	42
(5.4a)	Carmangay Structural Model from Seismic Data.....	43
b)	Claresholm Structural Model from Seismic Data.....	44
c)	Barons Structural Model from Seismic Data.....	45
(5.5)	Block Faulted Basement at Claresholm Gas Field.....	47
(5.6a)	Carmangay Isochron Profile with Fault Blocks.....	48
b)	Claresholm Isochron Profile with Fault Blocks.....	49
c)	Barons Isochron Profile with Fault Blocks.....	50

(5.7)	Isochron Profiles - Upper Cretaceous Layers.....	52
(5.8a)	Upper Cretaceous Clastics Isochron Map.....	53
b)	Lower Cretaceous Clastics Isochron Map.....	54
c)	Paleozoic Carbonates Isochron Map.....	55
(5.9)	Three-layer Constant Lateral Density Model Output.....	59
(5.10a)	Carmangay Surficial Deposits Profile.....	61
b)	Claresholm Surficial Deposits Profile.....	62
c)	Barons Surficial Deposits Profile.....	63
(5.11)	Example of Variable Cretaceous Density Well Log.....	66
(5.12)	Typical Density vs. Depth Plot.....	67
(5.13)	Carmangay Final Model and Output Comparison.....	69
(5.14)	Claresholm Final Model and Output Comparison.....	70
(5.15)	Barons Final Model and Output Comparison.....	71
(5.16a)	Upper Cretaceous Clastics Structure Contour Map.....	73
b)	Lower Cretaceous Clastics Structure Contour Map.....	74
c)	Paleozoic Carbonates Structure Contour Map.....	75
(5.17)	Contribution to Anomaly by Layer.....	77
(6.1)	Fault Trace Map.....	86
(6.2)	Density Distribution Maps.....	88
(6.3)	Density vs. Depth Graphs.....	91
(6.4)	Density vs. Thickness Graphs.....	92
(7.1)	One- and Two-Body Models.....	95

CHAPTER ONE - INTRODUCTION

1.1 - Introduction.

The purpose of gravity surveys in exploration is to define and interpret variations in the gravitational potential field of the earth which are generated by variations in the near-surface, (less than 10 kilometres deep), density structure. Such structural variations are caused by faulting, folding, intrusion, sedimentary patterns and other dynamic processes involving mass. The gravity method involves interpreting anomalies in the earth's gravity field in terms of subsurface geology and structure.

A limiting aspect of the gravity method is that a unique solution cannot be presented, i.e., there is always an infinite number of mass distributions which will generate the observed gravity anomaly. In comparison, the seismic reflection method does not depend as heavily upon additional control data. However, there are uncertainties such as velocity aberrations which may lead to erroneous interpretations. Integration of the seismic and gravity methods is therefore mutually beneficial as each diminishes the uncertainties which are inherent in the other. The two methods are complimentary and provide detailed information about the subsurface.

1.2 - Purpose of the Study.

The study has two objectives:

- (1) To determine whether or not the gravity method is capable of detecting variations in the earth's gravitational field caused by subsurface block-fault structures in southern Alberta.
- (2) To undertake a regional study of an area of southern Alberta to determine:
 - (a) The fault-block structure of the Precambrian basement and overlying sedimentary rocks.
 - (b) The density structure of the Mesozoic clastic wedge.
 - (c) The relationship between basement block faulting and gross sedimentary/stratigraphic variations.

These objectives were accomplished by means of an integrated gravity and seismic interpretation. The major component of this study was the collection and interpretation of gravity data. In addition to these data, seismic reflection sections were obtained in processed form for use as control in the integrated interpretation. These seismic sections are not included in an appendix because of constraints put upon their use by their supplier, however, general examples are included in the text.

CHAPTER TWO- BACKGROUND

2.1 - Gravitational Theory.

Newton's law of gravitation provides the basis for exploration by use of the gravity method. This relationship describes the gravitational effect of an ideal, spherical, non-rotating earth upon a unit mass:

$$\hat{g} = GM/R^2 \quad (2-1)$$

Where: \hat{g} = The acceleration experienced by a unit mass due to the gravitational potential of the earth, (m/s²).

M = The mass of the earth, (kg).

R = The radius of the assumed spherical earth, (m).

G = The Universal Gravity Constant, (6.67 x 10⁻¹¹ NM²/kg²).

However, in the case of the real earth, axial rotation causes centrifugal acceleration which opposes gravitational acceleration. In addition, the earth's non-sphericity results in varying radius, R, as a function of latitude, ϕ . Therefore, a measured acceleration at the earth's surface is affected by additional terms which modify equation (2-1). The equation which applies to the real earth is the 1967 International Gravity Formula given by Telford, et. al., (1976):

$$\delta_{\phi} = \delta \{ 1 + 0.0053024(\sin^2\phi) - 0.0000058(\sin^2 2\phi) \} \quad (2-2)$$

Where: δ = The equatorial value of gravity, 9.780318 m/s².

ϕ = The latitude of the station.

δ_{ϕ} = The latitude-corrected gravity station reading

From an exploration standpoint, the most important component of the earth's gravitational potential field arises from inhomogeneities in the density structure of the earth's crust which affect the magnitude of the local observed gravity field. The effects of crustal density variations represent one part in 10^6 of the total gravitational field, and can only be interpreted after reduction of the effects of latitude and elevation.

2.2 - Anomalies and Their Sources.

In gravity investigations, an anomaly is defined as the difference between a theoretical value and an observed value. The observed value is the drift-corrected field measurement with the calibration constant of the meter applied. The theoretical value is the value at the geoid level, calculated by means of equation (2-2) and corrected for elevation and terrain effects. The expression for calculation of Bouguer anomalies is:

$$(2-3) \quad \Delta g_{\text{boug}} = g_{\text{obs}} - \{ \delta_{\phi} + \Delta g_{\text{top}} + \Delta g_{\text{elev}} + \Delta g_{\text{slab}} \},$$

where: Δg_{boug} = The observed bouguer anomaly.

g_{obs} = The observed gravity reading.

Δg_{top} = The terrain correction, always negative.

(2-4) Δg_{elev} = The free-air correction = $-3.085(h)$.

(2-5) Δg_{slab} = The bouguer slab correction = $0.4188(h)(\rho)$.

δ_{ϕ} = The geoid value of gravity at latitude ϕ .

ρ = The density of reduction = $2.67 \times 10^3 \text{ kg/m}^3$.

h = The height of the station above sealevel datum, m.

In an absolute gravity survey, gravity station readings are tied into one or more of a world-wide system of measured gravity stations. However, in a relative survey, only station-to-station variations are of interest, and the gravity values have no meaning apart from each other. In such a relative survey, δ_ϕ is a constant for a base station, and Δg_{lat} accounts for the variation of the latitude effect over the survey area. This latitude correction is obtained by differentiating equation (2-2) which results in equation (2-6) below:

$$(2-6) \quad \Delta g_{lat} = (0.00812)(\sin^2 2\phi), (g.u./m)$$

This expression is not linear, but may be approximated as such over distances of up to four kilometres. With this latitude correction factor, equation (2-3) becomes:

$$(2-7) \quad \Delta g_{boug} = g_{obs} - \Delta g_{elev} - \Delta g_{slab} - \Delta g_{top} - \Delta g_{lat}.$$

for relative surveys.

The source of an anomaly lies in the relative mass excesses and deficiencies which arise from structural and density variations in the subsurface. Structural variations are the result of faulting, folding, or intrusion and density variations are caused by differential solution, differential compaction or varying depositional patterns. Anomaly wavelength is directly proportional to the depth to the anomaly source and anomaly amplitude is inversely proportional to depth.

2.3 - Gravitational Effects of Basement Structures.

At the start of this project, it was expected that basement block faulting would be found to generate gravitational anomalies by vertical movement of fault blocks relative to each other, since basement rocks were assumed to be of higher density than the overlying sediments. As seen in figure 2.1, upthrown fault blocks raise deeper, higher density rocks to create mass excesses in shallower, less dense layers. The result is the opposite in the case of down-thrown blocks which create relative mass deficiencies.

The greatest contribution to the anomalies is generated where overlying layers of large density contrast are vertically displaced by block faulting. In southern Alberta a density contrast exists between the average densities of the upper and lower Cretaceous clastic rocks, (Maxant, 1980). Actual density values are discussed in chapter five. These vertical density contrasts are thought to be the major sources of anomalies due to basement block structure. Precambrian basement to Paleozoic carbonate density contrast is less than contrasts higher in the section and thus does not generate a major contribution to the anomaly. In addition to these structurally-generated anomalies, density variations in the clastic wedge may affect local gravity readings. Density variations due to increasing depth of burial in the clastic wedge and differential compaction due to sedimentary drape over fault blocks are postulated.

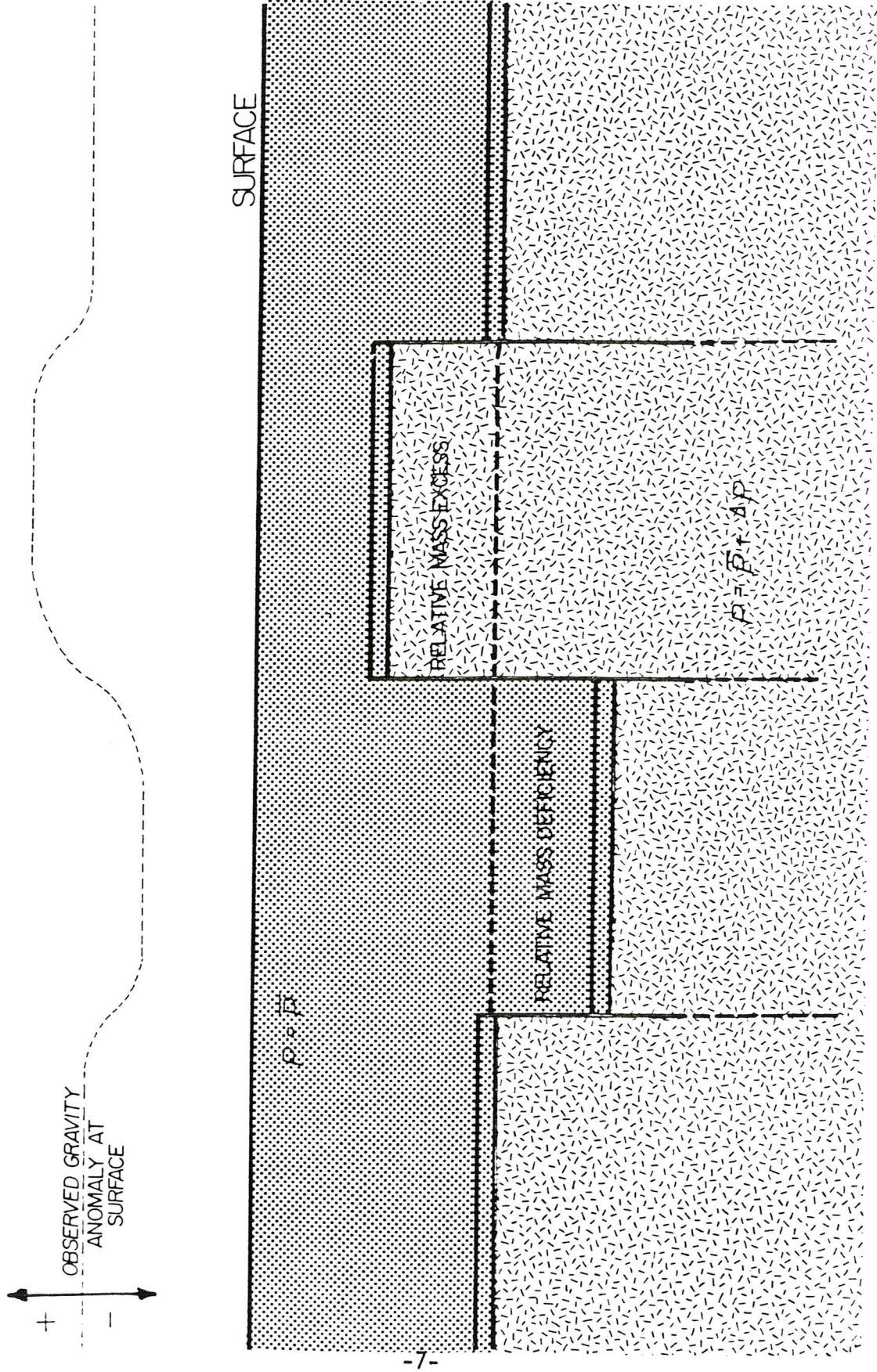


Figure 2.1: Diagram Illustrating the Effect of Basement Block Faulting upon Gravity Anomalies.

2.4 - Previous Related Work.

Previous gravity surveys in Alberta have been mostly regional in nature, (Garland, 1961; White, 1976), and specific studies of the Precambrian basement by the gravity method have explained regional variations in the gravity field in terms of broad, lithologic, rather than local, structural variations, (Burwash, 1957; Garland and Burwash, 1959). The lithologic variations were found to generate anomalies with wavelengths of more than 30 kilometres which are greater than the 5- to 20-kilometre wavelengths expected from the shallower sources represented by basement block faulting. Borowski's 1975 study of the crystalline basement in Banff and Kootenay National Parks indicates that the basement was probably not involved in the Cretaceous overthrust deformation of the overlying strata. Bally, Gordy, and Stewart, (1966), have also investigated basement character and structure in the region. Beyond these examples, little attention has been paid to the detailed investigation of basement structure with the gravity method.

However, in recent years, the effect of basement faulting and relief upon sedimentation and the stratigraphy of overlying Paleozoic and younger formations in sedimentary basins has been considered, (Weimer, 1978; and Davis, 1979). On a large scale, Weimer, (1978), has shown that basement arching extending from Arizona to Minnesota may have caused thinning of the

Niobrara formation in the Denver basin, in that a marked increase in thickness occurs in this formation in a direction perpendicular to the trend of the transcontinental arch. The Alberta and Denver basins are similar in that they are both flanked by positive basement features caused by tectonic activity which may have occurred during sedimentation. For this reason, sedimentary variations similar to those found in the Denver basin are postulated in the transitional area between the Sweetgrass Arch and Alberta Basin. These variations may include thinning and thickening of sedimentary strata over up- and down-thrown fault blocks, and differential compaction of sediments due to different burial depths created by block faulting.

CHAPTER THREE - GENERAL INFORMATION

3.1 - Study Location.

The study location is 130 kilometres southeast of Calgary in an area north of Lethbridge and east of Claresholm, Alberta, (see fig. 3.1). It is bounded by highway #2 on the west, the Little Bow River Valley on the east, and includes townships 12 and 13 and ranges 20 through 27 west of the fourth meridian, (see figure 3.2). This area was chosen for study on the basis of apparent block fault structure evident in available seismic reflection profiles.

The area is one of generally subdued topography with a gradual easterly slope away from the mountain front. An exception to this gradual gradient is the Blackspring Ridge which lies just to the west of the Little Bow River, trends north and south, and is generally about 100 metres above the surrounding area. This ridge is an erosional remnant of Tertiary clastic material. Elevations range from a maximum of 1040 metres above sea level in the western side of the area to 860 metres above sea level in the eastern side.

Within this area a three-profile gravity survey was conducted along existing section roads, involving a total of 508 gravity stations, (see fig. 3.2). These roads run directly east/west except for three minor deviations where detours to the north were necessary to avoid small lakes. The central

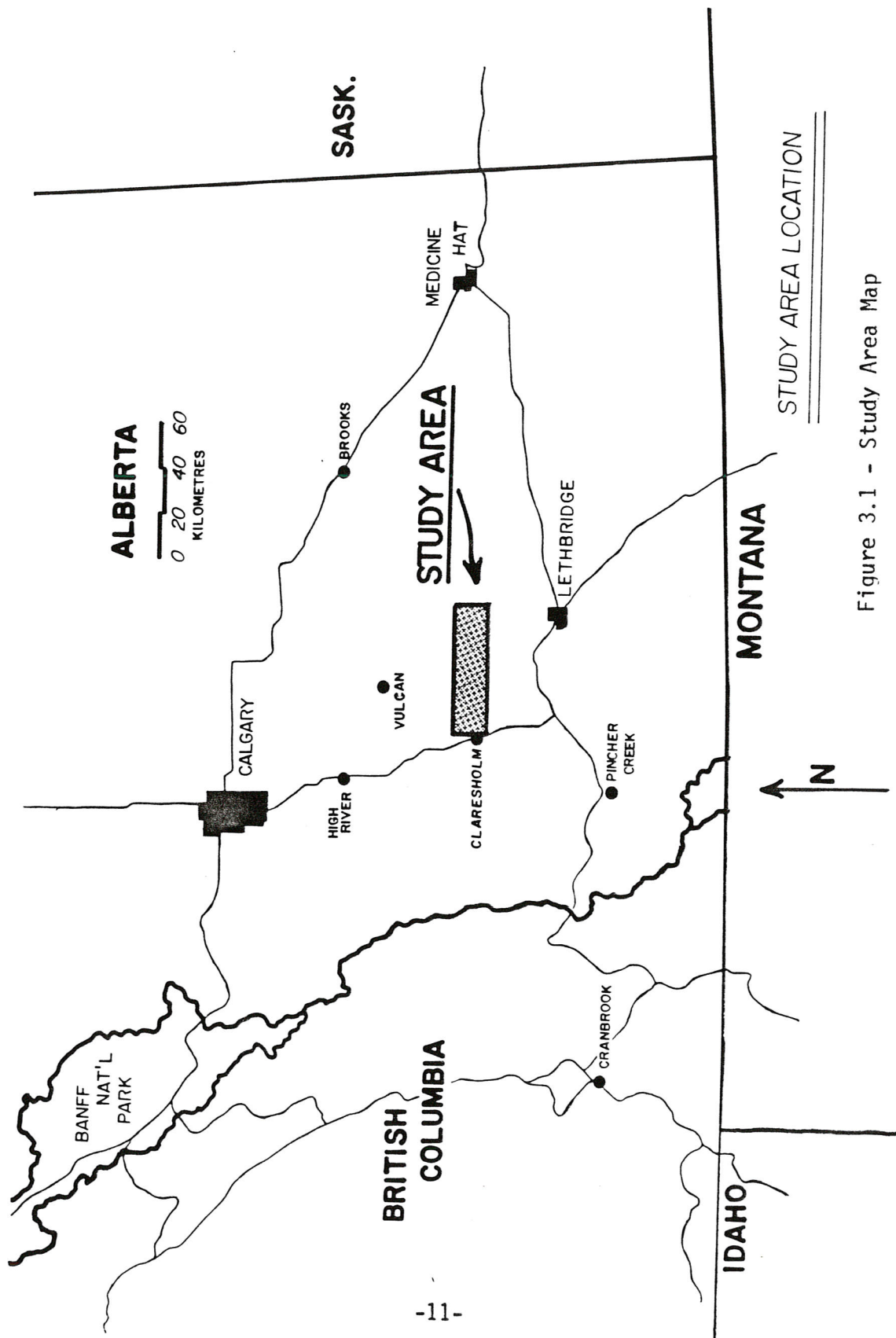
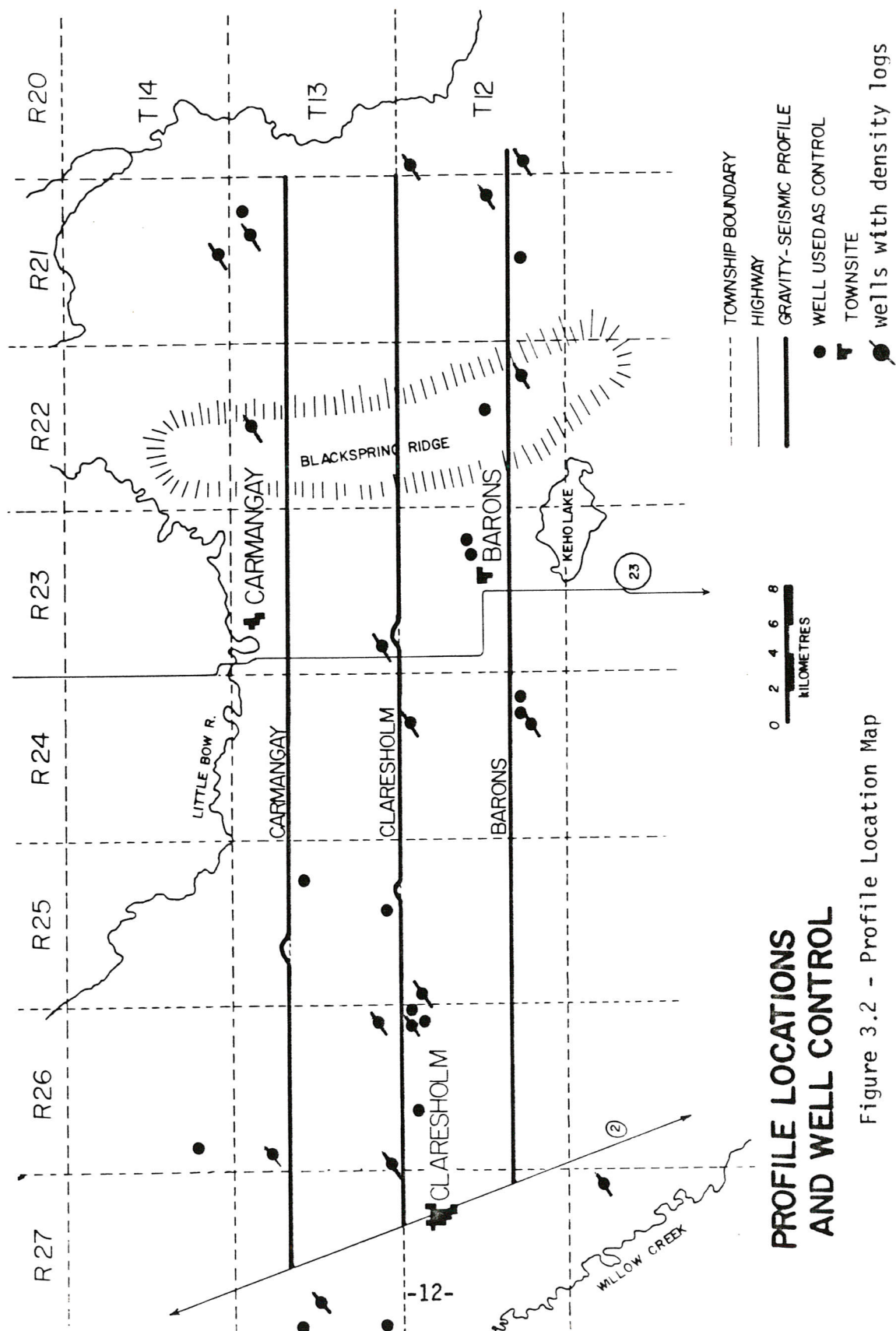


Figure 3.1 - Study Area Map



line crosses the Claresholm gas field 12 kilometres east of Claresholm and the southern profile crosses near the Barons oilfield one kilometre east of that town. Many producing oil and gas wells make up these fields, and are also found throughout the rest of the study area in lesser concentrations. The profiles, from north to south, are entitled Carmangay, Claresholm and Barons due to their proximity to those towns. Each profile is approximately sixty kilometres long.

3.2 - Geology of the Study Area.

The geologic history of southern Alberta has been described, (McCrossan, 1964), as that of a cratonic basin which has undergone a change in depositional environment from predominantly carbonate to predominantly clastic. A generalised stratigraphic column for the area, (see fig. 3.3), shows the crystalline Precambrian which will be referred to as basement. The basement lies beneath as much as 4,000 metres of Paleozoic carbonate and Mesozoic clastic rocks. McCrossan, (1964), and Nelson, (1970), present generalised geologic histories of the area from which the following discussion is condensed.

The Precambrian basement in the area consists mainly of gneissic and granitic rocks which have been dated by the potassium-argon method to be nearly 1800 million years old. These rocks are considered to be an extension, both lithologically and structurally, of the Precambrian shield which is exposed to the north and

GENERALISED SOUTHERN ALBERTA STRATIGRAPHIC COLUMN

CENOZOIC	QUATERNARY	
	TERTIARY	PASKAPOO
MESOZOIC	CRETACEOUS	EDMONTON
		BEARPAW
		BELLY RIVER
		PAKOWKI
		MILK RIVER SAND
		COLORADO
		CARDIUM (SHALE)
		2-ND WHITE SPECKS (SHALE SAND)
		FISH SCALE SAND
	JURASSIC	BLAIRMORE
		SUNBURST
	TRIASSIC	ELLIS
PALEOZOIC	PERMIAN	
	PENNSYLVANIAN	
	MISSISSIPPIAN	TURNER VALLEY
		SHUNDA
		PEKISKO
	DEVONIAN	BANFF
		EXSHAW
		WABAMUN
		WINTERBURN
		BIRDBEAR
		IRETON
		LEDUC
		COOKING LAKE
		BEAVERHILL LAKE
	SILURIAN	ELK POINT
	ORDOVICIAN	
	CAMBRIAN	CAMBRIAN
PRE-CAMBRIAN		CRYSTALLINE IGNEOUS

Figure 3.3 - Generalised Stratigraphic Column for Southern Alberta.

east in Saskatchewan and which forms the core of the North American craton. Subsequent to the late Proterozoic era, broad tectonic arching and subsidence belts were formed on the previously nearly planar basement surface. Subsidence in southern Alberta allowed for the transgression of an inland sea in which dominantly carbonate sedimentation was continuous up until the early Ordovician. Uplift at that time further differentiated the tectonic elements of the basement and caused the erosional loss of much of the Cambrian sequence. Reactivation of the uplift/downwarp zones was recurrent and eventually the Alberta Basin and Sweetgrass/North Battleford arch were formed. The study area lies in the area of transition between these negative and positive tectonic features.

General subsidence of the area in the Devonian period resulted in the formation of a large evaporite basin, and further subsidence in the Mississippian allowed for deep-marine carbonate deposition through the Permian period. Uplift again at the end of the Permian caused a lengthy period of erosion which led to severe truncation of Permian and Carboniferous strata. Triassic subsidence led to deposition of clastics, but early Jurassic erosion removed these beds from the plains areas. During the later Jurassic there occurred more subsidence, but the Sweetgrass Arch was not transgressed and remained a low land mass upon which significant erosion took place. According to Herbaly, (1974), the paleotopography of the Mississippian

surface is the "mold" over which Jurassic, Cretaceous, and Tertiary clastics have been deposited. The cause of this irregular surface has not been previously discussed, and one objective of this study is to attempt to relate features within the Paleozoic and Mesozoic sequences to basement relief due to faulting.

In the Cretaceous era, a major shift from deposition of carbonate rocks in deep seas to deposition of clastic rocks in shallow seas occurred within the miogeosyncline. A gradually retreating sea was the site of deposition of mostly sandstones until its final retreat allowed for the deposition of only terrestrial sedimentary rocks. This shallow body, called the Clearwater Sea, extended from the Arctic Ocean through southern Alberta to the Gulf of Mexico.

In the late Cretaceous, major tectonic crustal foreshortening to the west began and at this time the basement elements of the Alberta Basin and Sweetgrass/North Battleford Arch were completed. The geology seen today was completed by widespread glaciation in the Pleistocene when merging continental and alpine ice sheets left thick till deposits which fill valleys to obscure the pre-Pleistocene topography and drainage patterns.

Structure contour maps published by the Alberta Energy Resources Conservation Board, (1969, 1978), show that today the area lies to the east of the disturbed belt of Cretaceous thrust faulting. This boundary lies forty kilometres west of the town of Claresholm, (see fig. 3.4, after Herbaly, 1974), in the Porcupine

;

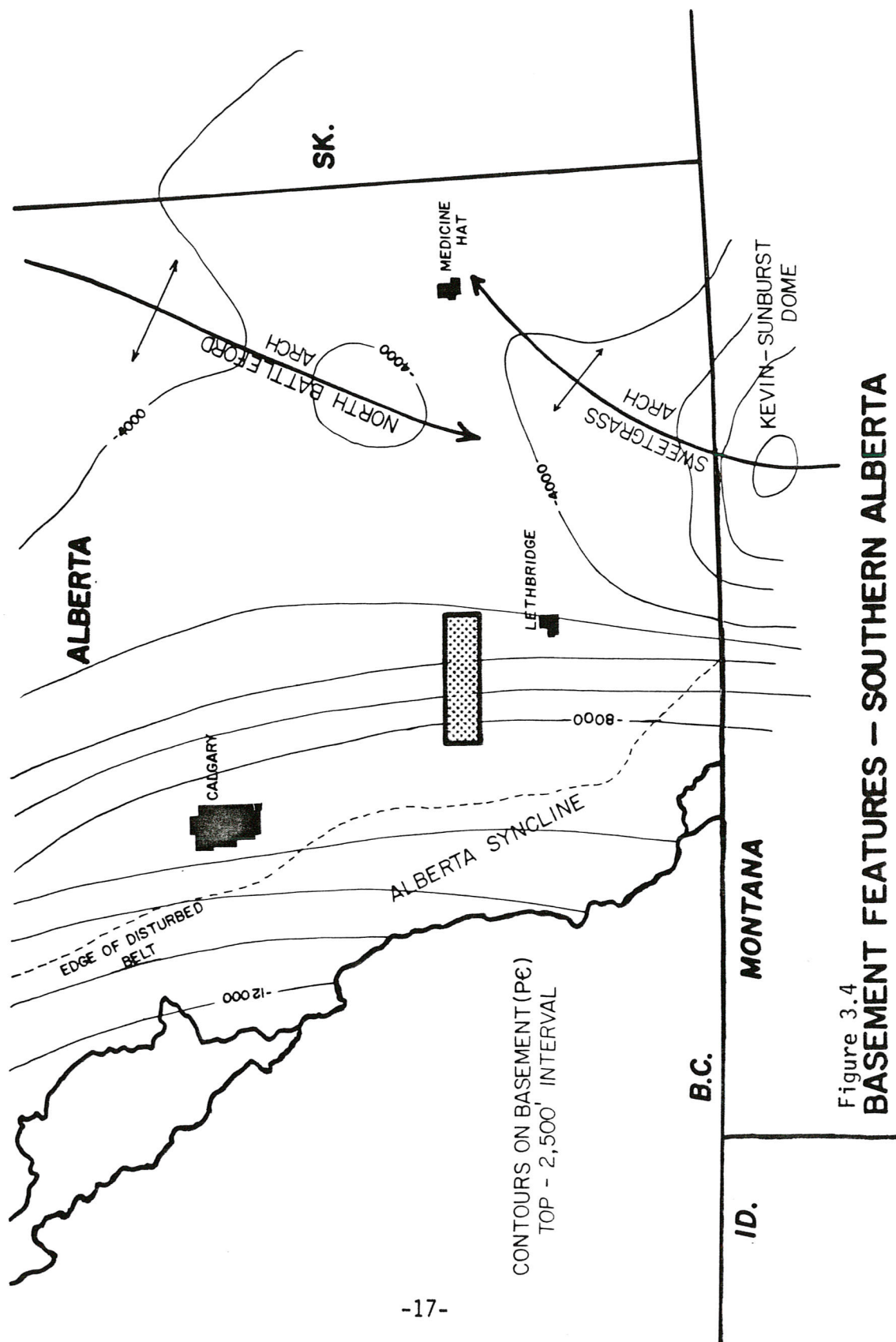


Figure 3.4
BASEMENT FEATURES - SOUTHERN ALBERTA

Hills. Beneath the surface the crystalline basement dips west away from the north/south trending axis of the Sweetgrass Arch toward the northwest/southeast trending axis of the Alberta Basin. Above the basement unconformity lie nearly 1,400 metres thickness of carbonate sediments of Cambrian, Devonian, and Mississippian age. A layer of Jurassic, Cretaceous and Tertiary clastic rocks ranging in thickness between 1,200 metres and 2,400 metres lies unconformably upon the Paleozoic carbonate sequence. Above this, till deposits of from 0 to 70 metres thickness smooth the pre-Pleistocene topography to the present-day flat to gently rolling terrain.

Data collected by Garland and Burwash, (1959), indicate that the basement under the study area is uniform in lithology, consisting mainly of granitic gneiss. For this reason, observed gravity anomalies were interpreted in terms of the structures described above, rather than in terms of a basement lithology/density variation.

CHAPTER FOUR - ACQUISITION AND REDUCTION OF DATA

4.1 - Description of Seismic Data.

Seismic reflection data were acquired for the entire length of the three gravity survey profiles, however north-south tie lines were not available. A characteristic example of the seismic data is shown in figure 4.1. The exact location of the seismic examples cannot be given due to constraints placed upon the use of the data by its supplier. The data are in the form of time sections with a record length of three seconds and are the result of conventionally-processed Vibroseis data. The data show numerous continuous seismic events which can be correlated throughout the profiles, and which are characterised by extensive linear sections interrupted by sharp discontinuities where arrival times abruptly increase or decrease in a step-wise fashion.

4.2 - Description of Well Data.

Log data were obtained for the wells shown in figure 3.2. These logs were both sonic and density logs, where available, and in many cases included driller's records of the contact depth of marker lithologies. Logs for over 30 wells in the area were obtained and studied. These wells are all located within two kilometres of the surveyed profiles.

A limitation arose in that most wells penetrated only to

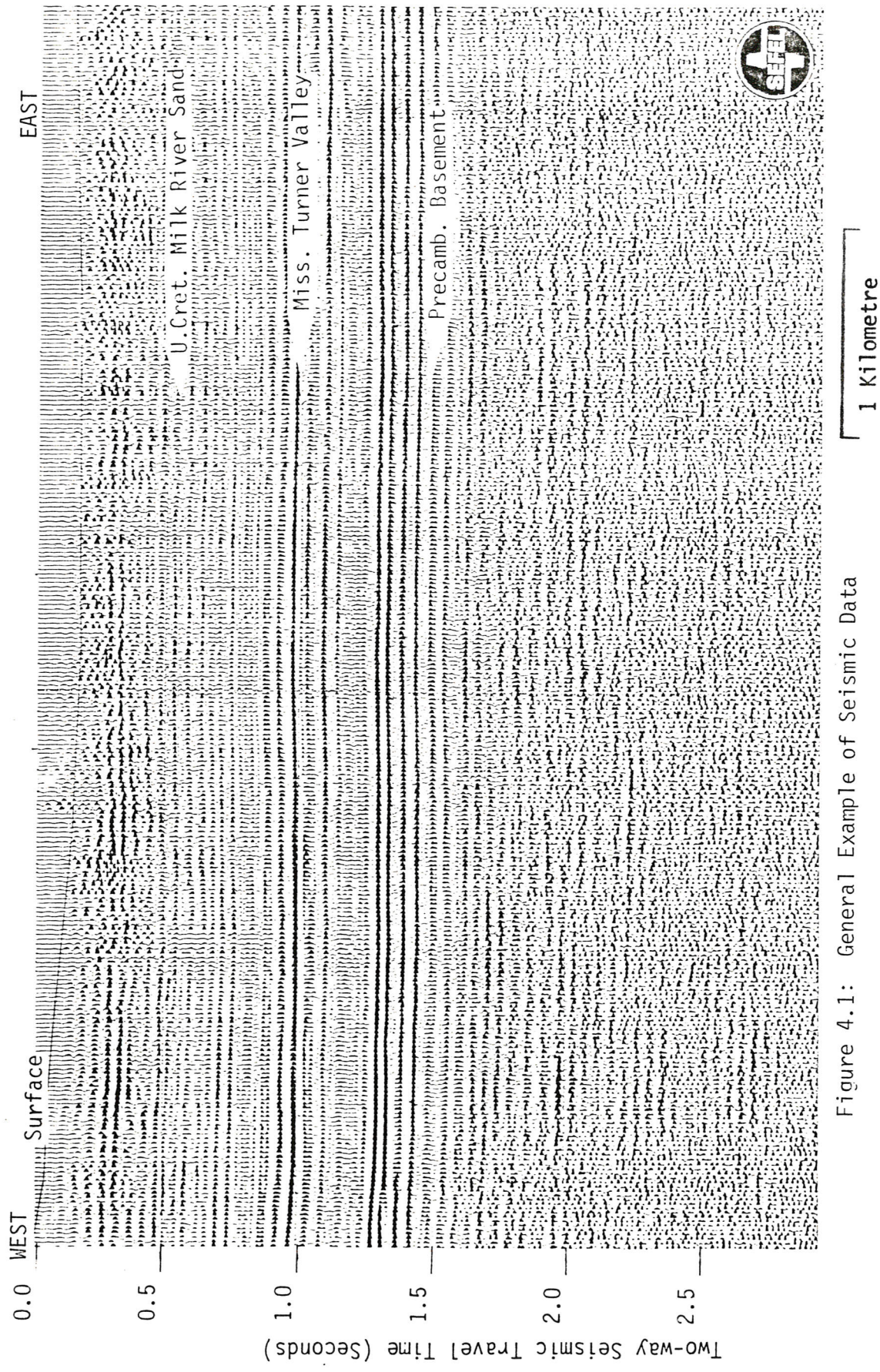


Figure 4.1: General Example of Seismic Data

the Mississippian surface. This resulted in poorer control for the thickness of the section from basement top to the Paleozoic-Mesozoic unconformity. However, log data from wells just outside the study area which penetrated to the basement show that carbonate seismic velocity is nearly constant at 6,100 m/s throughout the Paleozoic section. The thickness of this section was calculated by applying this velocity value to the time-thickness of the Paleozoic sequence.

The well log data show rapid, wide fluctuations in clastic average densities, (see figure 5.11, page 66). For this reason, accurate determination of average densities within the section was difficult. However, the few logs which encounter Paleozoic strata indicate less irregular density variation in that section.

4.3 - Description and Treatment of Gravity Data.

4.3.1: The Gravity Survey.

Gravity data were obtained in a gravity survey which was conducted between September 1980 and October 1981 using a Worden Master Gravity Meter belonging to the Department of Geology and Geophysics at the University of Calgary. The calibration constant for the instrument is 0.9584 g.u./scale division. Initially, measurements were made at 250-metre intervals along the centre profile, but after examination of reduced anomalies for this line it was determined that anomaly wave-

lengths were great enough to be sufficiently sampled by a 500-metre station interval. This station interval was used on the Carmangay and Barons lines, and results in the loss of higher-frequency variations which were not of interest to the study due to the fact that they are generated by shallow density variations. Instrument drift was assumed to be linear in nature and was corrected for by returning to a base station network every 2.5 hours, thereby allowing drift corrections to be calculated and removed from the observed data. Instrument precision is given as ± 0.5 gravity units by the manufacturer. Survey reliability was checked by closure of the two survey loops, which were in error by 1.9 and 1.3 scale divisions, or approximately 1.9 and 1.3 gravity units. These uncertainties are greater than the precision of the meter, but are insignificant in comparison to the magnitude of the observed anomalies. For this reason it was not considered necessary to distribute survey error around the survey loops. Gravity measurements were taken three times at every station and were found to be reproduceable to within 0.1 scale divisions or approximately 0.1 g.u.

4.3.2: The Elevation Survey.

The elevation survey was conducted simultaneously with the gravity survey using a Wild-T4 infrared distomat to obtain accurate elevations along each profile. Horizontal distances

between stations were measured and elevation differences were calculated from vertical angle measurements. Absolute elevations were determined by tying the survey into a Geodetic Survey of Canada elevation marker. Other Geodetic bench marks, Alberta Agriculture Survey markers and topographic map data provided checks on survey reliability.

Error in the elevation survey was determined through closure of two survey loops. The first loop was 139 kilometres long, contained 382 stations and closed to within 0.44 metres elevation. The second loop was 138 kilometres long, contained 383 stations, and closed to within 0.33 metres. These errors result in maximum uncertainties in Δg_{boug} of 1.3 and 1.0 g.u., respectively. These errors were not distributed due to their small magnitude relative to interpretable anomalies.

4.3.3: Reduction to Bouguer Anomalies.

Observed gravity readings were reduced to Bouguer anomalies by applying terrain, latitude, and elevation corrections according to equation (2-7). For the topographic corrections, gravitational effects of topography in Hammer zones (A) through (M), (Hammer, 1939), were calculated according to Bible, (1962), and found to be approximately zero even in the most topographically severe areas near Blackspring Ridge.

In that the profiles ran directly east/west, only a single latitude correction value was necessary for each line, except

for the three areas where the line deviated north around lakes. The total north-south separation of stations was 12.8 kilometres. It was considered satisfactory to assume a linear latitude correction over this distance, (equation 2-6), using a base station at the west end of the Claresholm line. Since each line has only a single-valued latitude correction, errors introduced by this assumption will generate only a small bulk shift to the data which is removed by the determination of the regional field.

In equation (2-7), the Δg_{elev} term is calculated according to equation (2-4). The reduction datum was chosen as sea level and thus (h) values are equivalent to station elevations. Δg_{slab} is calculated from equation (2-5) where the density of reduction, (ρ), was taken as $2.67 \times 10^3 \text{ kg/m}^3$ on the basis of the average density of basement core samples of wells sampled by Garland and Burwash, (1959). The average basement density was chosen as the reduction density so that the observed anomalies could be interpreted in terms of the density contrast between the Precambrian basement and the overlying sedimentary rocks. The resulting observed Bouguer anomalies thus reflect mass deficiency represented by sedimentary rocks with densities less than $2.67 \times 10^3 \text{ kg/m}^3$. A density of $2.20 \times 10^3 \text{ kg/m}^3$ was also employed in the Bouguer reduction process, and the resulting anomalies were not found to be significantly different than those calculated using the basement density, probably due to the generally subdued topography of the area.

The final computed Bouguer values were filtered by applying a three-point average filter. The filtering process involves averaging the Bouguer anomaly values of three adjacent stations, and then using that average as the filtered Bouguer value at the middle station. This type of filter was chosen in order to remove high-frequency variations generated by near-surface density variations and sharp variations in Quaternary till layer thickness. In addition, this process reduces the weight given to spurious variations due to instrument or operator error. Bouguer wavelengths less than one kilometre were considered to be noise and were filtered out in this way. The remaining longer wavelengths are generated by true and deeper mass variations which are the focus of this study.

The three filtered, observed Bouguer anomaly profiles are shown in figures 4.2a, b, and c. These profiles show numbers which are relative Bouguer anomaly values. All three profiles have a similar character which includes increasing eastward values. In each profile this regional eastward increase is interrupted by an area with relatively higher values at about kilometre 12. This area is followed in each case by an area of lower anomaly at approximately kilometres 18 through 34, after which a more constant increase in anomaly value is resumed to the east end of the profile. The curves are not smooth, as numerous sharp increases and decreases in Bouguer anomaly level are evident, specifically between kilometres 28 and 36. The total range

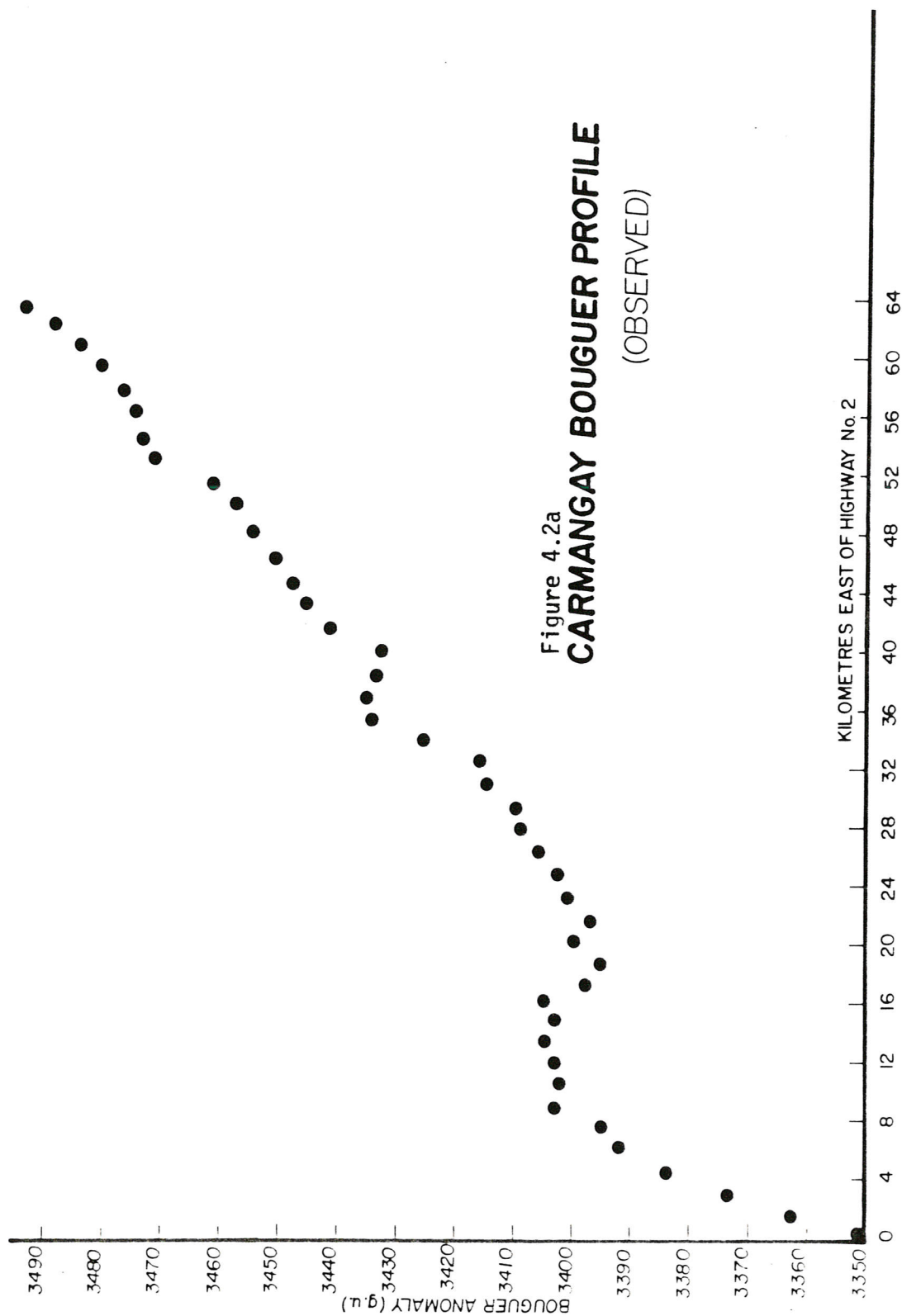
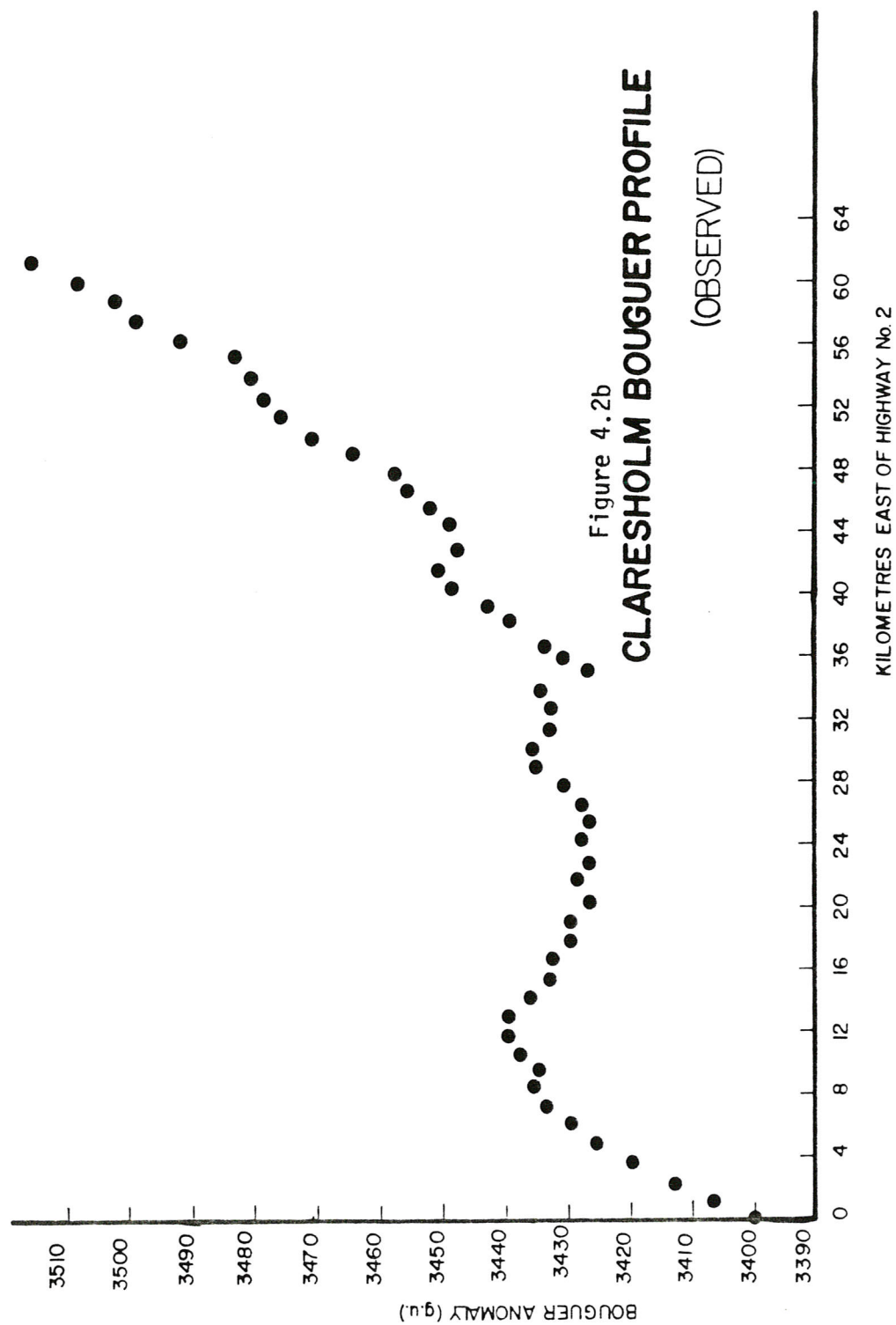
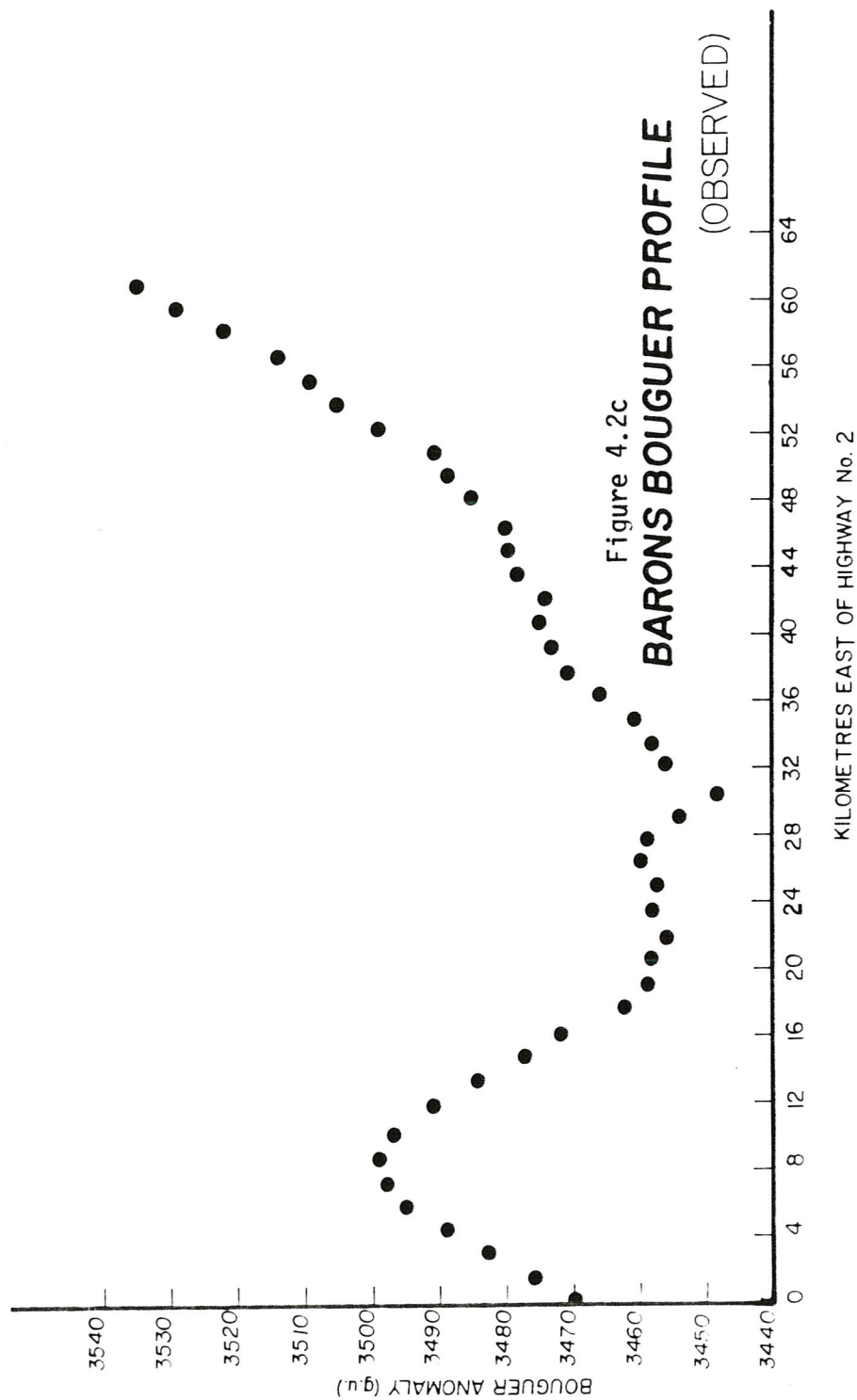


Figure 4.2a
CARMANGAY BOUGUER PROFILE
 (OBSERVED)





of anomaly values is approximately 180 gravity units.

The Bouguer profiles data in figure 4.2a, b, and c were plotted on a map of the study area and contoured to produce the relative Bouguer anomaly contour map in figure 4.3a. The map shows 10 g.u. contours with a general northeast/southwest trend and decreasing values to the northwest. A semi-circular area of rapid gravity increase is evident surrounding a high Bouguer anomaly area just southeast of Claresholm. The gradient in this area is as much as 10 g.u./kilometre, but gradients in the remainder of the area are consistently less, averaging only 4 g.u./kilometre. A large-scale gravity map of the area by Buck, (1967), (see fig. 4.3b), is in general agreement with figure 4.3a as far as range of anomaly values across the map and the highly anomalous area southeast of Claresholm are concerned. However, the general trend of contours in the published map is northwest as opposed to a northerly trend in figure 4.3a. This discrepancy is interpreted to be the result of a low station density of approximately one station per sixty square kilometres in the published map and also due to computer smoothing of the data from that source.

4.3.4: Regional Gravity Gradients.

To obtain residual Bouguer anomalies, the regional field must be subtracted from the observed Bouguer anomalies. This regional field is caused by deeper-seated crustal inhomogeneities which are not of interest to the study. The regional gravity

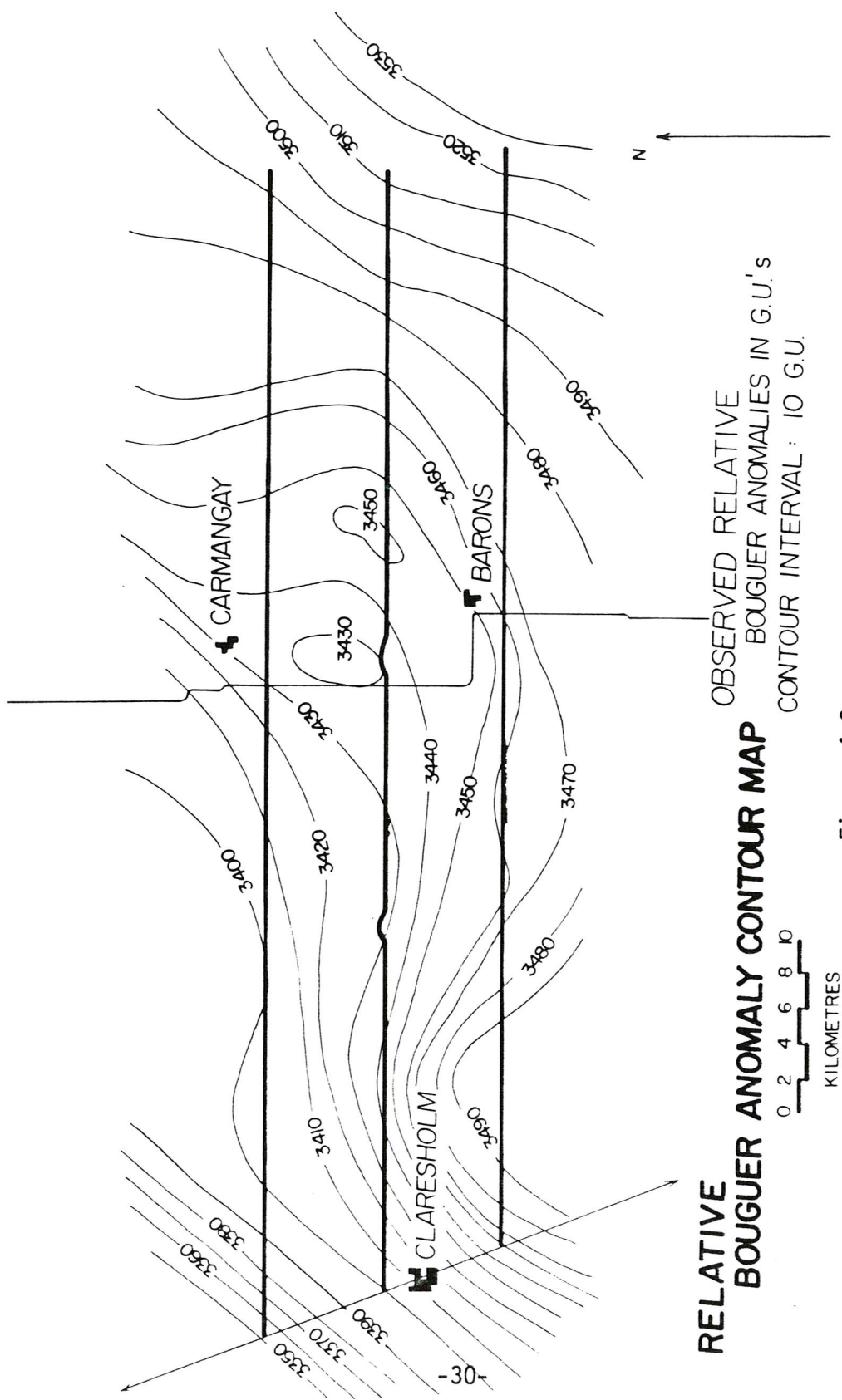


Figure 4.3a

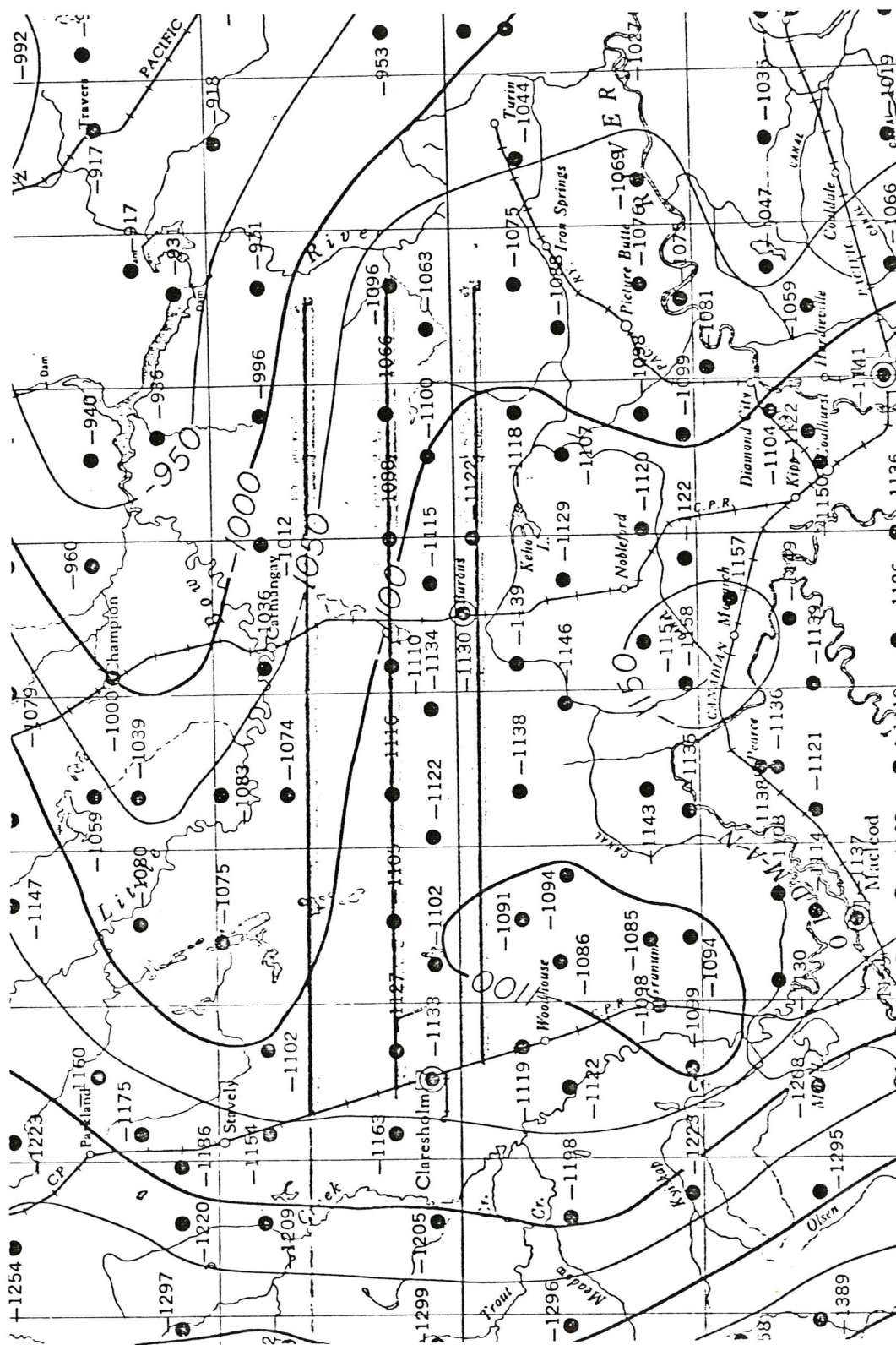


Figure 4.3b: Published Bouguer Anomaly Map of Study Area after Buck, (1967).
(East/West dark lines at centre are survey profiles).

fields were approximated by constant gravity gradients which extend over the lengths of the profiles. The depth to the source of regional fields results in long-wavelength anomalies which are assumed to be linear over the lengths of the profiles. These fields were established by actually defining the regional anomaly where good control was available from wells; i.e., by calculating the theoretical anomaly generated by Bouguer slabs at the end of each profile. The thicknesses and densities of these slabs were obtained from logs of wells near the ends of each profile, and anomalies were calculated with the following formula:

$$\Delta g = 2\pi G \Delta \rho h \quad (4-1),$$

where: $\Delta \rho$ = The density contrast of the Bouguer slab with respect to the density of reduction, ($2.67 \times 10^3 \text{ kg/m}^3$).

A sample calculation of the regional field value at one point at the western end of the Barons profile follows:

<u>Layer</u>	<u>Thickness(m)</u>	<u>Dens.Contr.</u>	<u>Total(g.u.)</u>
Till Layer	20	-0.72	- 0.60
U. Cret. Clastics	1350	-0.39	-21.06
L. Cret. Clastics	675	-0.15	- 4.05
Paleo. Carbonates	1340	-0.02	- 1.07
			<u>-26.78</u>

Subtracting the total of -26.78 from the observed gravity value at the western end of the Barons profile establishes the local magnitude of the regional field. Calculations at the two endpoints of the profiles establish the linear gradient

across the entire profile. The residual fields are those values which would be observed if the entire sedimentary section was replaced by material of basement density.

Figures 4.4a, b, and c show the observed Bouguer profiles of figures 4.1a, b, and c in relationship to the regional gradients calculated for each profile. The regional gradients dip gently to the east with changes of no more than 50 g.u. over the 60-kilometre long profiles. A steeper gradient is evident along the Barons profile than in the other two. This is due to the comparatively shallow basement depth at the eastern end of this profile which causes the total anomaly in that area to be less than at the eastern ends of the other profiles.

The residual Bouguer anomaly profiles obtained by subtracting regional field values from the observed anomalies are seen in figure 5.13a, 5.14a, and 5.15a for the Carmangay, Claresholm and Barons profiles, respectively. These figures show curves similar to those in figure 4.2a, b, and c but with negative values. The residual Bouguer anomalies are negative because the sediment densities are less than the basement reduction density. Thus, the residual anomalies can now be interpreted in terms of density and structure in the sedimentary wedge.

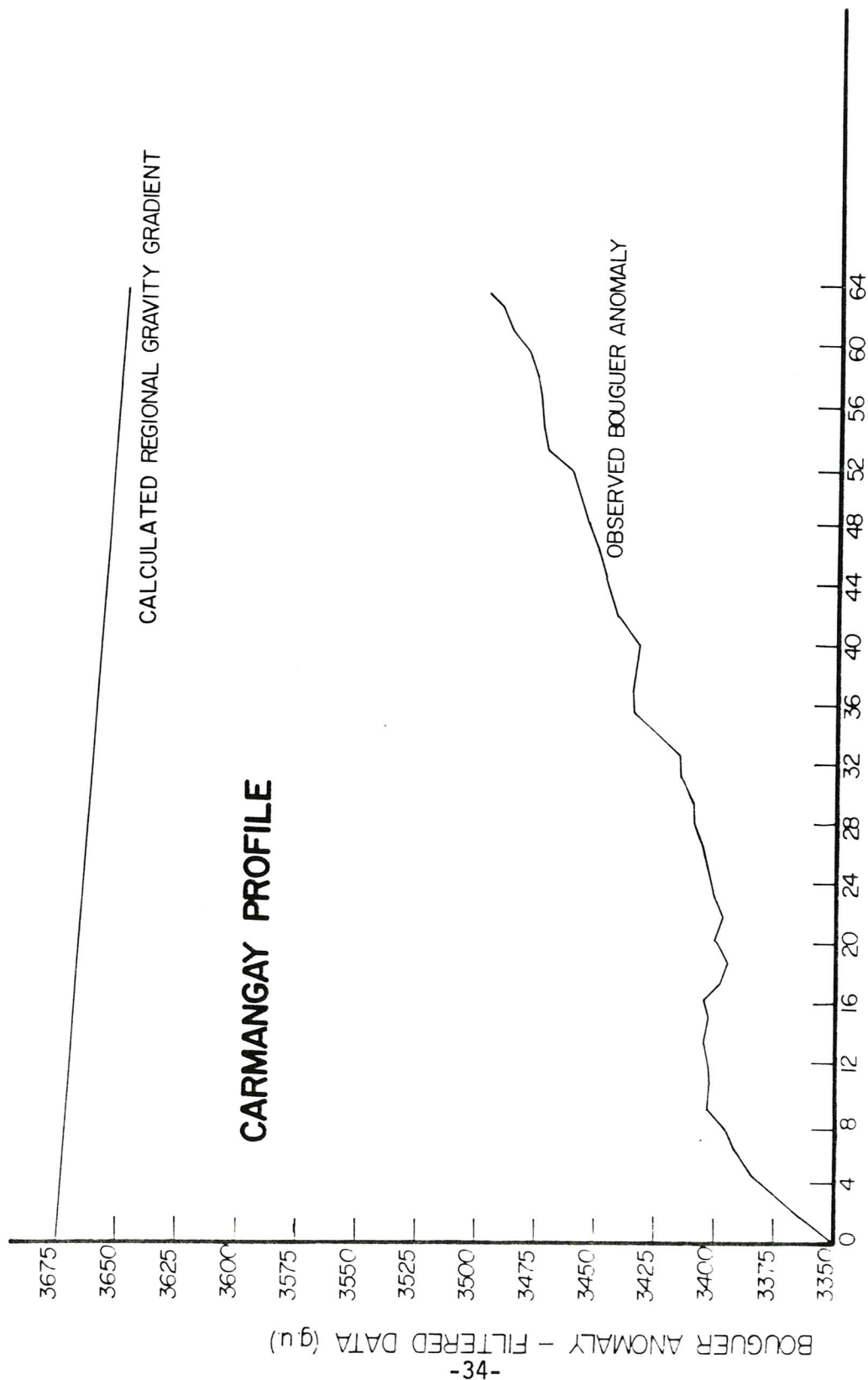


Figure 4.4a: Calculated Regional and Observed Bouguer Anomaly Profiles - Carmangay

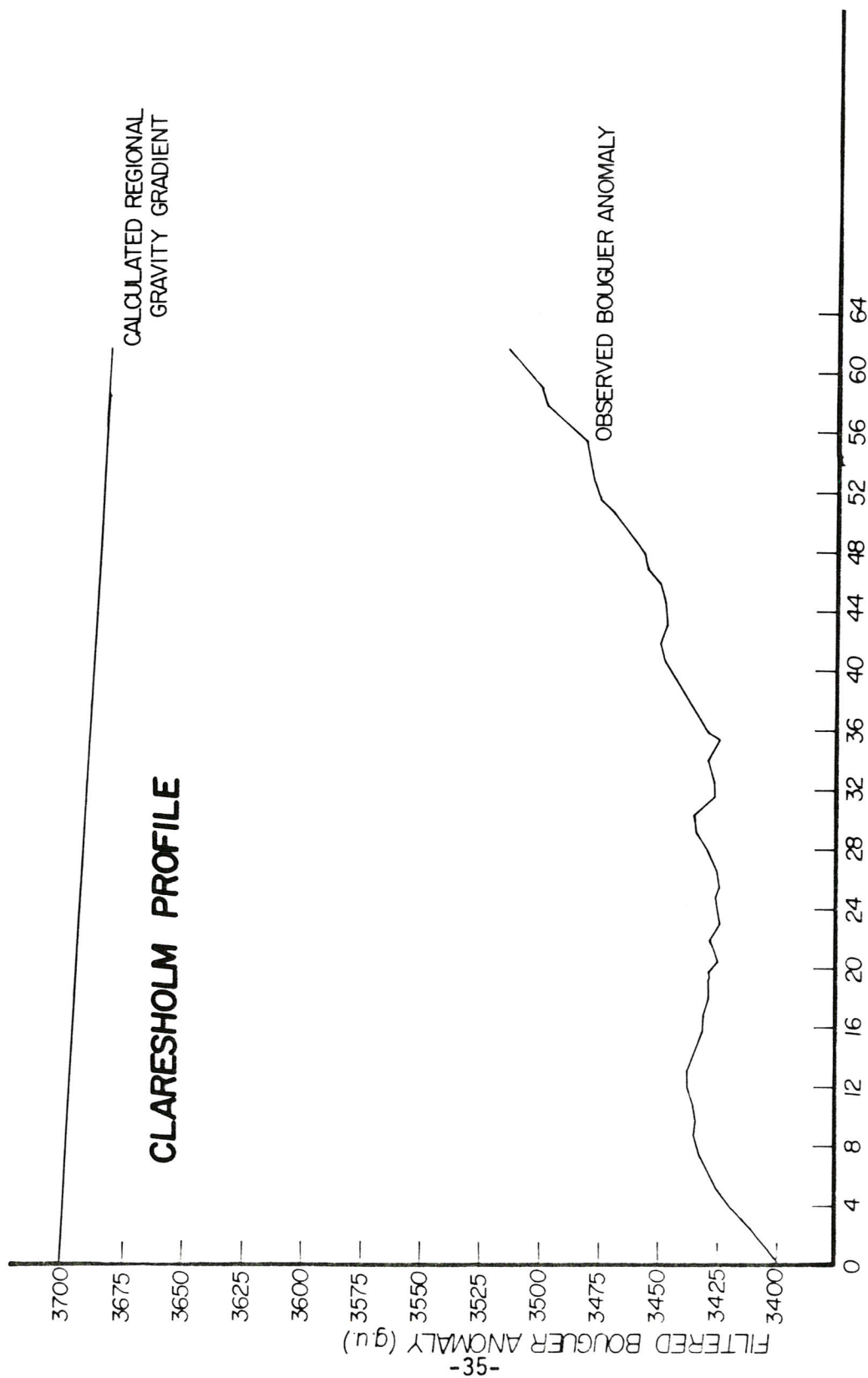


Figure 4.4b: Calculated Regional and Observed Bouguer Anomaly Profiles - Claresholm

CHAPTER FIVE - DATA ANALYSIS

5.1 - Analysis of Seismic Data.

5.1.1: Initial Model Construction.

The residual Bouguer anomaly curves presented in figures 4.4a, b, and c show amplitudes of as much as 50 g.u. and a variable character due to the subsurface density and structural variations. Interpretation of these data was accomplished by means of investigating the gravitational response of geologic cross-sectional models which were varied until their responses were in agreement with the residual Bouguer data. The first models were constructed from seismic control data, but further refinement led to more complex structure and density make-up.

Construction of the first models initially required identification of the continuous events seen in time sections. Geologic marker depth data and average velocity data from well logs allowed arrival times for individual markers to be predicted. Comparison of these predicted times with the arrival times in the time sections allowed events to be identified. The continuous nature of the reflections further allowed them to be traced through the length of the profile.

Three events were identified in the time sections; the upper Cretaceous Milk River Sand, the Turner Valley carbonate surface, i.e., the Paleozoic unconformity, and the reflection

off the top of the Precambrian basement, (see fig. 4.1).

Time-depth conversion of data was undertaken with the combined time section data and velocity data estimated from well logs. Average velocities to the upper Cretaceous Milk River Sand and Mississippian Turner Valley markers were found to be higher at the eastern end of each profile and lower at the western ends. To account for these variations, a linear eastward decrease in velocity was established along each profile. This approximation of linear velocity value changes was verified by logs of wells along the profiles. As stated in chapter four, carbonate layer thickness was obtained from a constant velocity which was applied to the time thickness measured in the section. The thickness calculated was added to the section below the Mississippian Turner Valley marker top.

Published structure contour maps of the Paleozoic surface and the lower Cretaceous Fish Scale member, based on well data, were obtained from the Energy Resources Conservation Board, (1969, 1978). Contour intervals on these maps are 100 feet and the maps confirm the accuracy of the initial models.

5.1.2: Features of the Seismic Data and Initial Model.

The seismic time sections show extensive linear events which are interrupted in a step-wise fashion by sharp to smooth variations in arrival time. These steps are as great as 0.12 seconds two-way travel time over the space of a

kilometres, (see fig. 5.1). Arrival time increases, generally, for all events from east to west, indicating a general westward dip. Evidence of faulting, in the form of diffraction and termination of events is seen at many of the discontinuities and in some areas listric normal faults are seen in the Cretaceous clastics above the larger vertical faults, (see fig. 5.2). In the Paleozoic carbonate sequence a reflection is seen to terminate against another reflection, indicating the depositional or erosional edge of a Paleozoic formation, (see fig. 5.3).

The initial model interpretations of these seismic data are shown in figures 5.4a, b, and c for all three profiles. In general, the sections show a block-faulted Precambrian basement of horst and graben structure. For the purpose of this study, the sedimentary wedge overlying the basement has been divided into three units; Paleozoic carbonates, lower Cretaceous clastics, and upper Cretaceous clastics. The faults bounding the basement blocks are continuous through the Paleozoic carbonates and terminate within the Cretaceous clastics. The basement and overlying strata slope away from an area of horizontal strata near the eastern end of the profiles, but this constant slope is interrupted occasionally by upthrown and downthrown areas.

In the Carmangay profile, nine faults are evident. A concentration of five faults surrounds an upthrown area near kilometre 26. To the east of this, a relatively downthrown area is evident, and a fault of larger than average throw is apparent

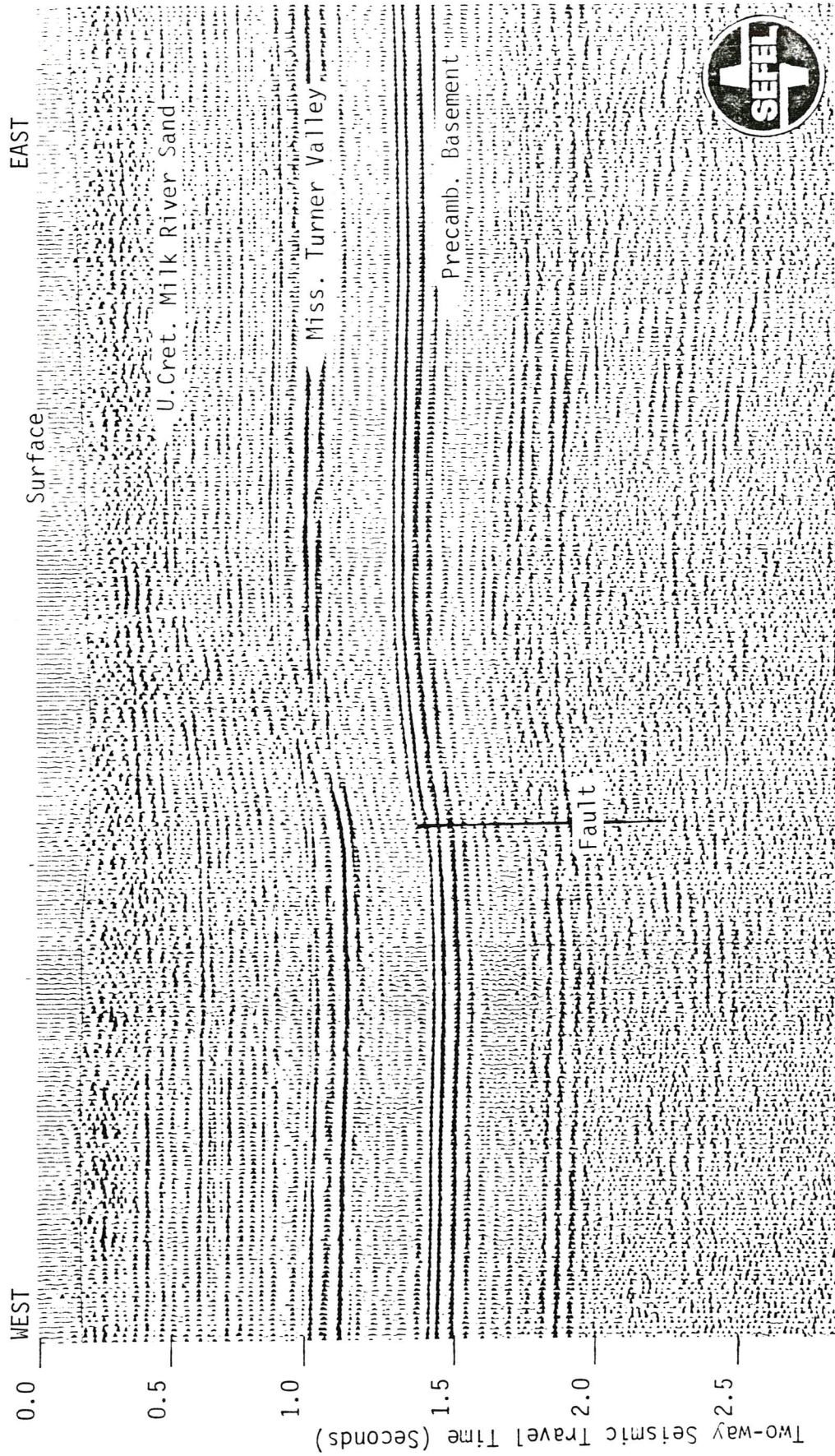


Figure 5.1: Example of Basement Fault in Seismic Profile.

1 kilometre

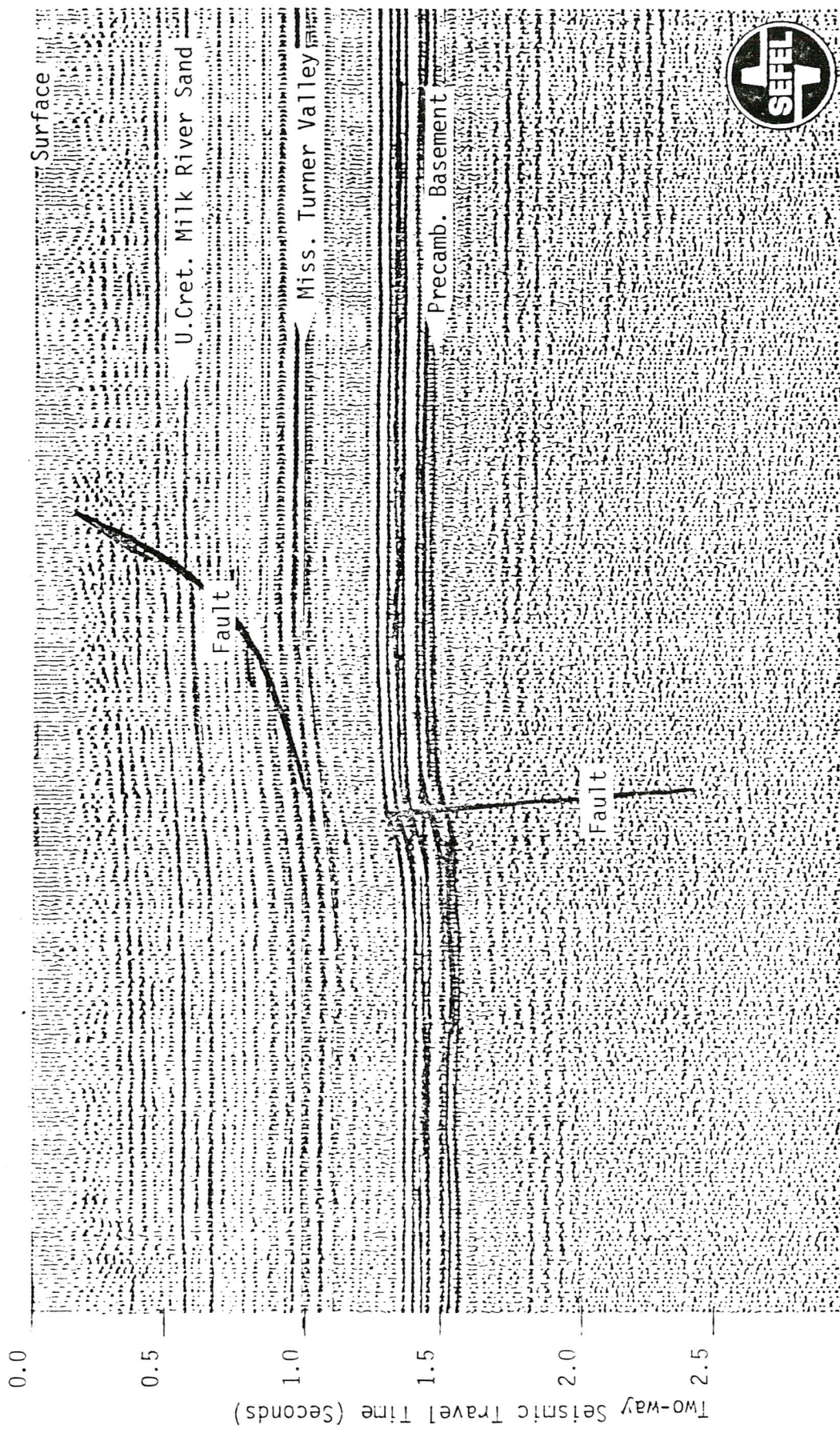


Figure 5.2: Example of Listric Fault in Seismic Profile.

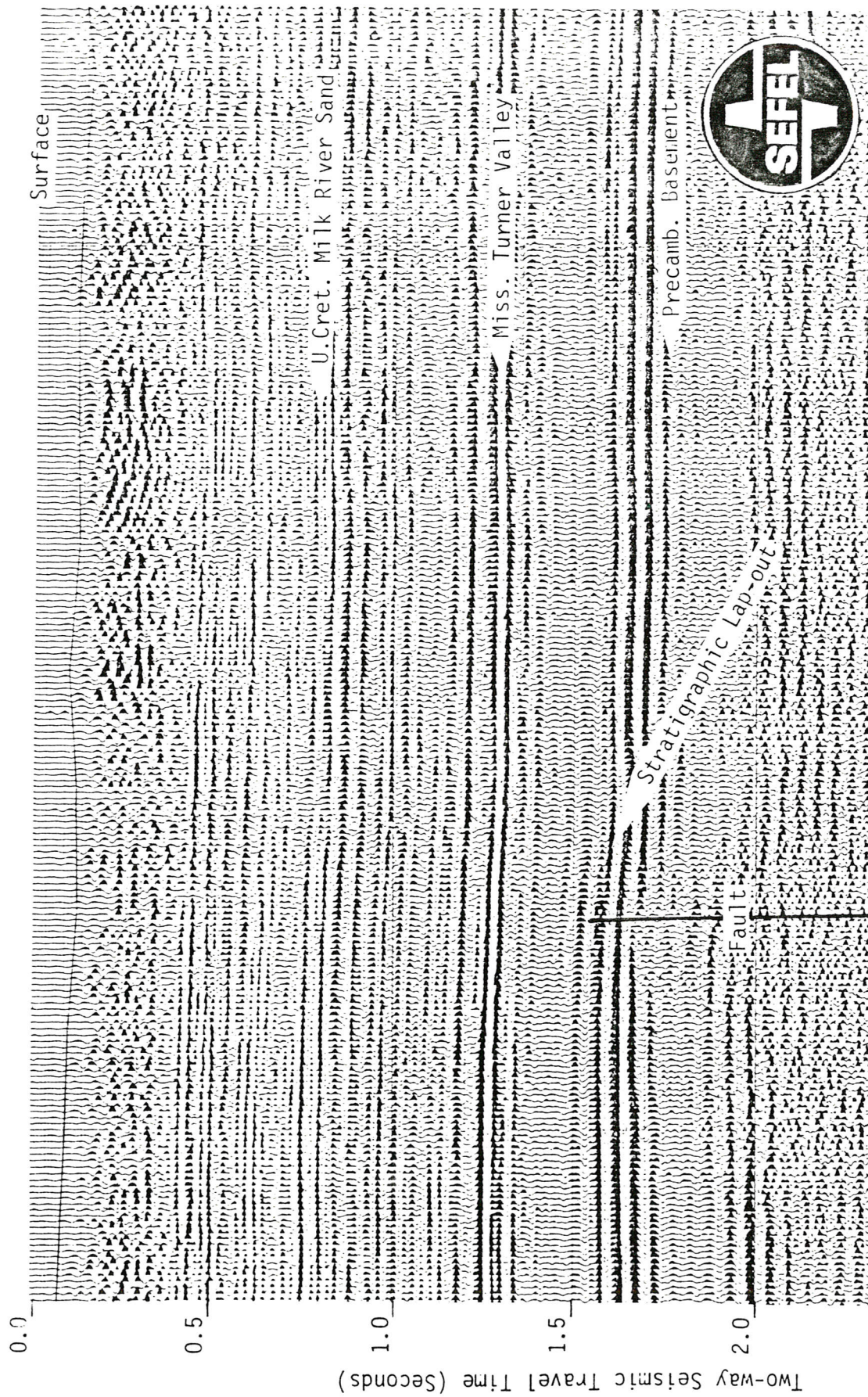


Figure 5.3: Example of Stratigraphic Termination in Seismic Profile.

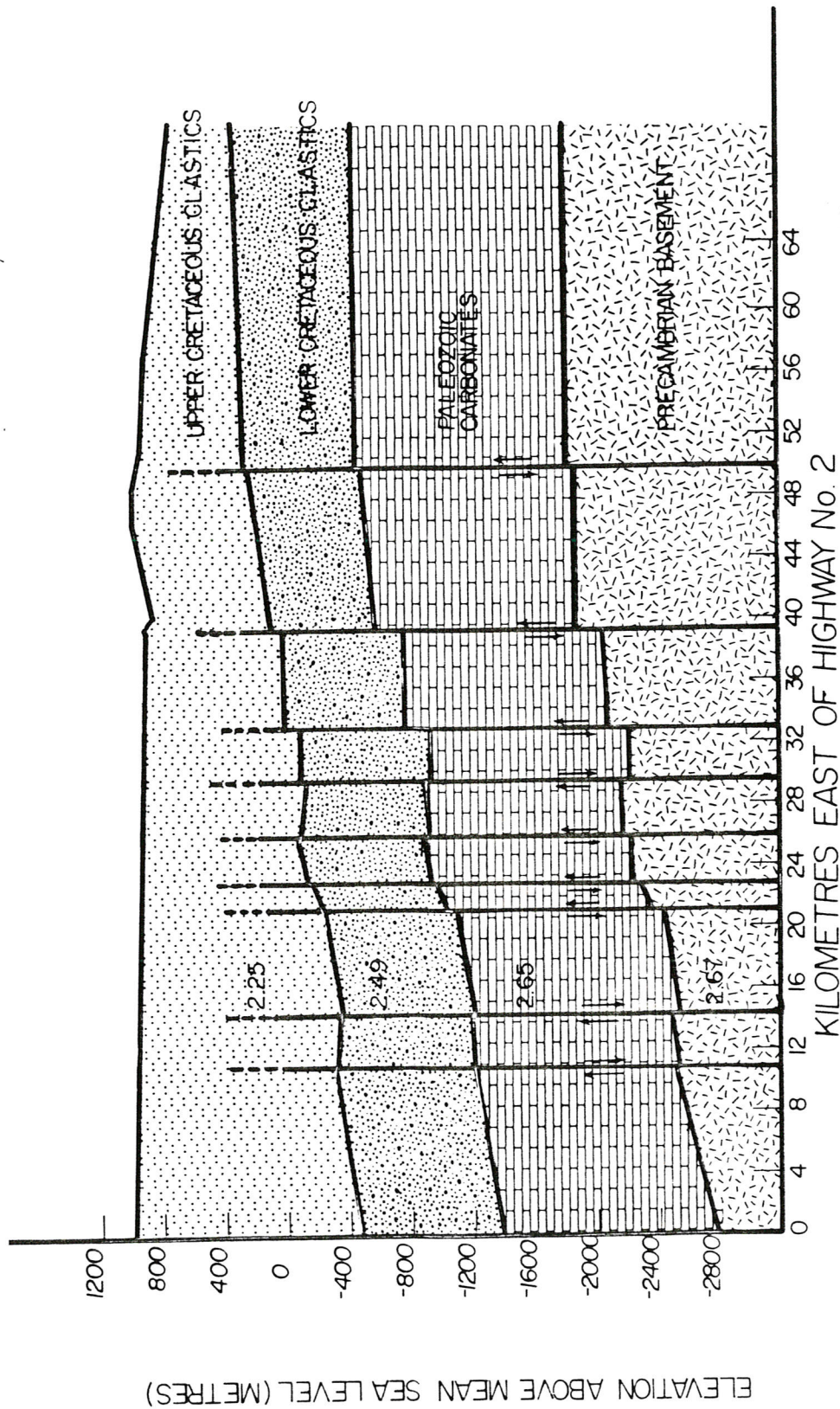


Figure 5.4a

SIMPLE STRUCTURAL MODEL FROM SEISMIC DATA – CARMANGAY

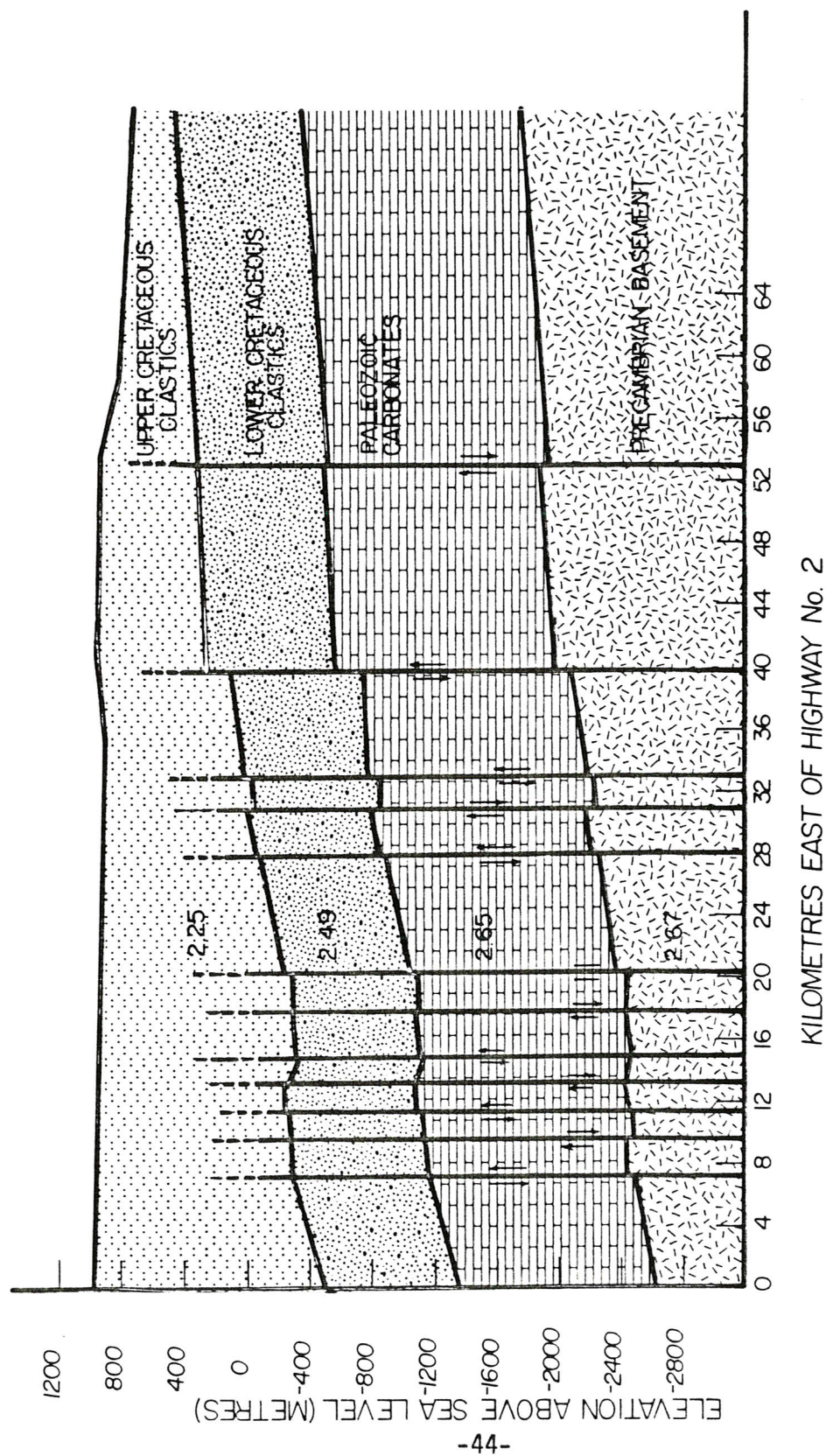


Figure 5.4b
SIMPLE STRUCTURAL MODEL FROM SEISMIC DATA -- CLARESHOLM

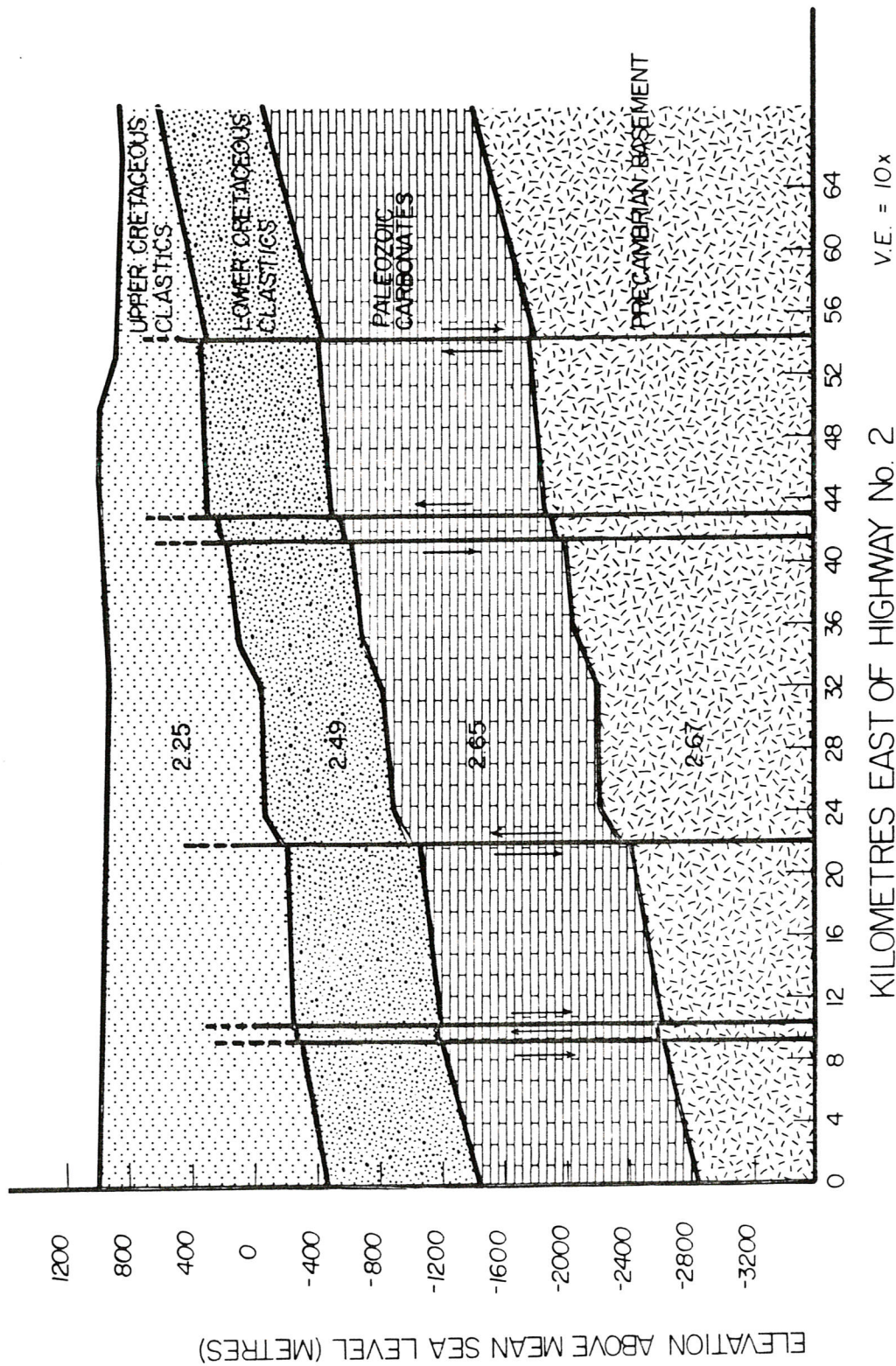


Figure 5.4c
SIMPLE STRUCTURAL MODEL FROM SEISMIC DATA - BARONS

at kilometre 39.

The Claresholm section shows more faulting than the Carmangay section, with a total of twelve evident. An interpreted portion of this profile is shown in figure 5.5. Here, five of the concentration of seven faults which surround an upthrown area at kilometre 14 are shown, and this is the location of the Claresholm gas field. A downthrown area flanks this to the east as in the Carmangay profile and another larger than average fault throw is evident at kilometre 40.

The Barons profile is markedly different from the two previously-discussed profiles in that only six widely-spaced faults are seen in section. The regional dip of the marker horizons in this profile is more constant, with no greatly upthrown or downthrown areas. Faults along this profile generally have smaller throws than faults in the other profiles.

5.1.3: Time Thickness Profiles and Isochron Maps.

Travel time data from the seismic sections were used to plot time thickness profiles for the upper and lower Cretaceous clastics and Paleozoic carbonate layers. In addition, for each layer an isochron map was constructed, showing points of equal time thickness.

Figures 5.6a, b, and c compare time thickness variations in the upper and lower Cretaceous clastic and Paleozoic carbon-

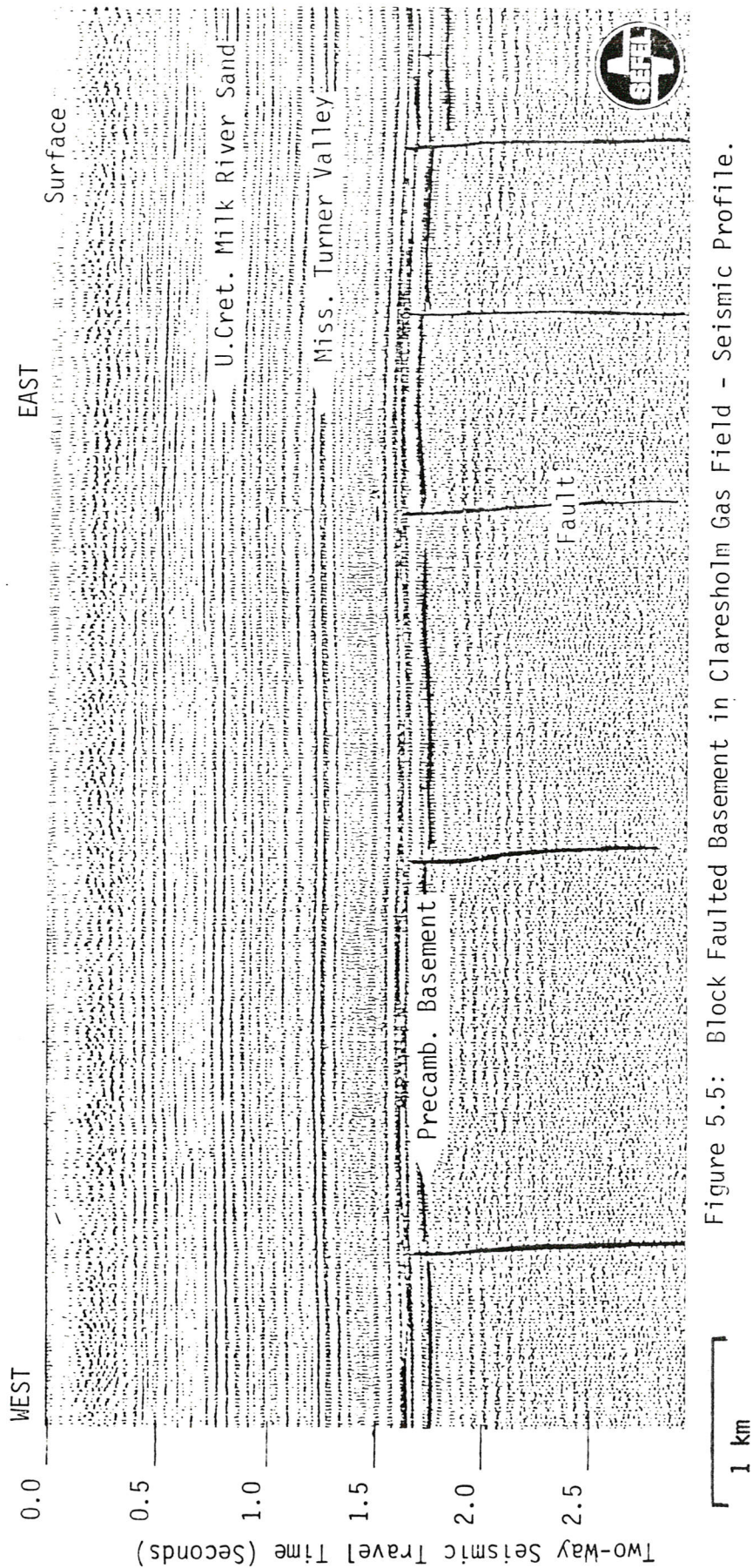
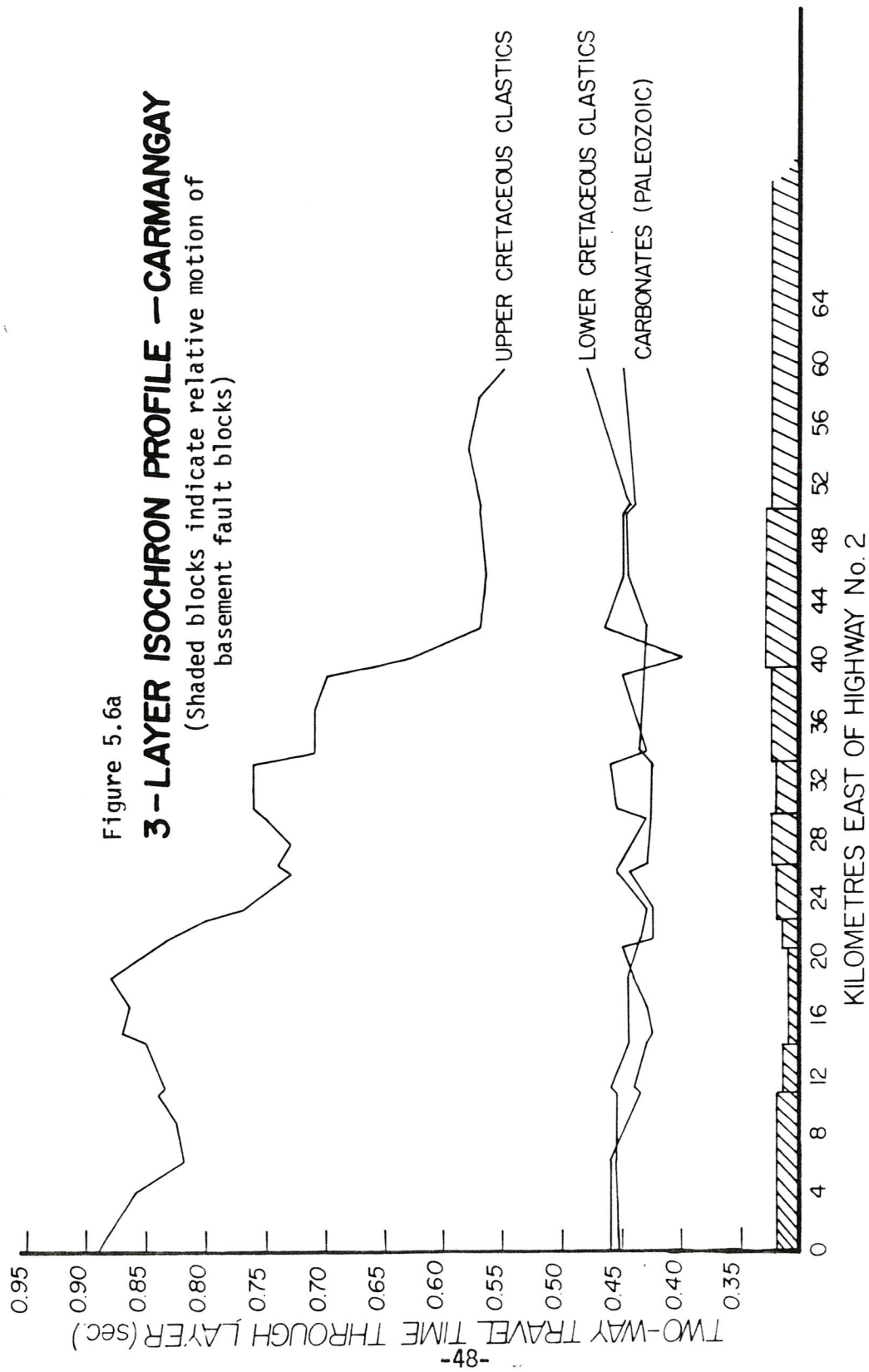
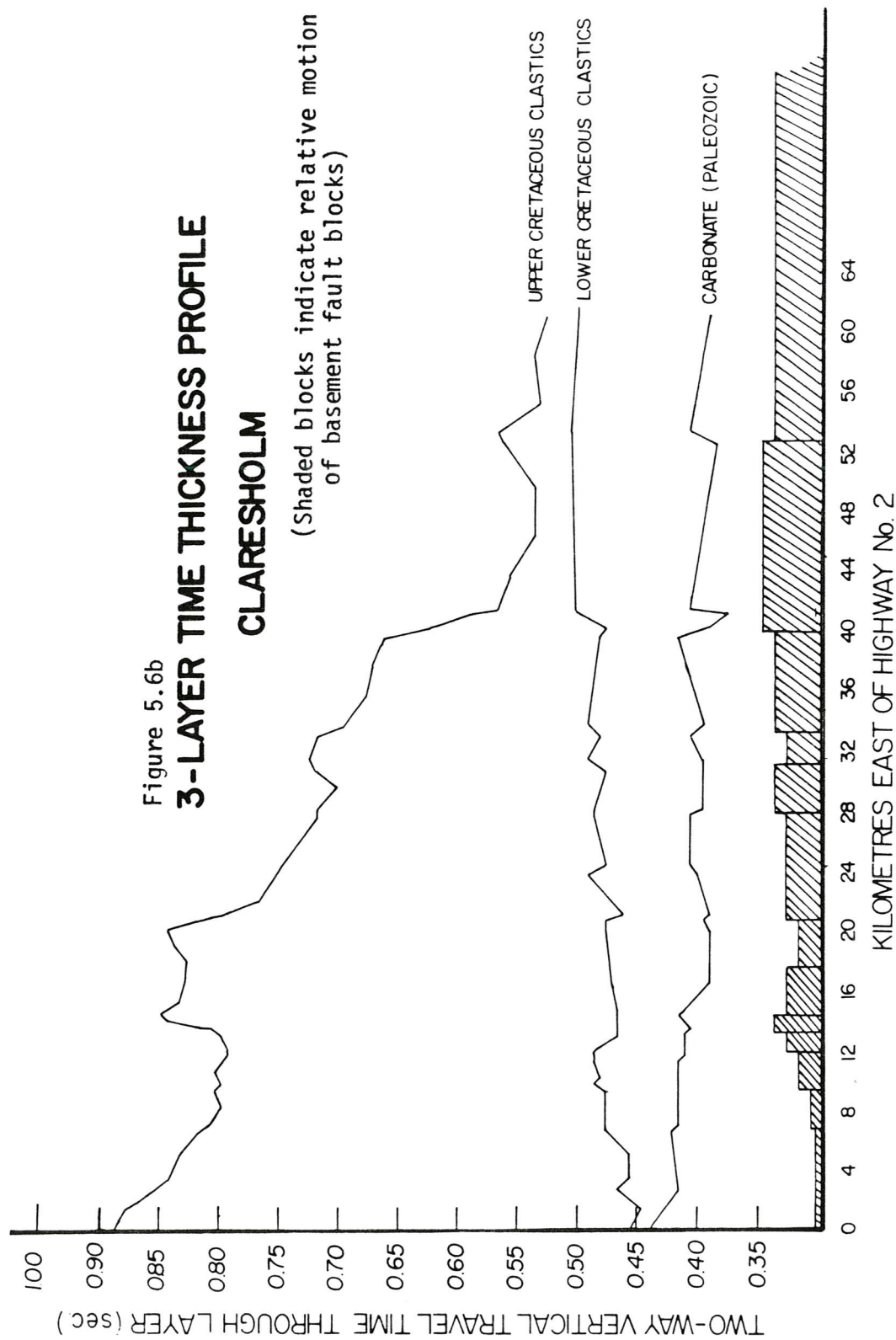
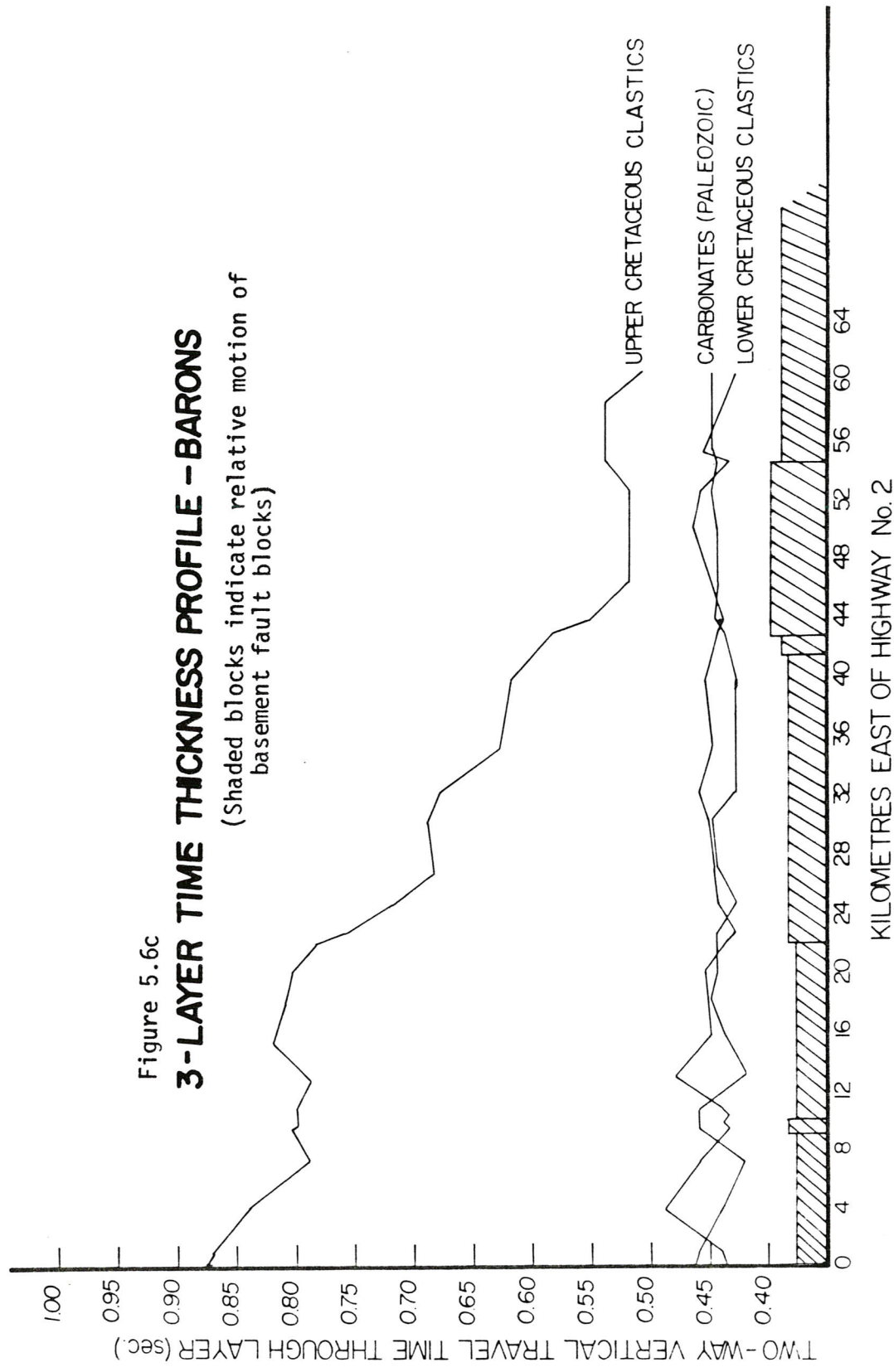


Figure 5.5: Block Faulted Basement in Claesholm Gas Field - Seismic Profile.



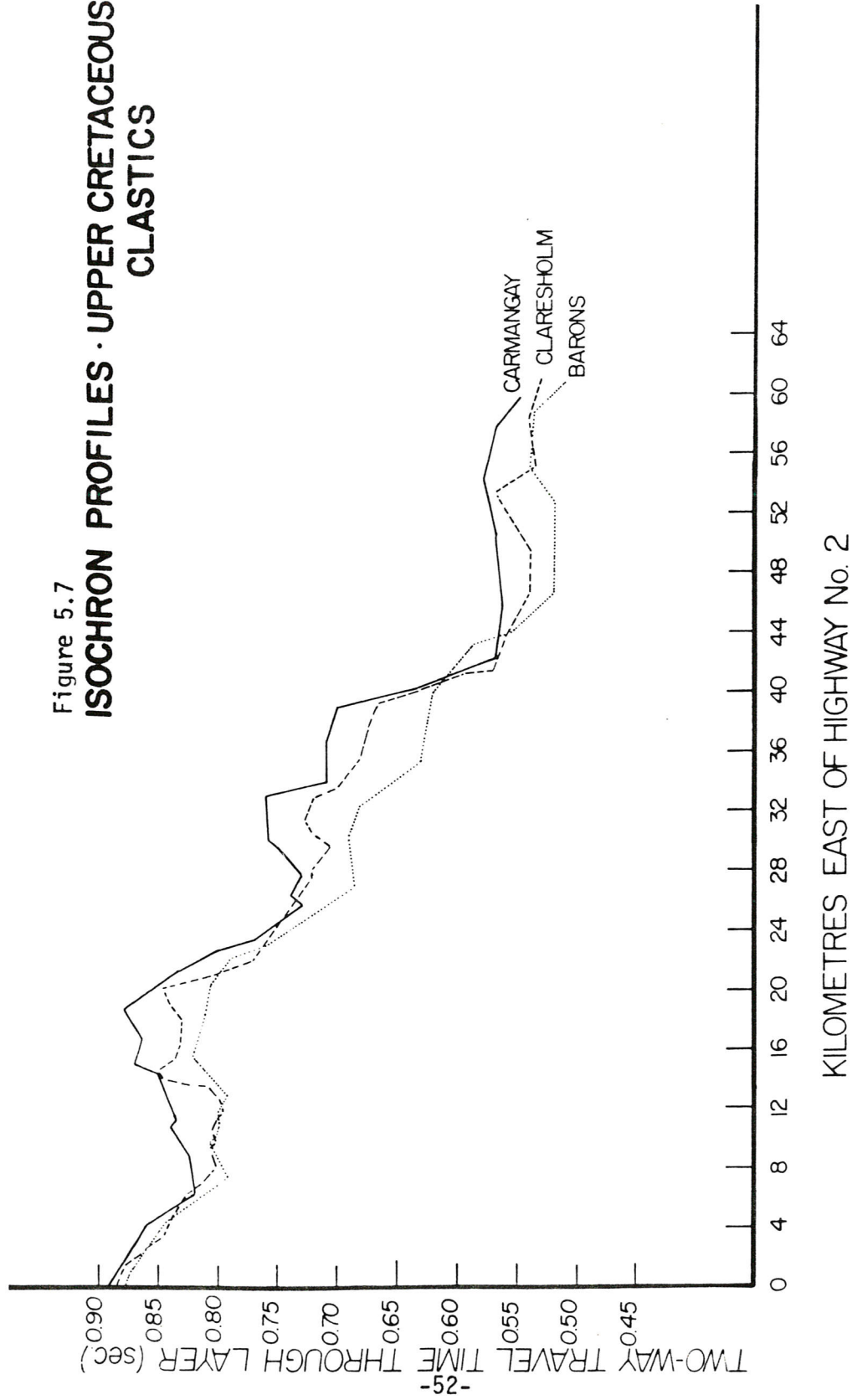




ate layers. Time thickness was measured at intervals across the seismic section and plotted along the profile. The curves are not smooth, partially due to the sampling frequency of approximately one sample every three kilometres and partially because of rapid thickness variations within the layers. The Paleozoic carbonate and lower Cretaceous clastic data indicate only minor variation in time thickness across the profiles. However, the upper Cretaceous clastic data show a general thinning through the clastic wedge along with local thickness increases of as much as 0.1 seconds two-way seismic travel time which interrupt the gradual easterly thinning. Figure 5.7 compares the upper Cretaceous clastic layer in all three profiles and shows that areas of increased thickness occur at nearly the same points in each profile, establishing a north-northwesterly trend to the thickness variations.

The isochron maps shown in figure 5.8a, b, and c show extrapolated contours in the areas between profiles. The upper Cretaceous clastics map reflects the general east to west thinning and shows two areas of very rapid thinning, one just south and west of Carmangay, and one midway between Carmangay and Claresholm. The trend of these contours is slightly west of north. Maps of the lower Cretaceous clastics and Paleozoic carbonates show less pattern. The lower Cretaceous clastic layer is thickest along the Claresholm profile and thins to the north, south and east. The Paleo-

Figure 5.7
**ISOCHRON PROFILES · UPPER CRETACEOUS
 CLASTICS**



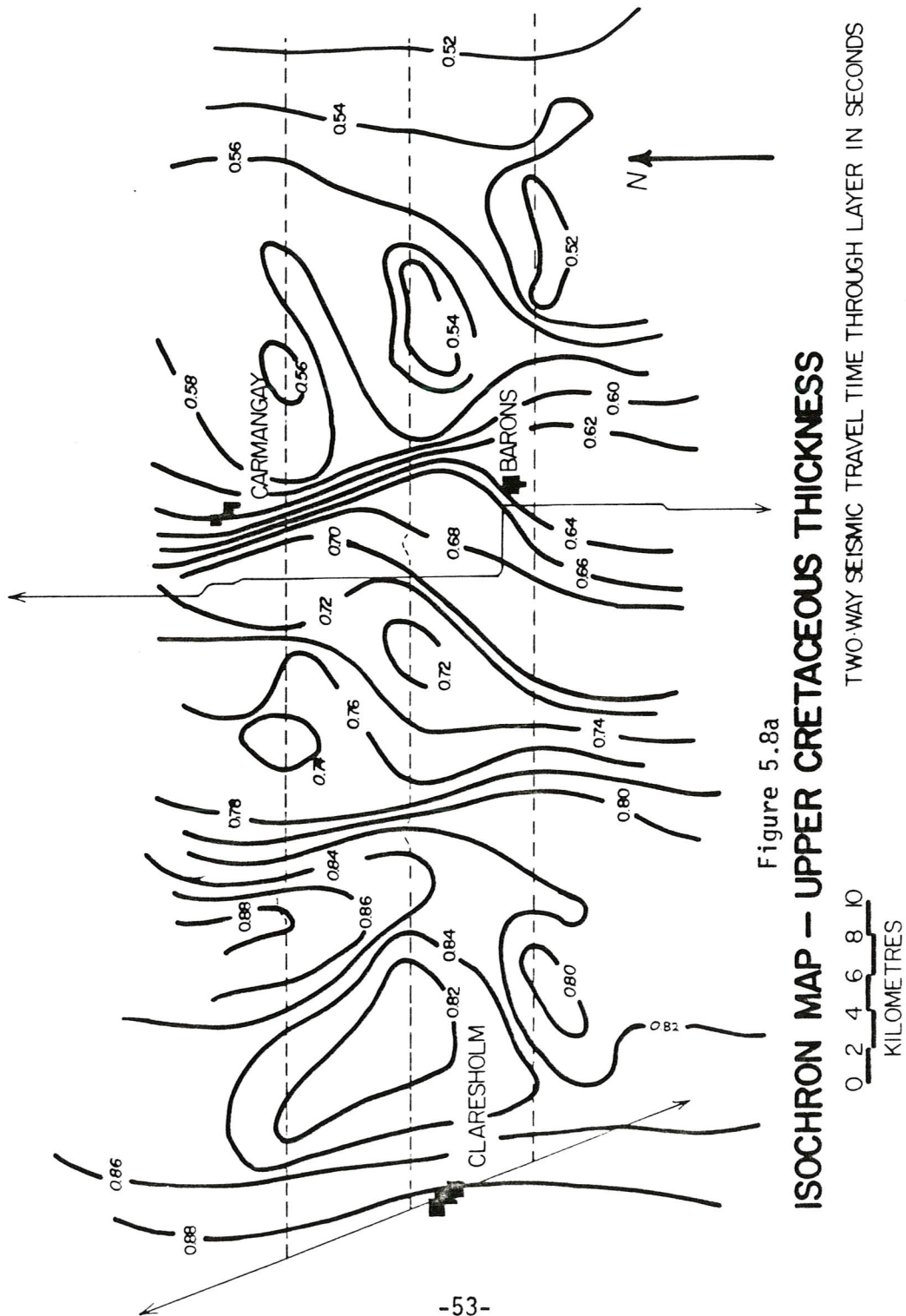


Figure 5.8a

ISOCHRON MAP -- UPPER CRETACEOUS THICKNESS

TWO-WAY SEISMIC TRAVEL TIME THROUGH LAYER IN SECONDS

0 2 4 6 8 10
KILOMETRES

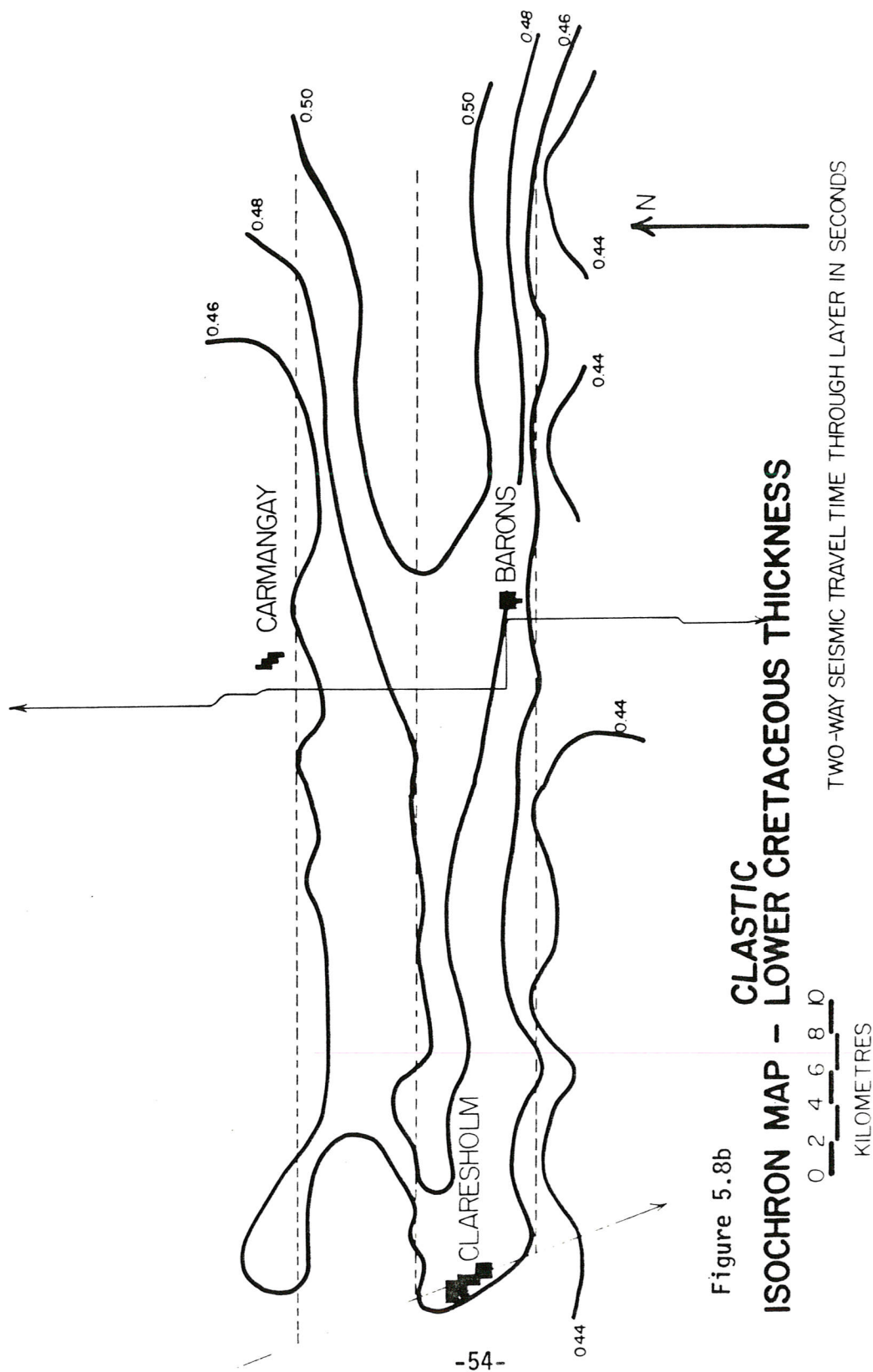


Figure 5.8b
CLASTIC
ISOCHRON MAP - LOWER CRETACEOUS THICKNESS

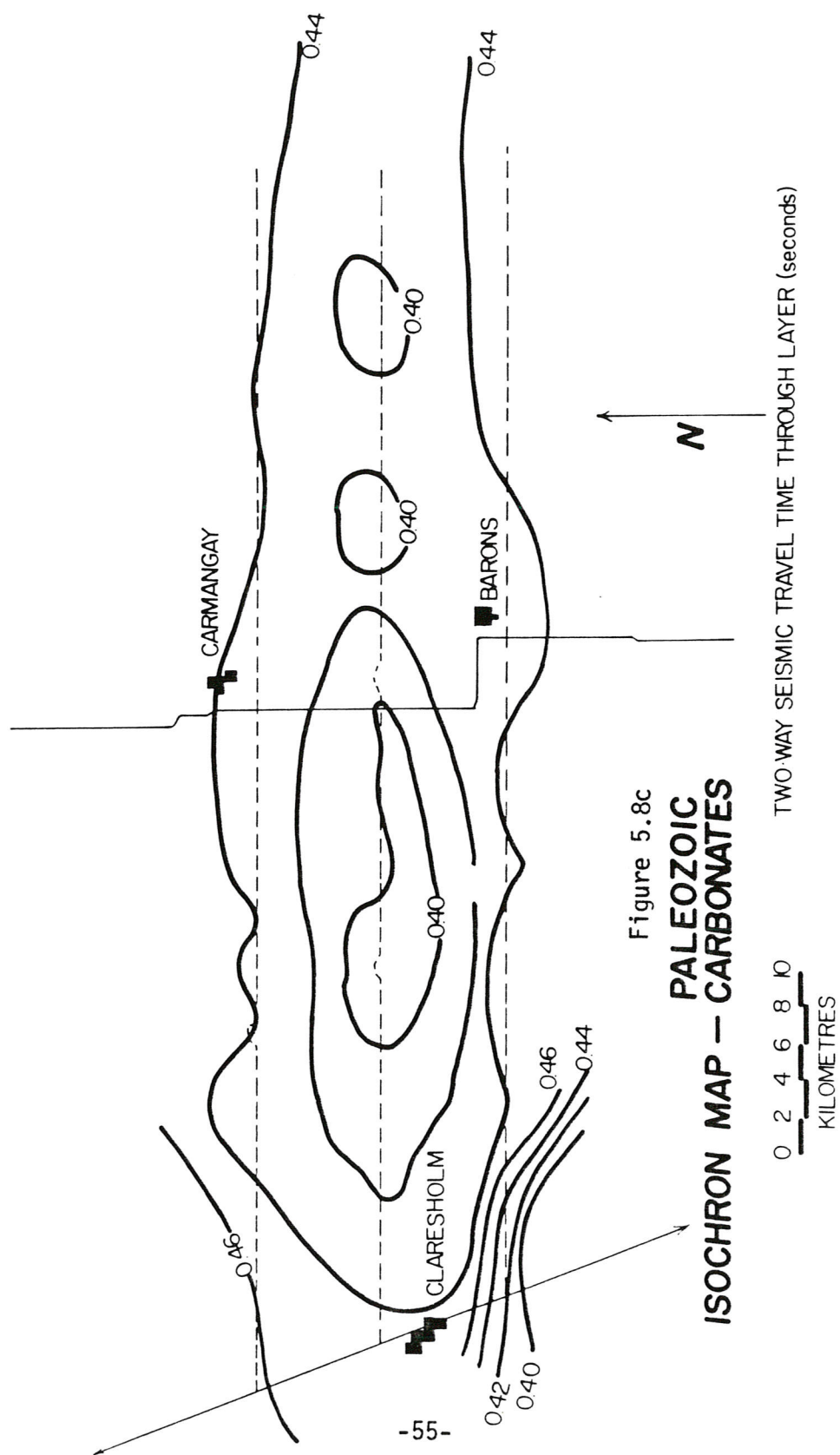


Figure 5.8c
PALEOZOIC CARBONATES
ISOCHRON MAP - CARBONATES

TWO WAY SEISMIC TRAVEL TIME THROUGH LAYER (seconds)

zoic carbonate contour trend is similar, but thickening occurs away from the Claresholm profile to the north and south.

5.1.4: Error Limits on the Structure Sections.

Average velocity values were calculated from sonic logs at two well sites on each profile and velocity gradients between these values were calculated and used in conjunction with arrival times to obtain depth values throughout the section. Accuracy of this method was confirmed as marker depths known at other well sites were within 100 metres of those predicted with average velocity and arrival times calculations.

Velocity logs were also examined to aid in determining accurate average velocities. Averages of interval velocities obtained from these logs were in agreement with the calculated velocity figures, to within 150 m/s. This uncertainty in estimated interval velocities results in depth uncertainties of from ± 40 metres at the east end of the profiles to ± 70 metres on the west for the upper Cretaceous Milk River Sand as increasing arrival time magnifies the uncertainty. Similarly, Turner Valley depth uncertainty varies between ± 75 metres on the east and ± 110 metres on the west. Logs show Paleozoic carbonate velocities to be nearly constant with depth and thus basement depth values are probably of similar accuracy. These values support a figure of ± 100 metres as an accurate upper limit of structural uncertainty within the profiles.

5.2 - Analysis of Gravity Data.

5.2.1: Density Data for Model Construction.

Density logs from well records provided approximate average bulk densities for use in the gravity modelling process. These values, by layers, are:

Upper Cretaceous Clastics above Milk River Sand:	2.25
Upper Cretaceous Clastics below Milk River Sand	
and Lower Cretaceous Clastics	: 2.49
Paleozoic Carbonates	: 2.65

These values are in units of $\text{kg/m}^3 \times 10^3$. Trott, (1981), determined an average density of $1.95 \times 10^3 \text{ kg/m}^3$ for glacial till in central Alberta and this value was used in this study. Maxant, (1975, 1980), provides maps of density distributions in western Canada with data obtained through well logs. Telford, et. al., (1976), was another source of density information. The values obtained from well log data are consistent with these sources however well log data fluctuate over short intervals and accurate averages are difficult.

5.2.2: Gravitational Response of the Initial Model.

A gravitational analysis of the initial structural model for the Claresholm profile, (see fig. 5.4b), was undertaken. Density values used in this model were the average upper and lower Cretaceous clastic and Paleozoic carbonate values listed in the previous section of this chapter. A comparison

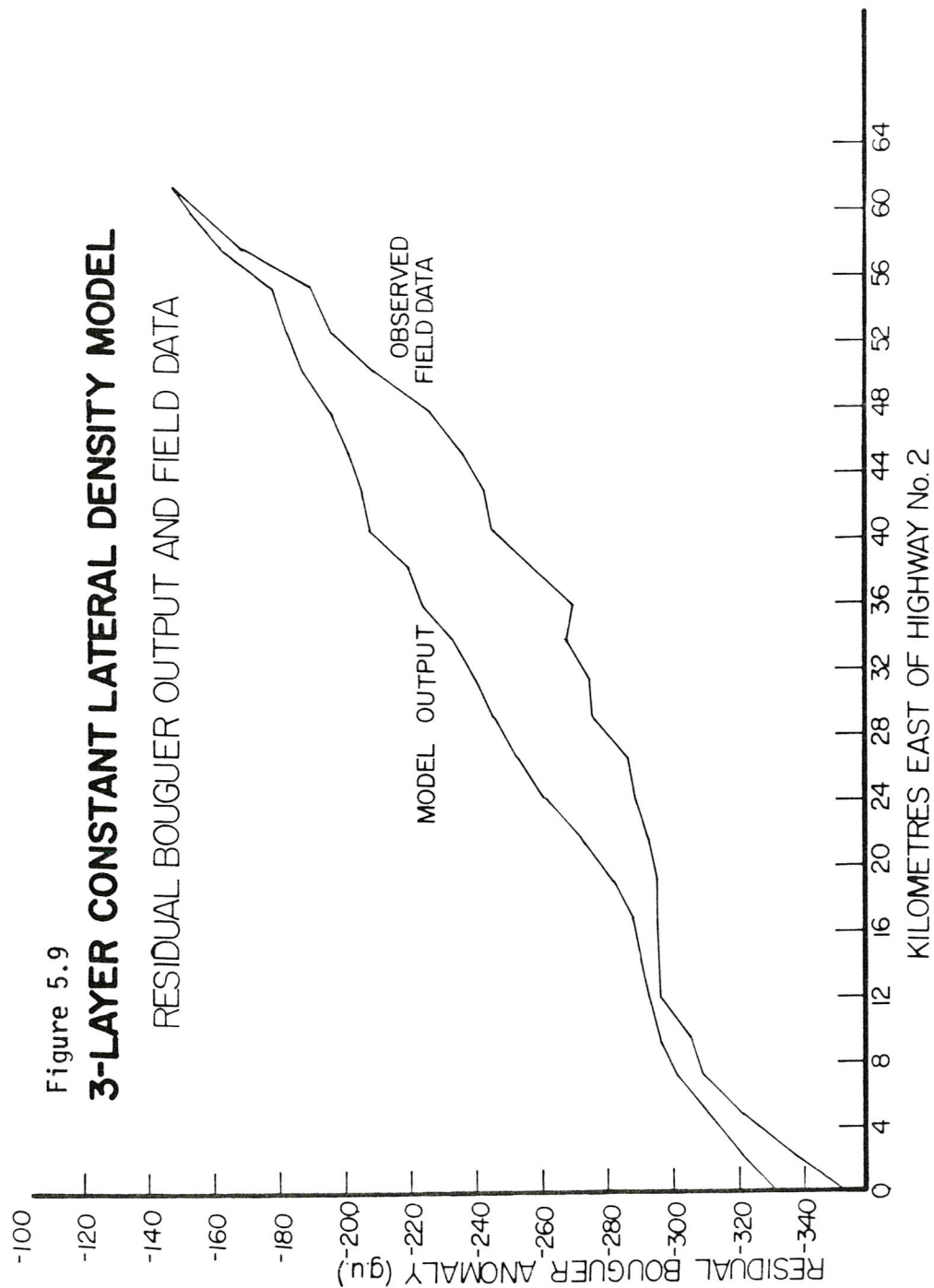
of the residual Bouguer anomaly data of the model response and field survey is shown in figure 5.9. This illustration shows discrepancies as large as 50 g.u. between the two profiles. The fit of the two profiles is very close at kilometres 12 and 64, which is expected since data at the end of the profile and kilometre 12 were initially used to define the regional field. However, between kilometres 20 and 56 a large section is evident where the initial model output disagrees with the residual curve. Similar results were obtained with the Carmangay and Barons data.

5.2.3: The Gravity Modelling Process.

The failure of the initial model's response to closely match the data observed in the field necessitates varying the model in one or more of the following ways:

- (1) Varying structure within the limits discussed in section 5.1.4.
- (2) Increasing the detail of the model.
- (3) Varying the density structure within the clastic and carbonate layers.

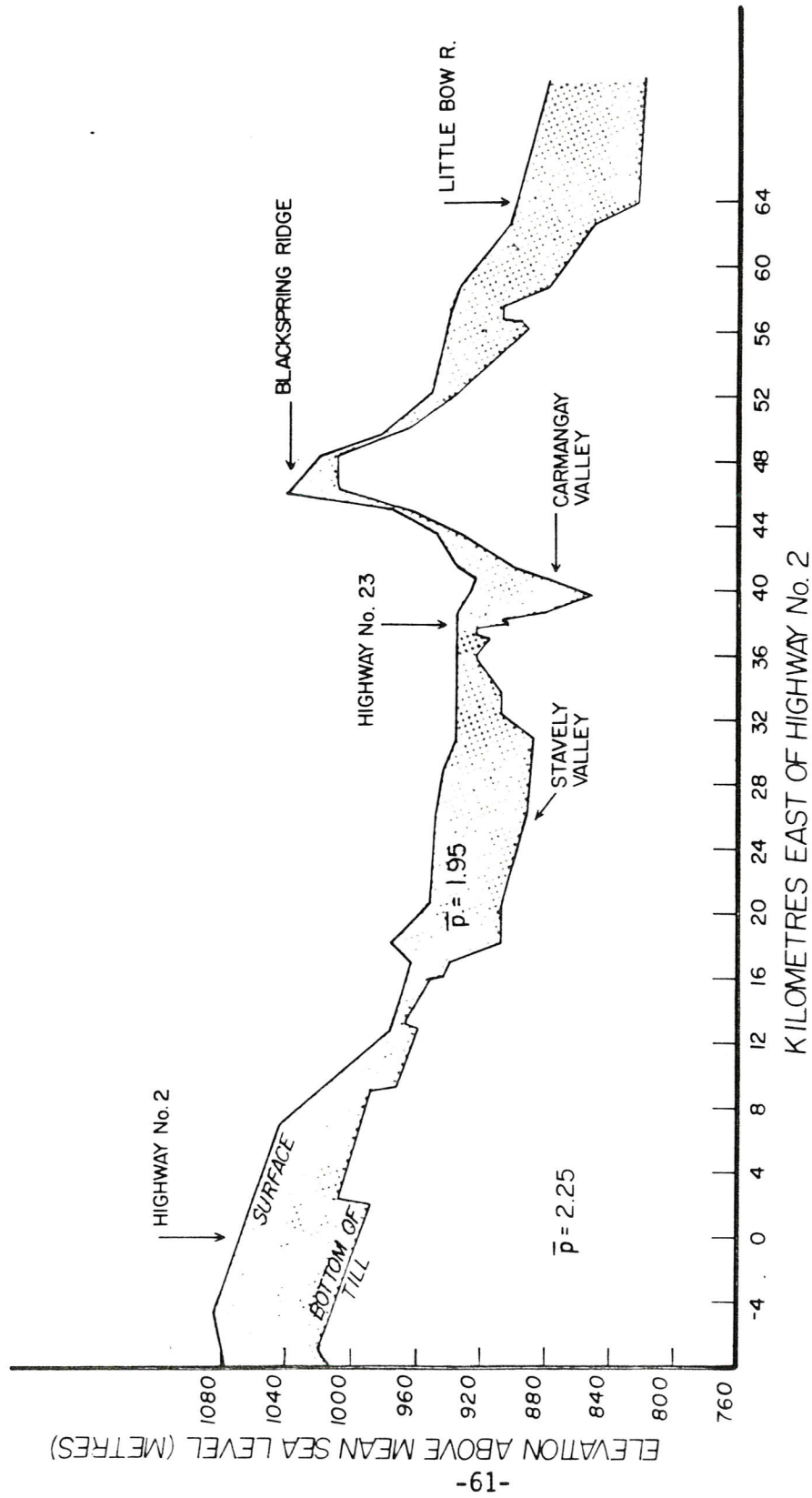
The first option, varying the structure, is the least reasonable in that control is greatest over the elevation data for the marker horizons. In addition, it was found that this approach was inadequate. Adjusting the marker horizons by the 100-metre elevation uncertainty resulted in maximum



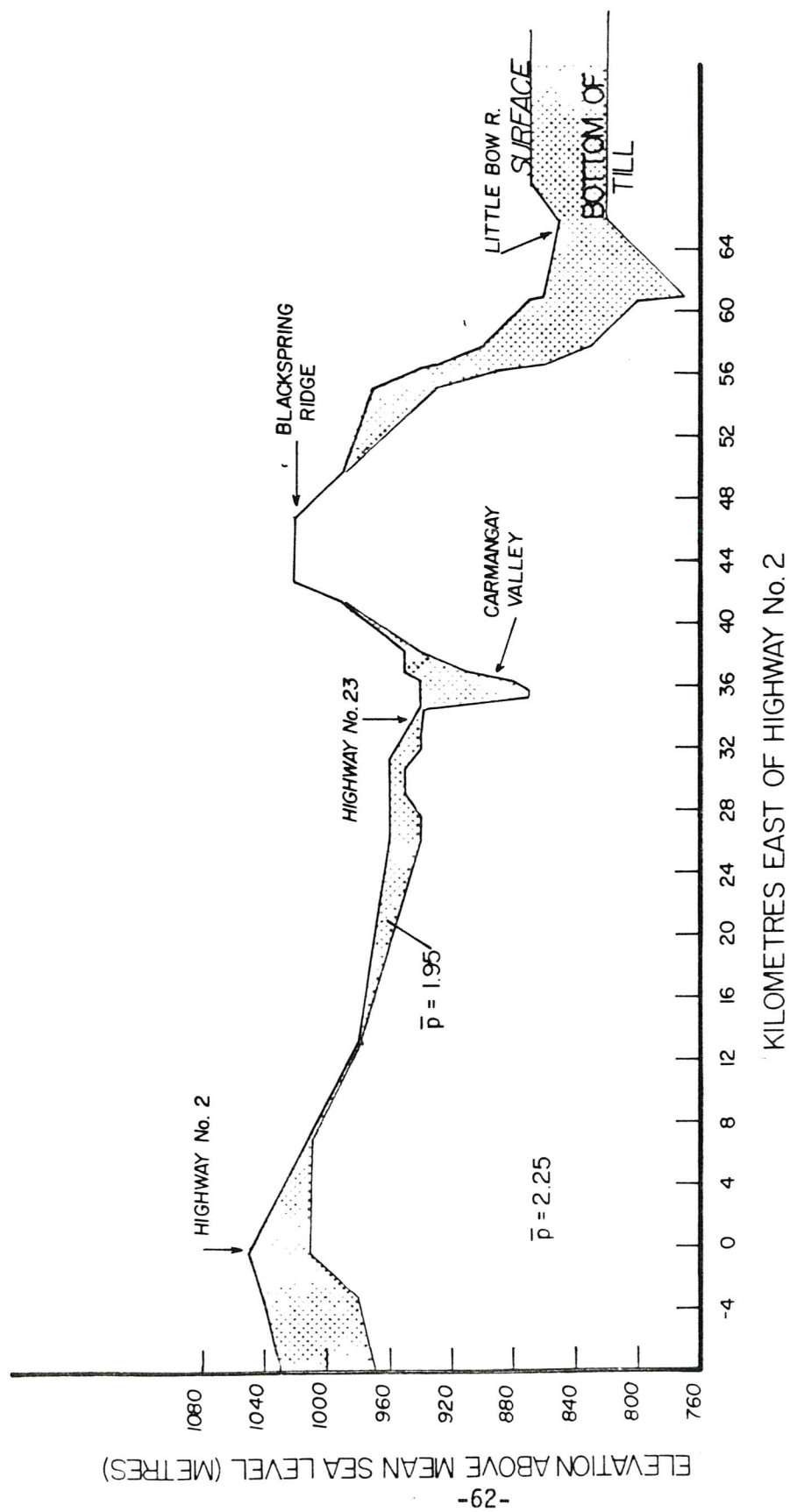
changes of only 15 g.u. in model output values, which are insufficient to reconcile the 50 g.u. discrepancies of the initial model.

Increased detail was gained in two ways. Firstly, a greater sampling frequency of depth data was taken. Secondly, an additional layer was added to the model which represents the thickness of Quaternary surficial deposits above bedrock. In general, this layer is made up of glacial till and alluvial outwash gravel deposits. Data for the thickness profile of this layer were obtained from the Alberta Research Council, (Geiger, 1967), which has published maps of bedrock structure contours for the area. The large scale profiles in figures 5.10a, b, and c are constructed from data in Geiger's map and topographic maps from the Department of Energy, Mines and Resources. These profiles indicate that the pre-Pleistocene topography in the study area includes paleo-stream valleys which cross the profile lines and have been infilled with as much as 70 metres of Quaternary till deposits. A density of 1.95×10^3 kg/m³ was assigned to these till deposits after Trott, (1981).

The density structure of the clastic wedge was varied by dividing layers into density regimes or prisms with assigned values representative of the average bulk density in that area of the profile. The upper and lower Cretaceous clastic layers in each profile were individually divided into approximately twelve prisms of 3 to 12 kilometre east/west extent.



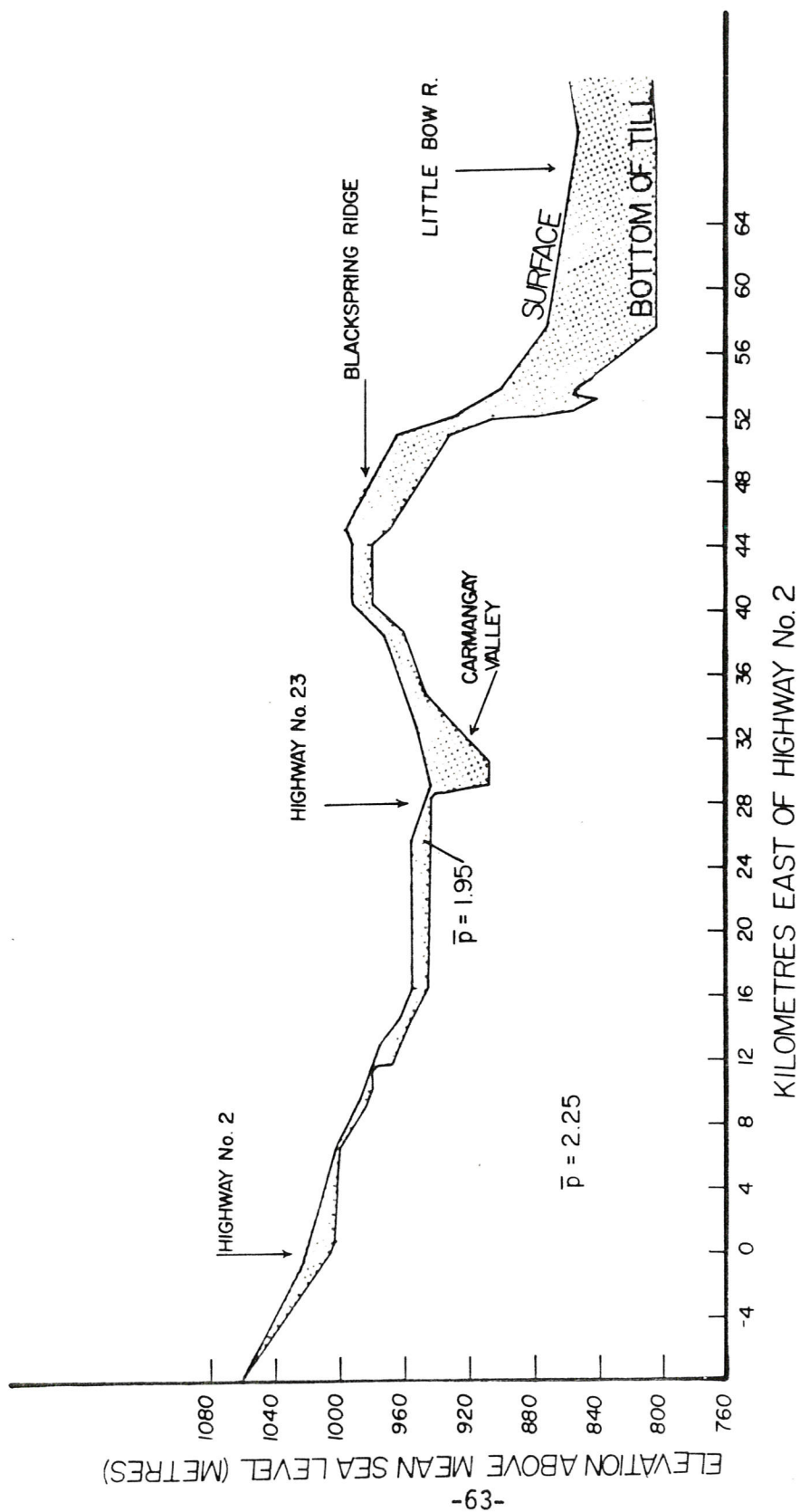
ELEVATION AND SURFACE DEPOSITS PROFILE - CARMANGAY
 VERTICAL EXAGGERATION 100X
 Figure 5.10a



ELEVATION & SURFICIAL DEPOSITS - CLARESHOLM PROFILE

Figure 5.10b

VERTICAL EXAGGERATION: 100 x



ELEVATION & SURFICIAL DEPOSITS - BARONS PROFILE

Figure 5.10c

VERTICAL EXAGGERATION - 100 x

Gravity modelling was undertaken by means of a program written by Talwani, et. al., (1959). This program calculates the summed effect of all density prisms in the profile at each gravity station for comparison to field data. The modelling process is iterative, and involves varying the density of each prism from the initial, laterally-constant average value. The result is a model with many prisms of differing densities which generates a response which is in agreement with the residual Bouguer anomalies. The criteria for density variations were:

- (1) Relative difference between values of residual Bouguer anomalies and model output.
- (2) Wavelength of anomaly.
- (3) Amplitude of anomaly.

The relative difference between values indicates whether density values must be increased or decreased to achieve agreement. Anomaly wavelength is influential in that process since it is directly proportional to the depth of the anomaly source; thus long wavelength discrepancies generally call for deep source adjustment. Anomaly amplitude is indicative of the magnitude of density adjustment required.

In this study, Paleozoic carbonate density was assumed to be constant for two reasons. Firstly, well logs show the density of this sequence to be nearly constant from top to bottom. Secondly, the largest variation reasonably expected,

($\pm 0.10 \times 10^3 \text{ kg/m}^3$), would generate very low frequency, low amplitude anomalies due to the depth of the density variation. These anomalies would be negligible when compared to those generated by the clastic wedge. In the process of modelling, the validity of such a constant-density assumption was investigated by varying the density of large, (3 to 5 kilometre width), sections of Paleozoic carbonate material within a $\pm 0.10 \times 10^3 \text{ kg/m}^3$ range. Such density variations generally resulted in Bouguer variations at the surface of less than 10 g.u. which lies within the range of uncertainty caused by till layer variations and elevation error.

An attempt was made to check prism density data in the final model against data from wells in the respective prisms. This check proved inconclusive due to the large uncertainty associated with average densities estimated from well logs in this area. The uncertainty from well logs is at least $\pm 0.05 \times 10^3 \text{ kg/m}^3$ and the entire range of density values is a little more than twice this figure. Thus, average densities from well logs are too uncertain to reflect the density structure indicated by gravity data. An example of well log density data is shown in figure 5.11, and figure 5.12 illustrates the general density variation with depth in the area.

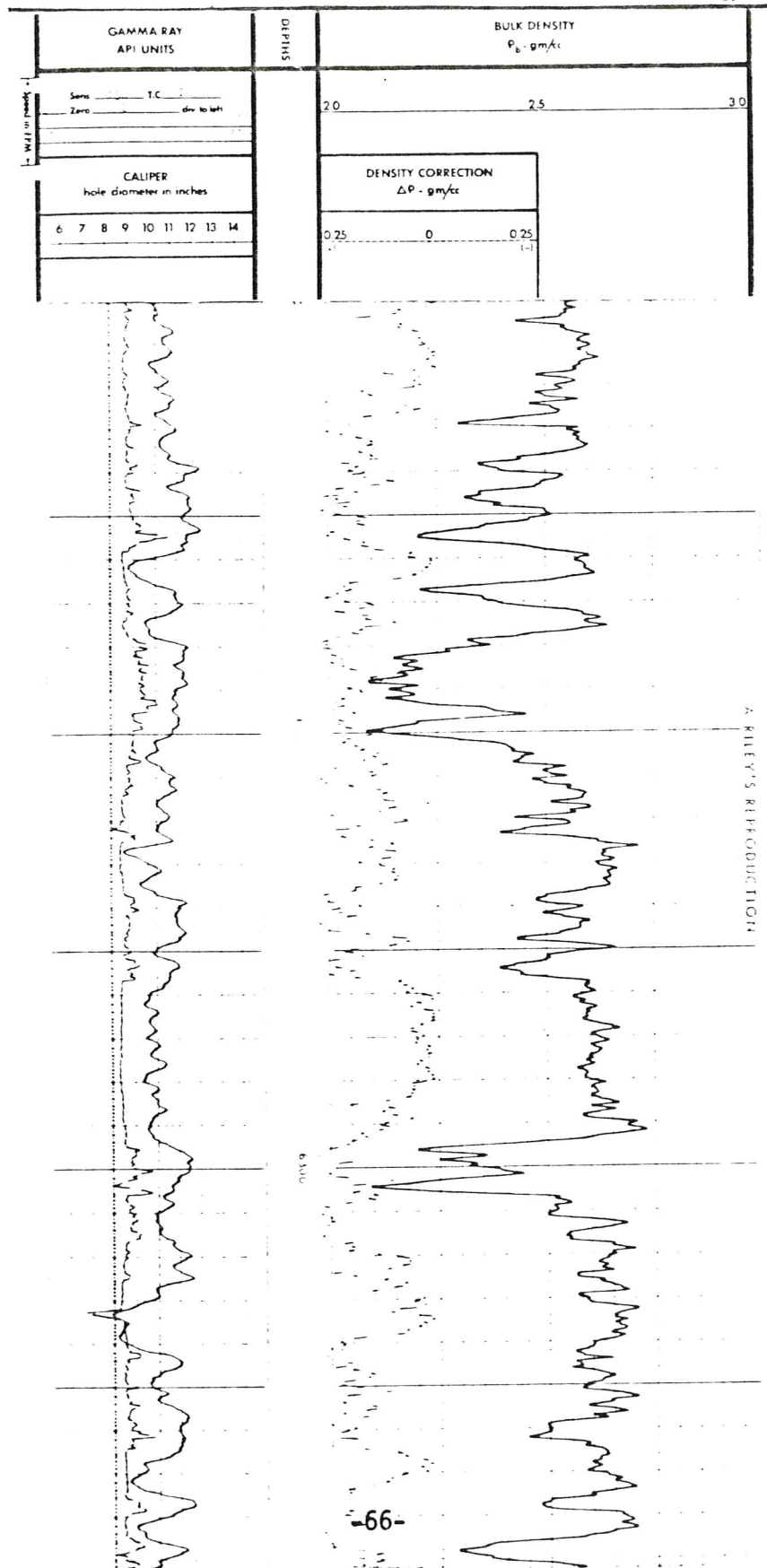
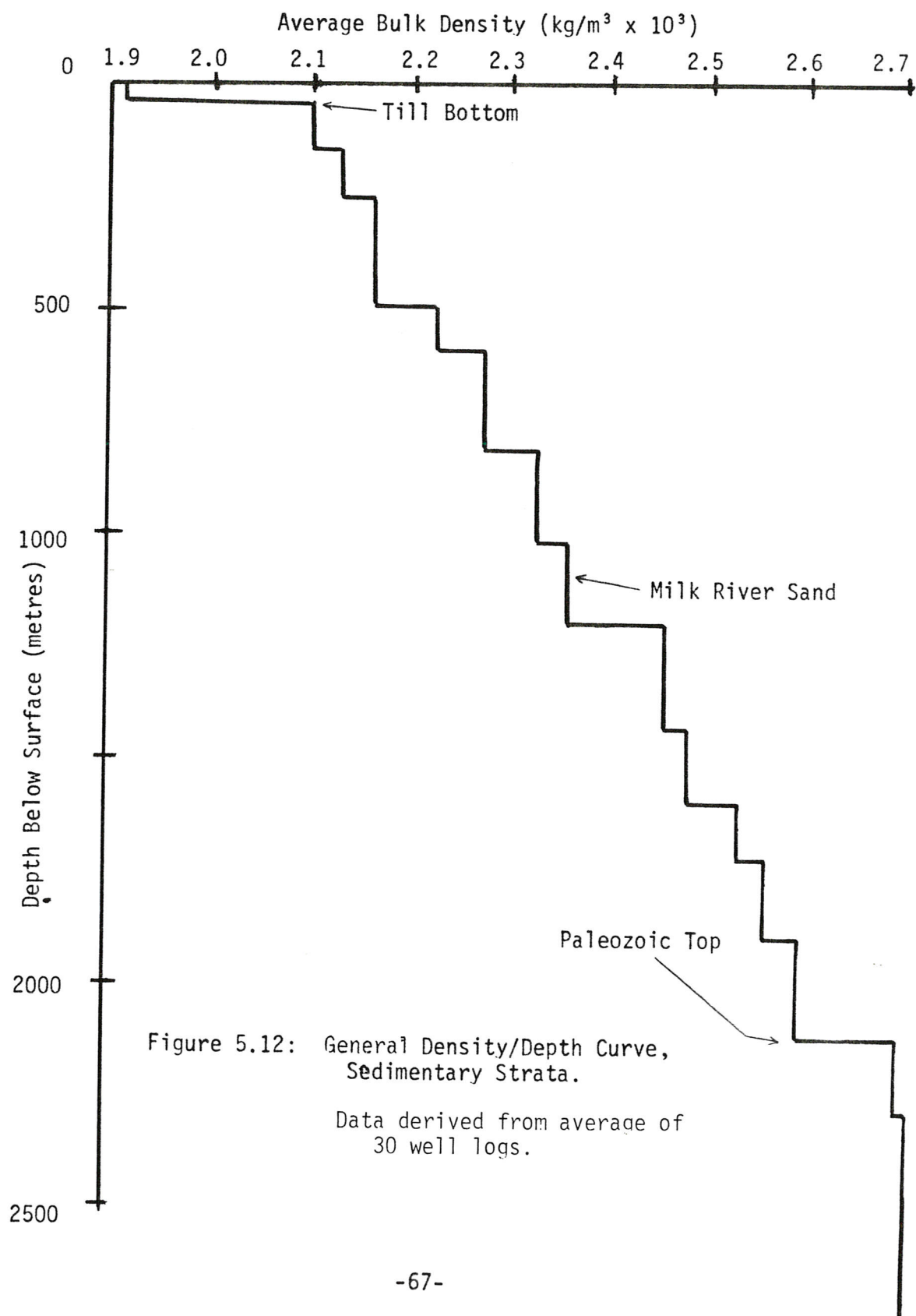


Figure 5.11: Example of Variable Density Data in Lower Cretaceous Sequence.



5.2.4: Description of the Final Models.

Figures 5.13, 5.14, and 5.15 show the final cross-sectional models and comparisons of field data and model response. In general, these profiles show structure similar to that seen in the initial models, but with additional complexity due to increased detail and due to the addition of density structure within the clastic wedge. The Carmangay profile shows the basement surface at an elevation ranging from 1,800 to 3,000 metres below sea level and overlain with approximately 1,400 metres of Paleozoic carbonate strata and 1,400 to 2,600 metres of Cretaceous and Tertiary clastics. The Precambrian basement and Paleozoic carbonate tops are nearly parallel and fault throws at both surfaces are within 20 metres of each other. The upper Cretaceous Milk River Sand surface is characterised by more subtle changes in contrast to the Paleozoic carbonate and Precambrian basement tops, and in places throws are 60 metres less at this horizon than at deeper horizons. The Claresholm profile is similar, but shows more complex topography due to additional faults and more subtle topography due to smaller fault throws. The Precambrian basement in this profile is, on the average, higher than in the Carmangay profile. The Barons profile shows the basement at an elevation of nearly 3,200 metres below sea level at one point near kilometre 12. A more constant dip is evident here in all horizons due to the fact that only six faults are evident.

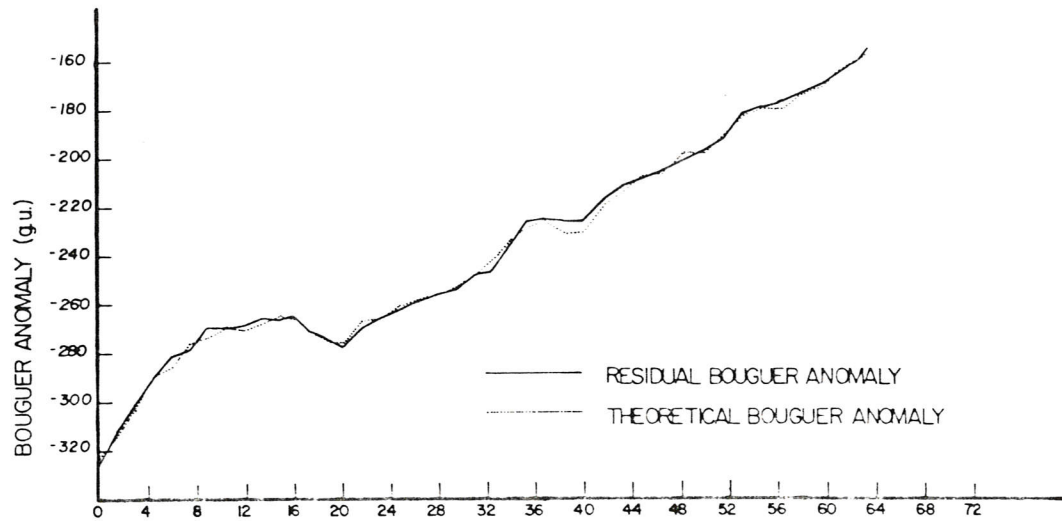
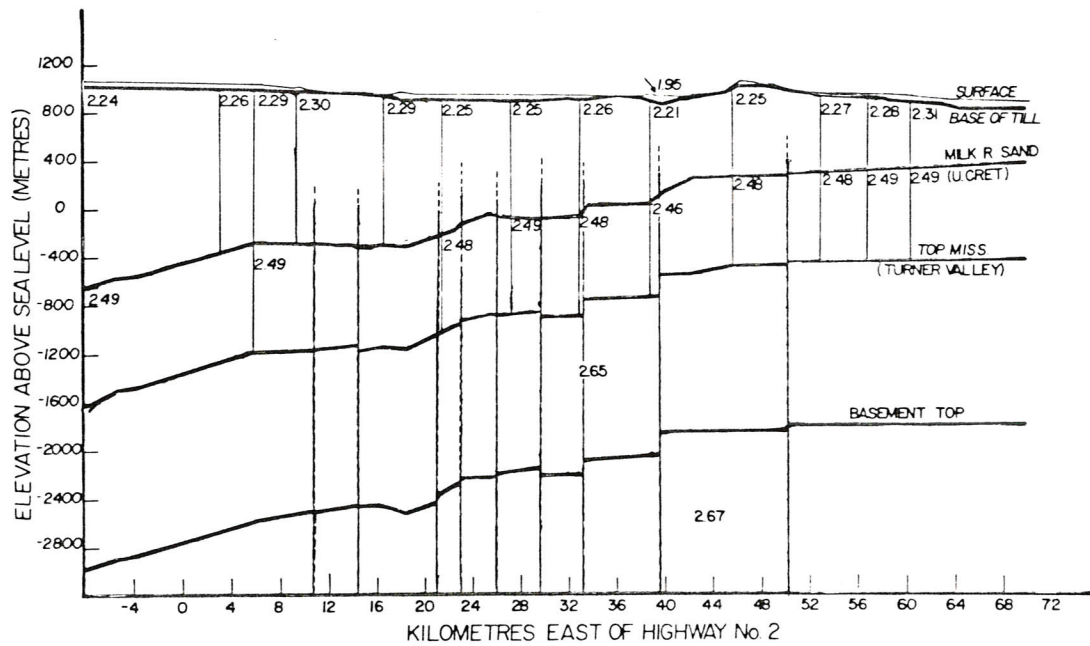


Figure 5.13a KILOMETRES EAST OF HIGHWAY No 2
RESIDUAL BOUGUER ANOMALIES CARMANGAY PROFILE
 (FIELD DATA & MODEL OUTPUT)

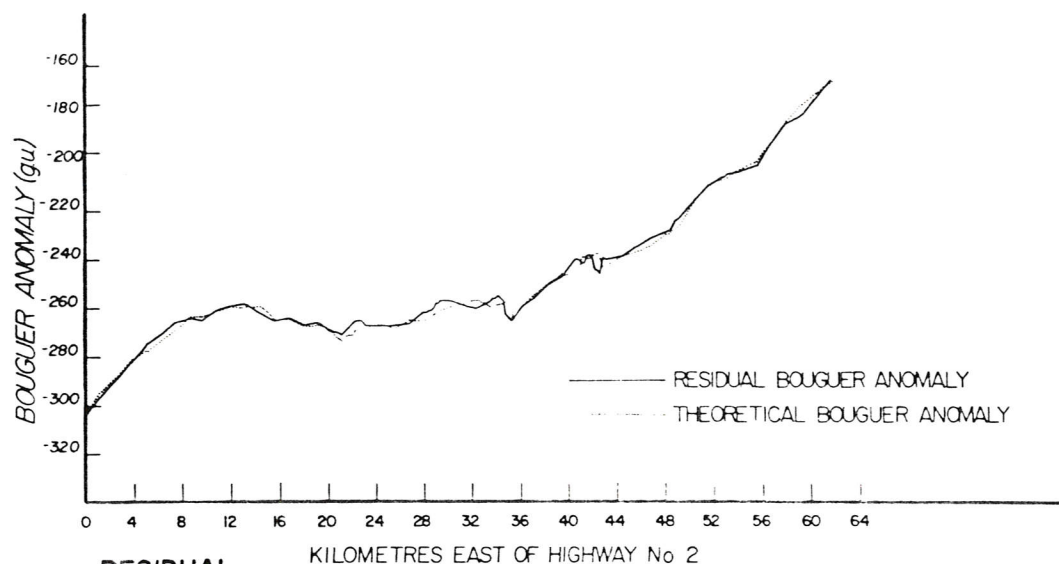


(2.25): PRISM AVG. DENSITY
 IN ($\text{kg}/\text{m}^3 \times 10^3$)

CARMANGAY DENSITY MODEL

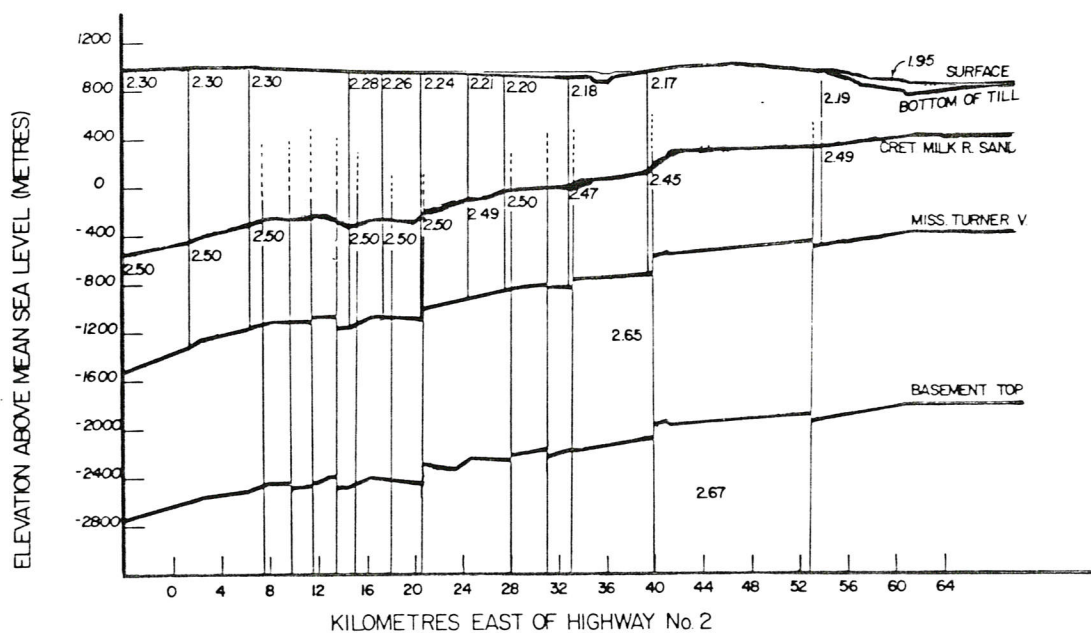
VE = 10x

Figure 5.13b



RESIDUAL BOUGUER ANOMALIES
FIELD DATA & MODEL OUTPUT - CLARESHOLM PROFILE

Figure 5.14a

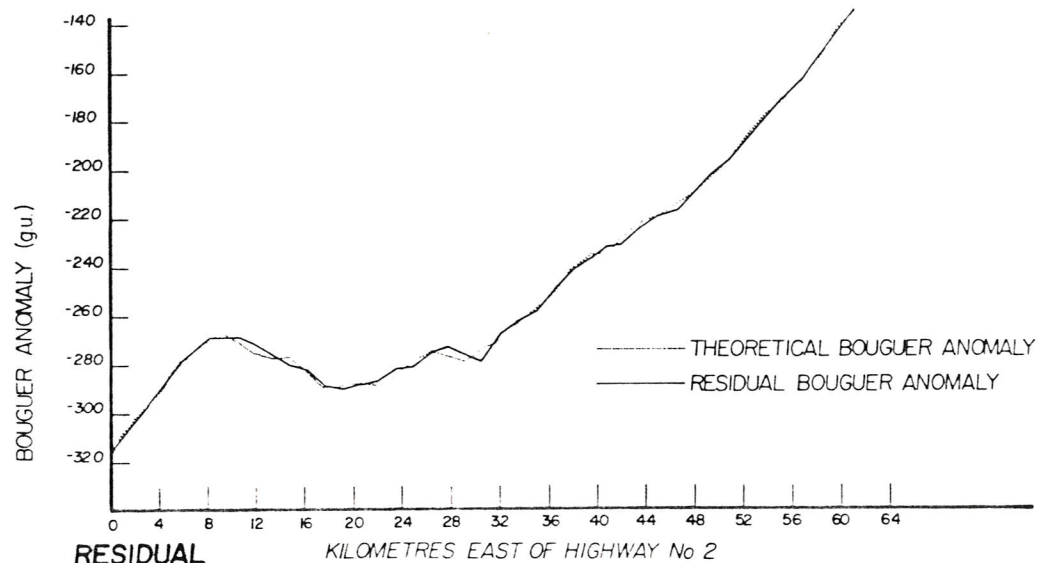


CLARESHOLM DENSITY MODEL

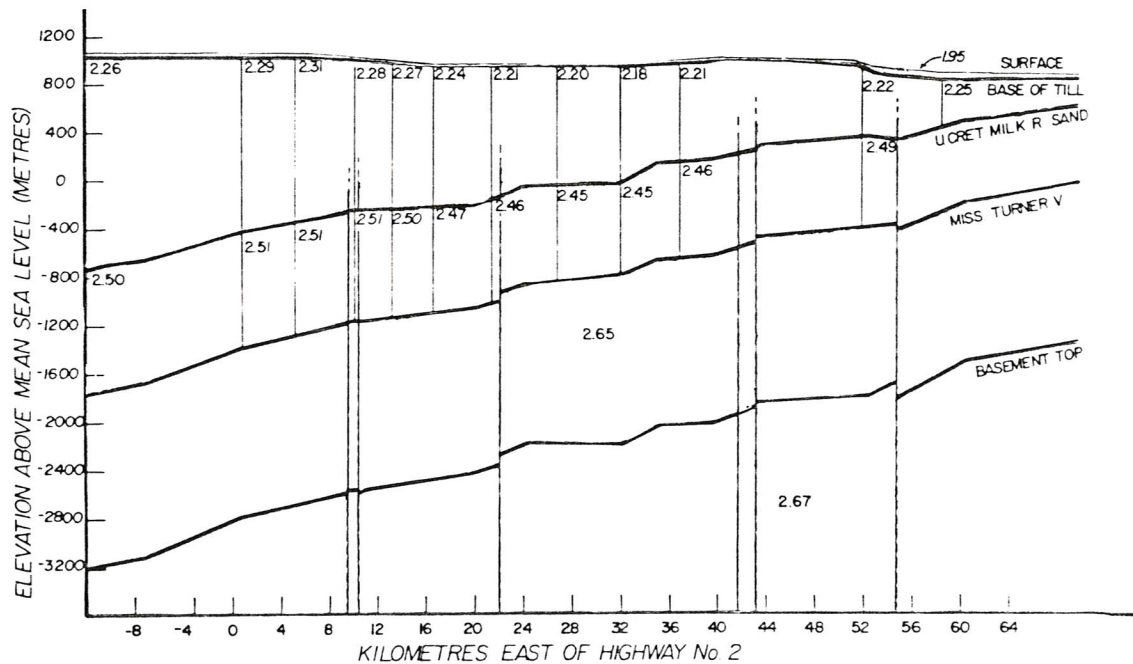
Figure 5.14b

VE = 10x

2.25: PRISM AVERAGE DENSITY
 IN ($\text{kg}/\text{m}^3 \times 10^3$)



RESIDUAL
BOUGUER ANOMALIES
FIELD DATA & MODEL OUTPUT—BARONS PROFILE
Figure 5.15a



BARONS DENSITY MODEL - (2.21) PRISM AVG DENSITY ($\text{kg/m}^3 \times 10^3$) V.E = 10x

Figure 5.15b

The density structure of the models indicates density variations of as much as $0.13 \times 10^3 \text{ kg/m}^3$ across the length of a profile in the upper Cretaceous clastic layer. The lower Cretaceous clastic layer shows less variable densities, as little as $0.03 \times 10^3 \text{ kg/m}^3$ across a profile. In the Carmangay profile, (see fig. 5.13b), two areas of high density are evident near kilometre 14 and at the eastern end of the profile. A low density area is evident near kilometre 40. Density values range from 2.21 to $2.31 \times 10^3 \text{ kg/m}^3$ in the upper Cretaceous clastics and between 2.46 and 2.49×10^3 in the lower Cretaceous clastics. The density pattern in the Claresholm cross-section, (see fig. 5.14b), shows upper Cretaceous clastic densities decreasing from west to east from 2.30 to $2.17 \times 10^3 \text{ kg/m}^3$. Lower Cretaceous clastic densities are nearly constant at $2.50 \times 10^3 \text{ kg/m}^3$ in the western half of the profile, with a low density area between kilometres 32 and 52. In the Barons profile, (fig. 5.15b), both upper and lower Cretaceous clastic layers show an area of high density near kilometre 8. From this area, densities decrease until the vicinity of kilometre 36 and then increase to the end of the profile. Density values range between 2.18 and $2.31 \times 10^3 \text{ kg/m}^3$ in the upper Cretaceous clastics, and between 2.45 and $2.51 \times 10^3 \text{ kg/m}^3$ in lower Cretaceous strata.

Figures 5.16a, b, and c show 100-metre structure contours which have been constructed from elevation data in the final

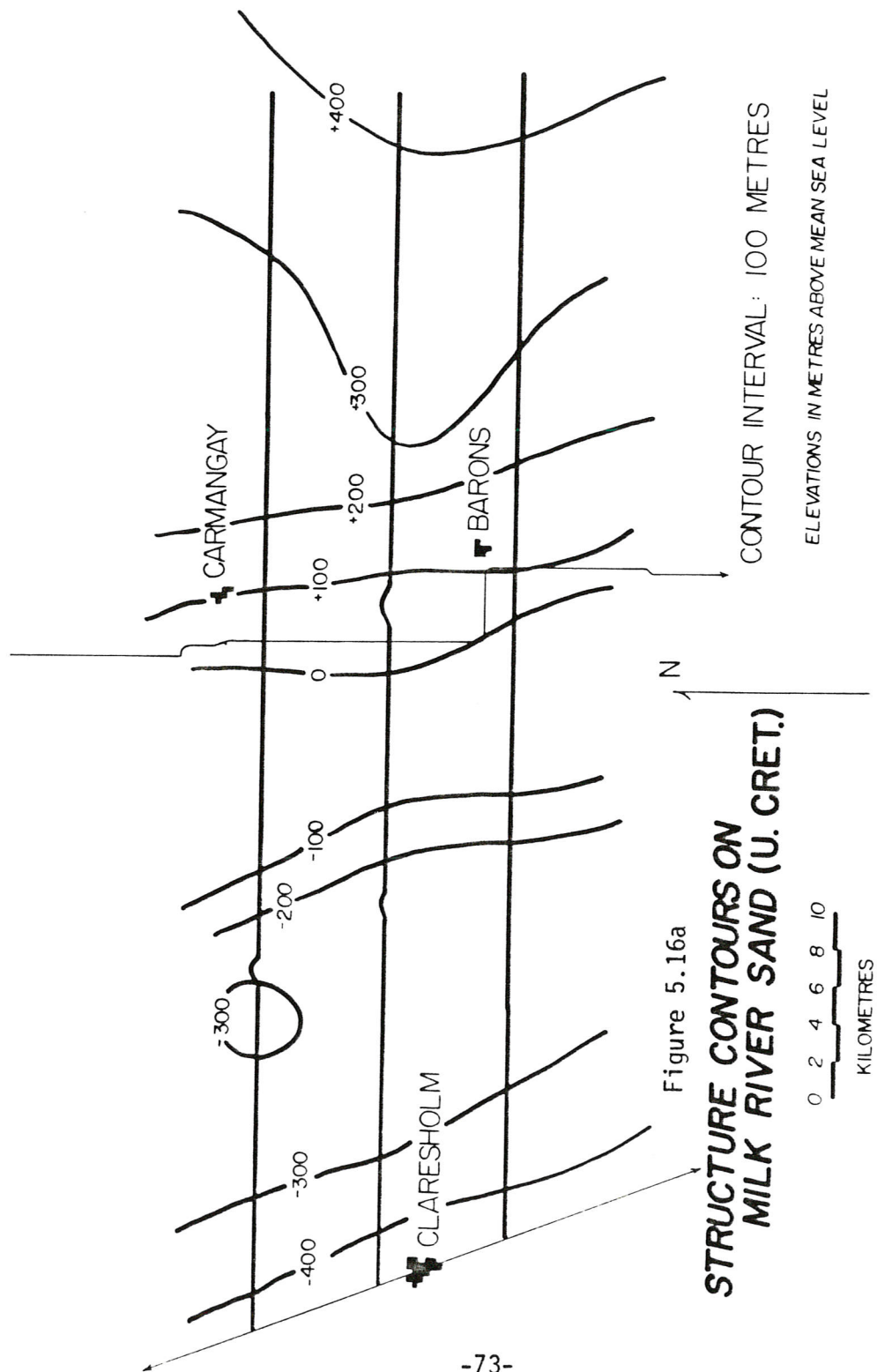


Figure 5.16a

STRUCTURE CONTOURS ON MILK RIVER SAND (U. CRET.)

CONTOUR INTERVAL: 100 METRES

ELEVATIONS IN METRES ABOVE MEAN SEA LEVEL

0 2 4 6 8 10
KILOMETRES

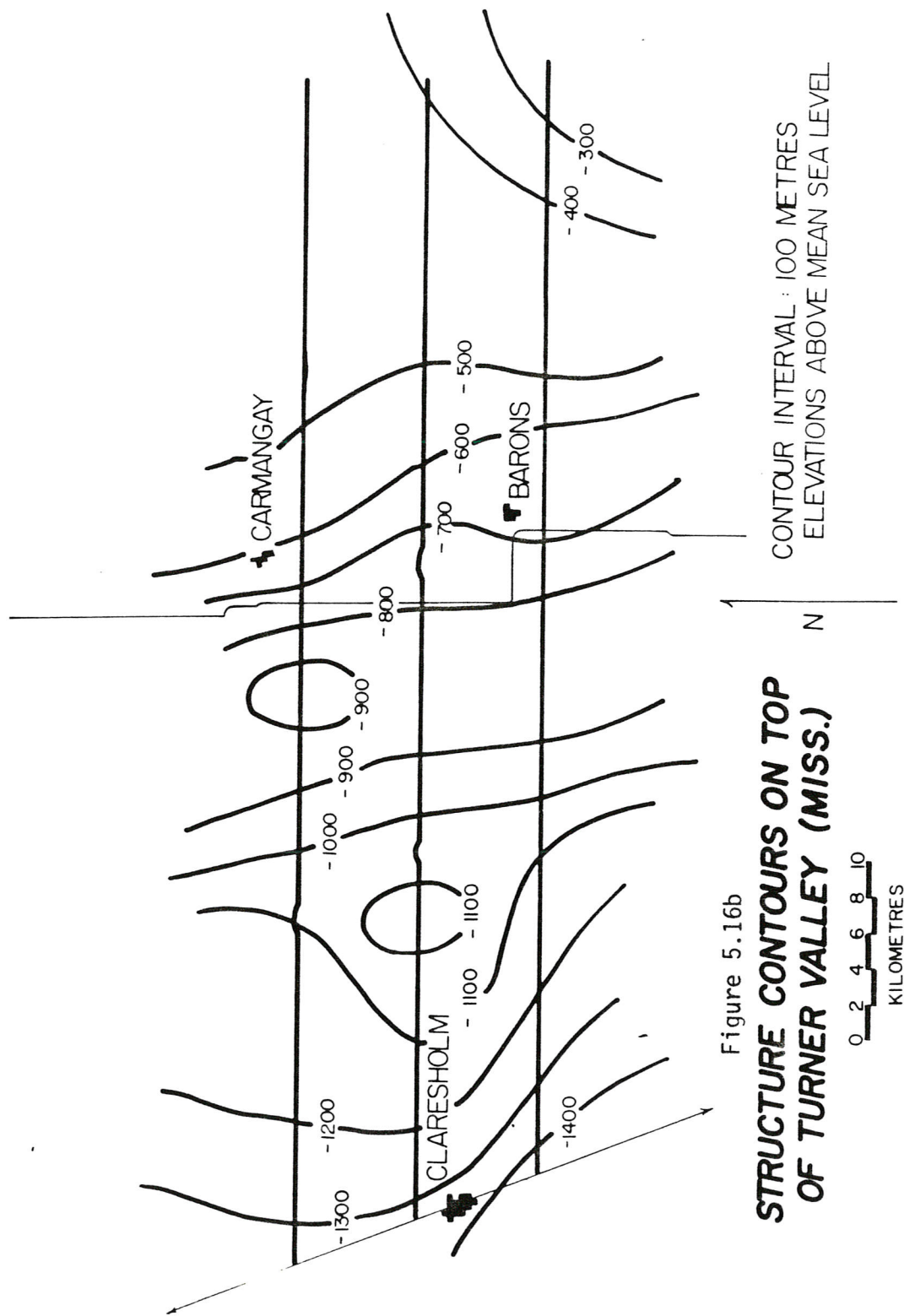


Figure 5.16b

STRUCTURE CONTOURS ON TOP OF TURNER VALLEY (MISS.)

CONTOUR INTERVAL : 100 METRES
ELEVATIONS ABOVE MEAN SEA LEVEL

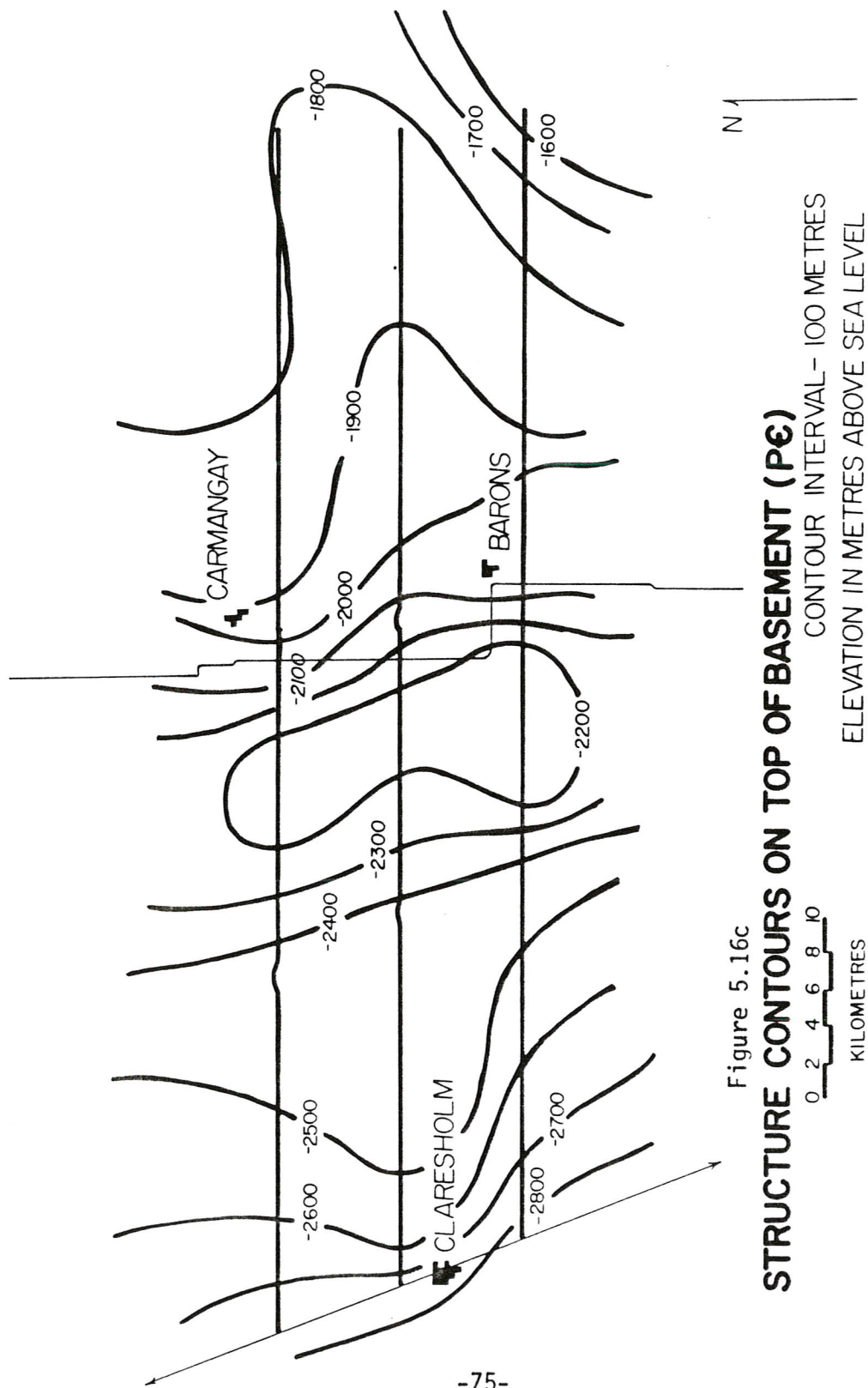


Figure 5.16c

STRUCTURE CONTOURS ON TOP OF BASEMENT (P6)

CONTOUR INTERVAL - 100 METRES

ELEVATION IN METRES ABOVE SEA LEVEL

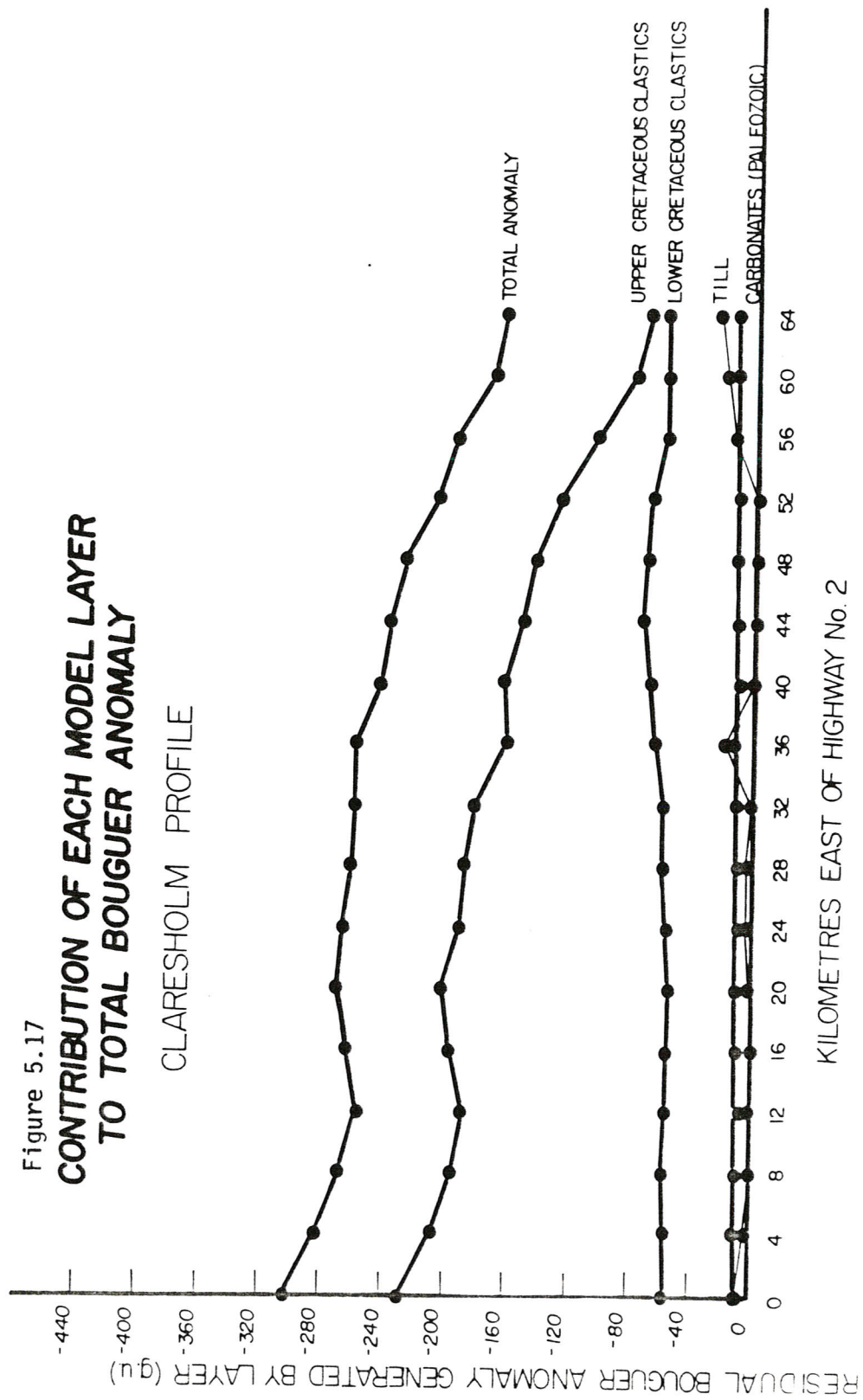
0 2 4 6 8 10
KILOMETRES

N

model profiles. A general northwesterly trend is characteristic of contours at all three stratigraphic levels, reflecting the transition between the Alberta basin to the west and the Sweetgrass Arch to the east. Structure contours on the upper Cretaceous Milk River Sand show high areas northwest of the towns of Claresholm and Barons. The variable spacing of the structure contours indicates a step-wise change in elevation for this marker. The trend of structure contours on the Mississippian Turner Valley top is less consistent. High areas are noted west of Carmangay and in the vicinity of the Claresholm gas field, 12 kilometres east of Claresholm. The step-wise elevation changes are seen here, also, as in the basement where contours near the ends of the profiles depart from the north-northwesterly trend common in the younger strata.

A gravity analysis of the final models was undertaken to determine the contribution of each stratigraphic layer to the total Bouguer anomaly. Typical results of this analysis are shown in figure 5.17 for the Claresholm line. The approximate contribution for each layer, in percent, is:

Quaternary Till Layer	:	3
Upper Cretaceous Clastics:		64
Lower Cretaceous Clastics:		29
Paleozoic Carbonates	:	4



5.2.5: Error Limits on the Density Interpretation.

Due to limited computer program capacity, the models cannot be divided into an unlimited number of prisms in order to achieve a perfect fit of model data to residual Bouguer data. Rapid changes in density over a short area were necessarily contained within two or three bodies, thus density figures for prism centres are more accurate than those near the edges of the prisms where an abrupt density change is a poor approximation.

An attempt was made to achieve model to field data fit of within ± 3 g.u. This was achieved for more than 90% of the gravity stations. Most of the remaining stations were in areas of high frequency variation where further modelling would only result in changes to near-surface densities. Likewise, refinement to agreement within ± 3 g.u. would require division of the till layer into density prisms and would provide no additional information about deeper structure which is accurately modelled.

Accuracy of the density values relative to each other is estimated as $\pm 0.02 \times 10^3 \text{ kg/m}^3$ in upper Cretaceous clastic prisms and $\pm 0.04 \times 10^3 \text{ kg/m}^3$ in the lower Cretaceous clastics. These are the relative uncertainties in density values as the result of a structural uncertainty of ± 100 metres. By experimentation with the models it was found that density changes of this magnitude had a gravitational effect similar to a

100-metre change in the Turner Valley and Milk River Sand elevations at the centre of the profile. Increased and decreased depths to horizons at the ends of the profiles make these uncertainties greater to the west and slightly less to the east.

CHAPTER SIX - DATA INTERPRETATION

6.1 - Stratigraphic Interpretation.

6.1.1: General Stratigraphic Description.

Stratigraphic interpretation is based on isochron profiles which are seen in figure 5.6a, b, and c. The time-thickness profiles show the thinning of the upper Cretaceous clastics updip in the clastic wedge. The Paleozoic carbonate and lower Cretaceous clastic layers appear nearly uniform in thickness in these profiles, but since velocities generally decrease from west to east, true-thickness in reality also decreases slightly from west to east in the lower Cretaceous clastics. The time-thickness profiles for these layers also show rapid thickness variations. However, the amounts of time-thickness variation in the Paleozoic and lower Cretaceous layers are less than 30% of the large time-thickness changes seen in the upper Cretaceous clastic layer. The Claresholm profile is notably different from the Carmangay and Barons profiles in that the lower Cretaceous clastic layer here is thicker, and the Paleozoic carbonate layer thinner, than in the other two profiles.

6.1.2: Effect of Faulting on Sediment Thickness.

The effect of the movement of the faulted basement is seen

in figures 5.6a,b, and c, which show the time-thickness variations of the upper Cretaceous clastics. Also shown in the figures is the relationship of thickness to relative fault block motion. Here, a definite pattern of thickness variation is evident in the upper Cretaceous clastics. Significant, sharp increases and decreases in thickness are evident which represent anomalies with respect to the constant regional west to east thinning of the layer. Examples of anomalous areas of the thickness profiles are seen at kilometres 16 and 32 of the Claresholm profile, (fig. 5.6b), and kilometres 20 and 32 of the Carmangay profile, (fig. 5.6a). While these variations are most common and pronounced in the upper Cretaceous clastic sequence, they appear with lesser frequency and magnitude in the lower Cretaceous clastic and Paleozoic carbonate layers.

Thickness variations in the upper Cretaceous clastics are determined by the motion of basement fault blocks. Sharp variations in thickness occur consistently above fault block boundaries. The thickness of the upper Cretaceous clastics increases above relatively downthrown blocks, and conversely decreases over upthrown blocks. These variations are interpreted as having been caused by erosion and depositional infilling on the paleotopography induced by block faulting. These processes have transferred eroded sediment from the tops of upthrown blocks and deposited it on the adjacent lower blocks, resulting in a layer of variable thickness. The fact that thickness variations are not evident

in the lower Cretaceous clastic and Paleozoic carbonate layers indicates that these sequences were less affected by the basement tectonism; that is faulting was less common and severe during the deposition of these sequences. In places, an inverse relationship is evident between block motion direction and thickness, i.e., thickening over upthrown blocks, (kilometres 46-55, fig. 5.6c). This suggests that the faults were active during Paleozoic and lower Cretaceous deposition but that relative motion in some cases was the reverse of that which occurred during the late Cretaceous era.

6.2 - Structural Interpretation.

6.2.1: Vertical Extent and History of Faulting.

It is the relationship between block fault motion and sediment thickness variations which indicates that motion has occurred along basement faults as recently as the late Cretaceous era. Vertical extent, and thus the absolute age of this fault activity cannot be determined from examining the seismic sections alone, as the vertical continuity of the faults in seismic data is uncertain. Faults are easily identified in the Precambrian basement top and Paleozoic carbonate top where they result in discontinuity of seismic events and diffraction patterns. However, higher in the sections, discontinuities are replaced by smoother, continuous transitions between arrival times. This change in

transition character can be interpreted in two ways: (1) By sedimentary drape of clastic Cretaceous strata over topographically-reflected fault motion prior to deposition, or (2) By faulting of clastic Cretaceous strata in response to basement motion subsequent to deposition. Lower Cretaceous clastic strata show little thickness variation which is consistent with the latter interpretation. Variations in the upper Cretaceous clastics thickness are consistent with the first interpretation, thus fault motion occurred probably after deposition of the upper Cretaceous Milk River Sand formation.

Fault throws across the Precambrian basement top and the Mississippian Turner Valley top are nearly the same for most faults. Fault throws were calculated from average velocities of 3,000 m/s in the upper Cretaceous clastics, 3,300 m/s in the lower Cretaceous clastics, 6,100 m/s in the Paleozoic carbonates, and the arrival time difference across the fault. Elevation changes of the Milk River Sand event are calculated to be 20 to 40 metres less than those deeper in the section. The equivalent Precambrian and Paleozoic fault throws indicate that the basement and Paleozoic carbonates were faulted simultaneously in most places. Therefore, the faults were generally inactive during the Paleozoic, if they existed at that time. The reduced fault throws across the upper Cretaceous clastic strata indicate a growth-fault nature of recurrent activity in the upper Cretaceous.

The general strike direction of the faults is 330 degrees, (see section 6.2.2), and this closely parallels the strikes of the major thrust planes caused by tectonic foreshortening in the Rocky Mountains, (McCrossan, 1964). These thrust sheets begin only 50 kilometres to the west of the study area and the parallelism of regional tectonic features here suggests a common genesis and age. These data further support the interpretation of late Cretaceous motion along the faults.

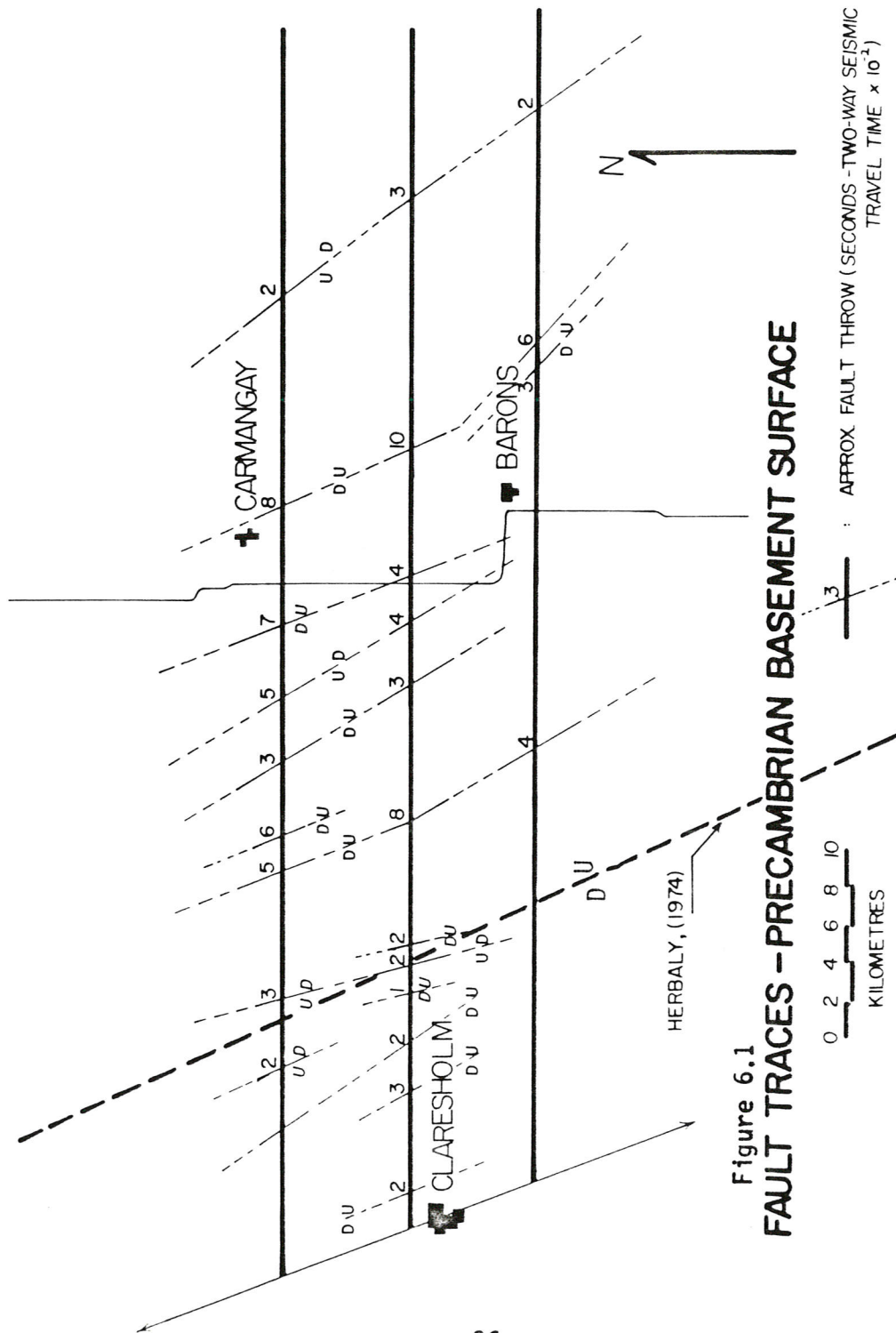
A synoptic history of the basement faults in the Claresholm area, based on results of the study, assumes initial formation of the faults in the late Precambrian uplift, (McCrossan, 1964). The faults were generally inactive until the end of the Paleozoic when reactivation displaced both the Precambrian surface and the Paleozoic carbonate sequence. The faults then remained inactive during the deposition of the lower Cretaceous clastics, allowing deposition of a rather uniform layer. Tectonism associated with Laramide overthrusting to the west reactivated the faults, which cut the lower Cretaceous strata. The Paleotopography created by this reactivation during deposition of the upper Cretaceous clastics has determined the thickness variations in the upper Cretaceous strata.

6.2.2: Active Length and Orientation of Faulting.

A study of the known locations of faults was undertaken to determine the active length of these vertical faults. Rel-

ative movement and fault throws were compared between lines to determine if specific faults are continuous between profiles. A large fault appears in all three sections beneath the area of the Blackspring Ridge. This fault was interpreted to trend northwest/southeast throughout the profiles on the basis of its larger throw and characteristic associated listric faults in the Cretaceous clastics above, (see fig. 5.2). Other faults were interpreted to be continuous across the three profiles on the basis of throws and similar relative motion seen in each section. Another factor which tends to confirm the continuity of these faults is that fault trace intersections with the profiles form nearly straight lines on a map of the study area, which strongly suggests linear continuity.

A map is shown in figure 6.1 which shows the interpreted system of parallel faults. The faults range in size from a throw of more than 300 metres, (kilometre 41, figure 5.6b), to faults with very little net relative motion. These values were obtained using the same velocities as in section 6.2.1. The trend of these faults is very consistent, varying only between 310 and 345 degrees. The average is approximately 330 degrees. This trend is in agreement with published maps by Herbaly, (1967), which show a single fault with similar trend which crosses the study area. This fault cuts the Cambrian, Devonian, and Mississippian carbonates, was interpreted from evidence based on fluid contacts in reservoir rocks, and is



also indicated in figure 6.1.

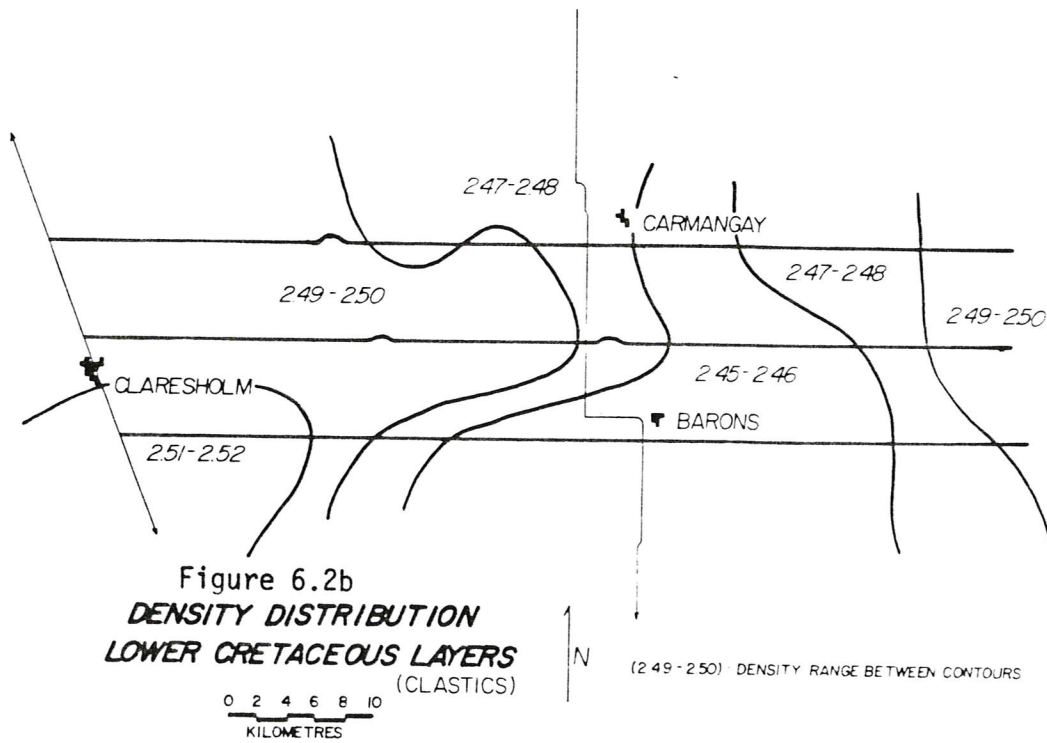
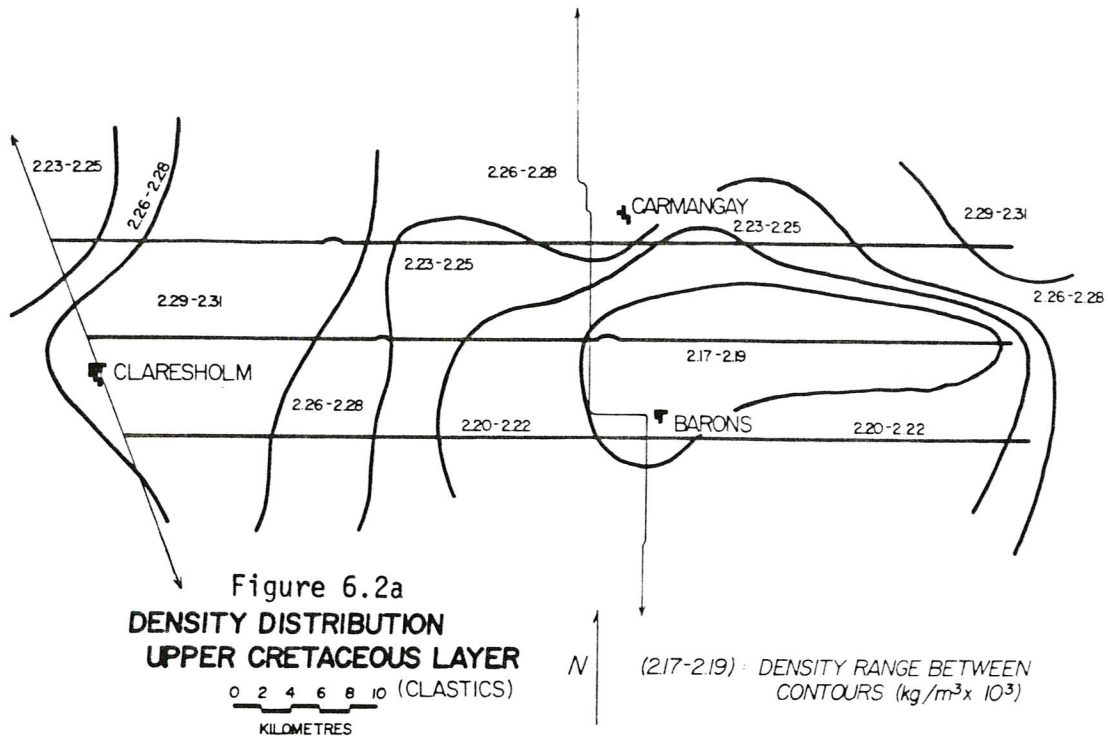
Fault throws along individual faults are in some cases very consistent, but in others vary quite substantially, indicating in the latter case that some degree of rotation or other differential motion occurred. Faults are shown to be as much as 15 kilometres in northwest/southeast extent. However, many faults seen in the northern two profiles die out before reaching southward to the Barons profile.

6.3 - Density Variation Interpretation.

6.3.1: Description of Density Structure.

Density data from prisms in the three profiles were used to construct maps of density distribution within the upper and lower Cretaceous clastic sequence. These maps, (figure 6.2), show contours which divide areas of different subsurface density.

The upper Cretaceous clastics maps, (fig. 6.2a), show a circular area of lower density sediments which covers the eastern two-thirds of the study area. This low density area is flanked on the west by north-south trending areas of varying density. Moving west, these areas increase to their highest density near the beginning of the surveyed profiles and then decrease in value.



The lower Cretaceous clastics map of figure 6.2b shows an area of higher density clastics at the east end of the Barons profile. To the east of this, roughly north-south trending areas decrease in density value to a minimum at about kilometre 40 and then begin increasing again.

6.3.2: Effect of Faulting on Sediment Density Variation.

Block faulting affects both depth of burial and thickness of Cretaceous layers by vertical movement of strata. These variables, in turn, affect the density of a given layer. The map patterns and values seen in figure 6.2a and b suggest a relationship between fault-structure and sediment density variations in that the contour trends parallel fault trends and areas of increasing depth and thickness tend to be areas of higher density. In the western half of the study area, densities increase toward the west in the upper Cretaceous clastics in accordance with the increasing structural depth evident from structure contours. The broad, low-density area in the eastern half of the upper Cretaceous clastics map coincides with the structurally high area here. Only a general relationship is seen here, and the anticipated changes in density over local structural highs and lows are not evident in the density distribution maps.

To investigate these structural/stratigraphic relationships, graphs were made of prism average bulk density vs. prism average

thickness, and of prism average bulk density vs. prism centre depth, for prisms in both the lower and upper Cretaceous clastic layers. These graphs are seen in figures 6.3 and 6.4. A general relationship between increasing depth or thickness and increasing density is evident. While this trend appears somewhat linear when certain sections of the profiles are considered, the overall scatter of the data is too great to allow any quantitative conclusions to be made. The cause of these density variations is interpreted to be the basement faulting process which controls variations in depth and thickness. Increases in both of these variables cause an increase in average density due to compaction in response to additional depositional load. The scatter of the data illustrates that this variable stratigraphic load is not the only factor which affects prism average bulk density. Varying sedimentation patterns and differential compaction probably have also affected densities throughout the sections.

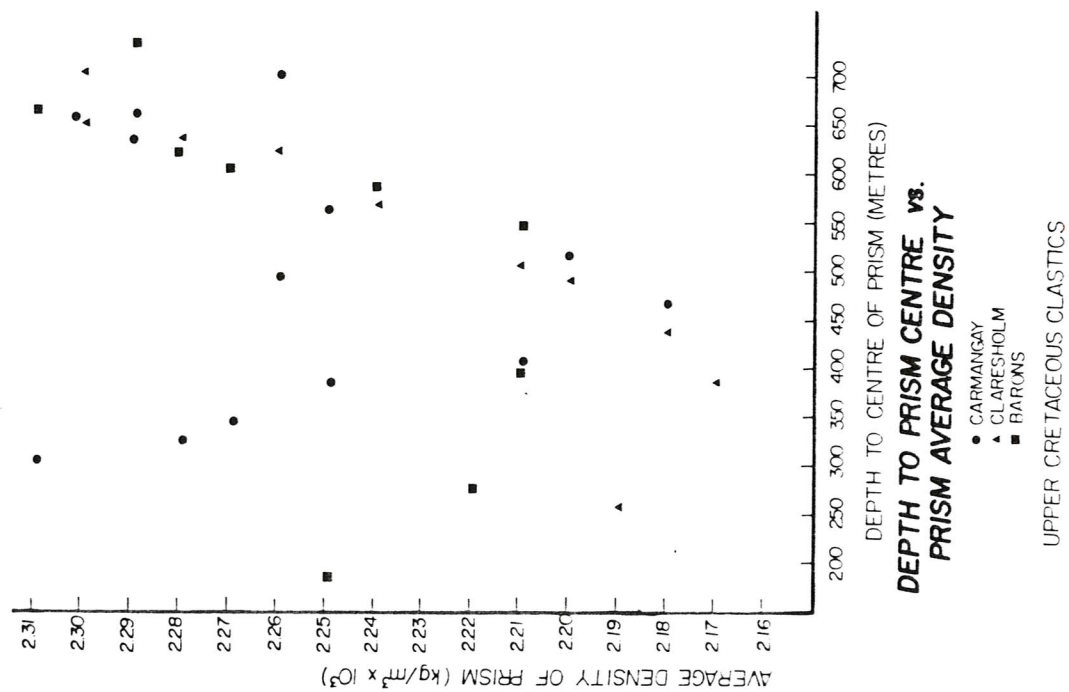


Figure 6.3a

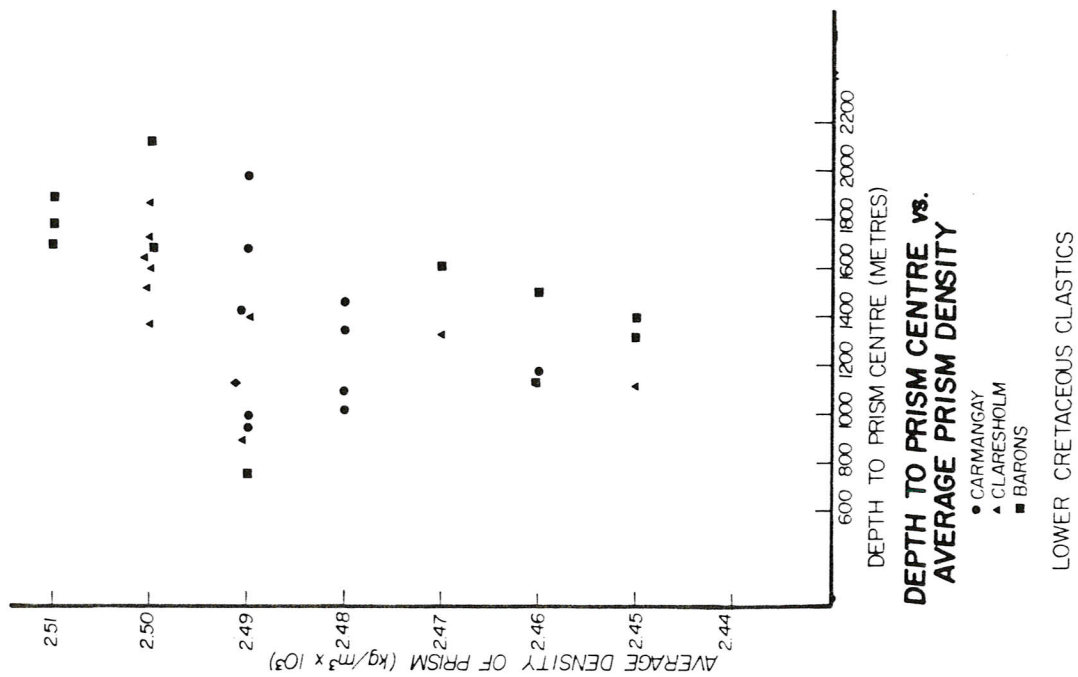
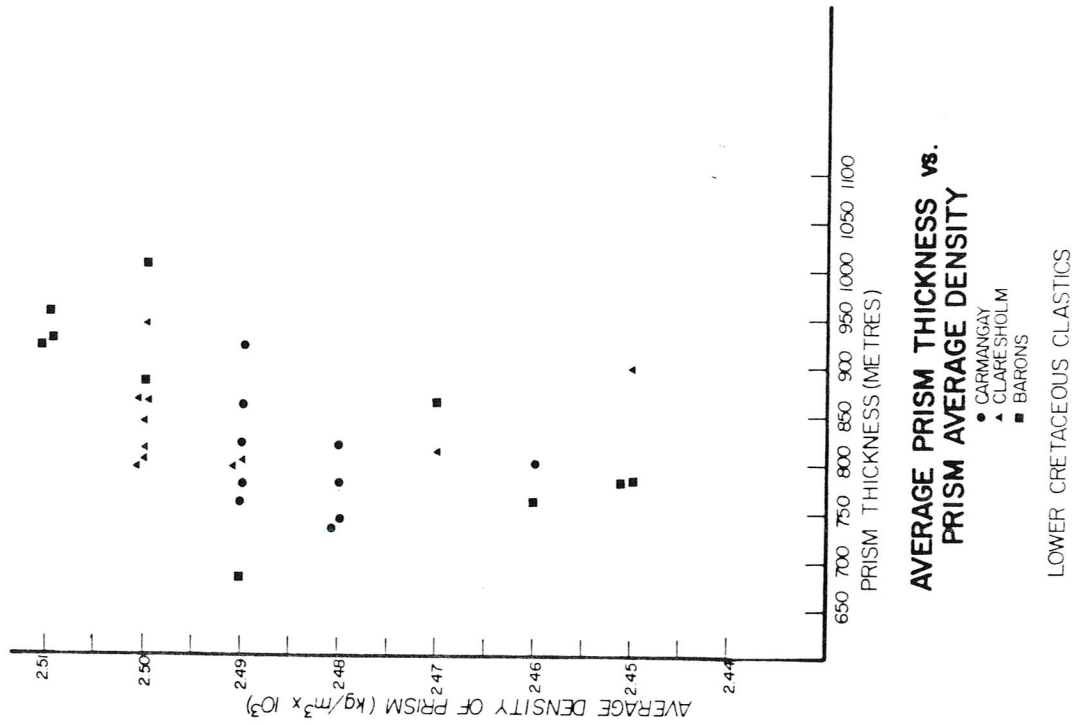
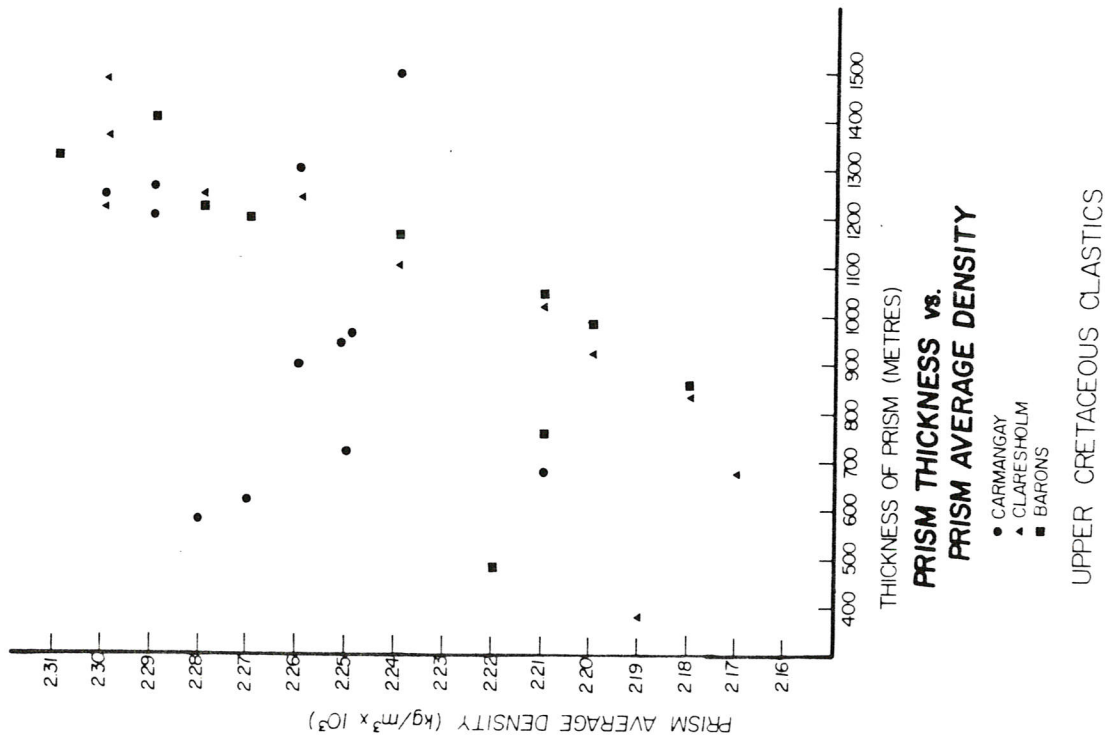


Figure 6.3b



CHAPTER SEVEN - CONCLUSIONS

7.1 - Summary.

The Claresholm gravity survey was conducted in an area where detailed control data were available from seismic profiles and well logs. Access to these data made possible a more in-depth study of the geologic structure of an area of southern Alberta than would otherwise have been possible. This integrated study allows the following conclusions to be made:

Relative Bouguer anomaly data in the Claresholm area exhibit variations which must be interpreted not only in terms of Precambrian basement block faulting, but also in terms of a variable density structure within the overlying Mesozoic clastic wedge. Models interpreted from integrated data indicate basement fault block structure including faults with throws of up to 300 metres, and upper Cretaceous clastic density variations of as much as $0.13 \times 10^3 \text{ kg/m}^3$ within an area of 60 x 13 kilometres. Both of these geologic variations contribute to the observed gravity anomaly and one cannot be considered apart from the other without access to independent information about basement depth or Cretaceous density variations.

The Precambrian basement and overlying strata are shown to be cut by a series of parallel faults trending north-northwest. Late Precambrian, late Paleozoic, and late Cretaceous motion along these fault planes is interpreted on the basis of fault

throws, comparison of tectonic trends, and thickness variation patterns in upper Cretaceous clastic strata. Stratigraphic thinning and thickening in this sequence have been determined by continued growth of these faults during deposition. Paleotopography induced by fault activity has resulted in upper Cretaceous thickening over downthrown blocks and vice versa. Density variations are also shown to be in part affected by fault block motion. Differential displacement of fault blocks creates variation in burial depths and compaction occurs in response to this variable load.

7.2 - Significance of the Gravity Study.

Without the use of control data, the gravity method is found to be incapable of providing a unique model. This is because of distortion due to the interfering effects of upper and lower Cretaceous clastic density variations. Figures 7.1a and b show final models based on gravity modelling with depth control limited to two well logs. Also included for comparison are horizons interpreted from seismic data.

Figure 7.1a shows a one-body model which includes the entire sedimentary sequence above basement with an average density of $2.48 \times 10^3 \text{ kg/m}^3$. The elevation of the basement surface was varied to achieve agreement between field data and the model's gravitational response. The basement surfaces interpreted from gravity and seismic data disagree substantially as elevation discrepancies of as much as 900 metres are evident.

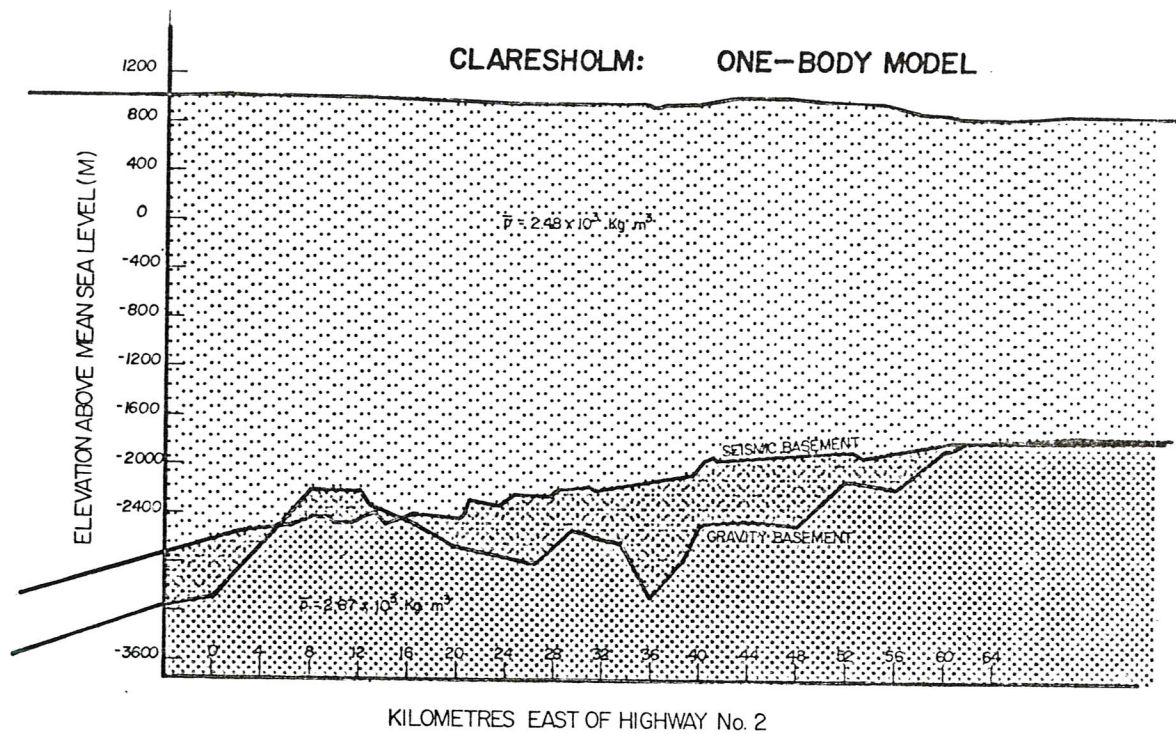
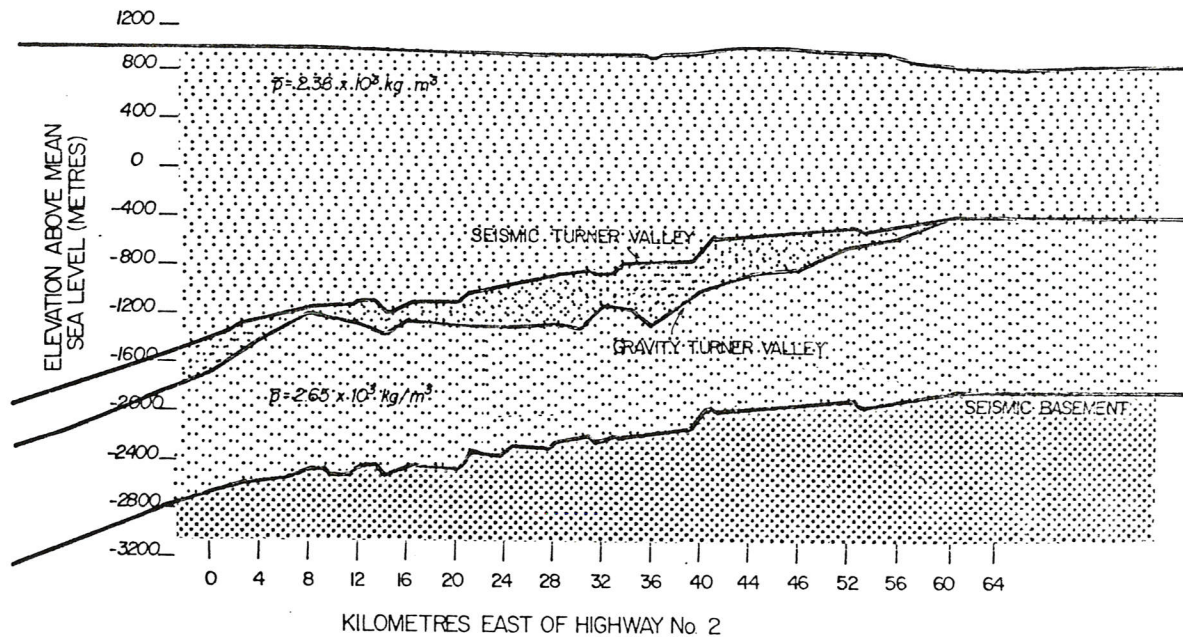


Figure 7.1a



TWO-BODY MODEL — CLARESHOLM PROFILE

Figure 7.1b

A similar example in figure 7.1b involves a two-body model where basement elevations interpreted from seismic control are fixed and the elevation of the Paleozoic carbonate surface is varied to achieve agreement between observed anomalies and model response. Again, there is disagreement, as much as 500 metres, although it is evident that increasing control here contributes to greater accuracy than that seen in figure 7.1a.

Control data are necessary for detailed interpretations of gravity data. However, general interpretations are possible in the absence of such data. A comparison of Bouguer profiles to final models indicates that high gravity gradient areas of the profiles, (kilometres 16, 34, Carmangay; 28, 31, Claresholm; and 42, Barons), correspond to transition areas across faults. It is evident that Cretaceous density variations do not completely obscure the gravitational effects of basement faults and that the location of larger faults, (greater than 150 metres in throw), may be interpreted on the basis of gravity data alone. Comparison of the model to Bouguer data also indicates that regionally upthrown and downthrown areas are reflected in the observed data by the lower-frequency characteristics of the data. These findings encourage the use of the gravity method alone to delineate major faults in and regional trends of the basement surface.

7.3 - Significance and Application of Integrated Studies.

Integrated studies of this nature are appropriate in that

they allow additional detail in model interpretation. For example, depth control in this study allows density interpretations to be made. Conversely, density control in gravity studies results in greater reliability in depth determinations. Control data in this way allow the anomaly of interest to be isolated from other sources.

While reconnaissance of basement faulting structure has been shown to be viable here, gravity surveys are best suited to integration in the manner of this study. This generally would involve follow-up of areas of interest delineated by seismic methods.

7.4 - Implications of the Study to the Tectonic History of Western Canada.

The normal or reverse orientation of faulting in the basement near Claresholm is difficult to determine with certainty from the seismic data. However, block faulting generally indicates a tensional tectonic regime which is paradoxical in consideration of the major compressional thrust-fault zone of the Rocky Mountain foothills, Front, and Main Ranges just to the west. Two explanations are considered here:

Firstly, load applied to the basement beneath the front ranges and foothills by overthrust build-up has depressed the basement, and created a fore-deep area which extends east of the disturbed zone. A tensional regime existed during the late

Cretaceous for the basement in this area as the load was applied and the basement was depressed, more to the west and less as one moves away from the loaded area. These tensional stresses were resolved along the pre-existing faults formed during late Precambrian warping of the basement surface and thus down-faulting was predominant.

A second possibility is that the compressive stresses inferred from thrust faulting of the Mesozoic wedge were transferred through the basement and again were resolved via reactivation of basement faults. The faults represented the easiest way of resolving compressional stress in the late Cretaceous, by up-thrusting of fault blocks.

Borowski's 1975 study of the basement within the disturbed belt supports a thin-skinned tectonic model where compressional stresses were not resolved in deformation of the basement, thus also supporting the former case here. Alternatively, Molnar and Tapponier, (1978), have found high-angle faults oriented roughly parallel to thrust fault trends in the compressive zone between India and Asia. They interpret these steep faults to be due to transmission of stresses through Tibet to the north where stresses are resolved in an area of weaker crust by high-angle compressive block faulting with a strike-slip component. This model is similar to the second case above. However, since the absolute motion of the fault blocks cannot be determined there is no data in this study to support either theory as

predominant in southern Alberta.

The location of the Claresholm gas field with respect to basement structures suggests a relationship between basement block faulting and hydrocarbon entrapment. The Claresholm gas field, located at kilometre 12 of the Claresholm profile, (see fig. 5.12b), is an area of active gas production from Mississippian carbonate strata. The reason for this is evident in figure 5.12b where an anticlinal structure is evident in the Mississippian Turner Valley marker just above the producing depths. This structure is a reflection of a similar basement feature deeper in the section, and is interpreted as having been caused by relative uplift of the fault block beneath the field and the adjacent block to the west. The hydrocarbon trap is the result of these blocks being relatively higher than their surroundings and is probably enhanced by subtle drag folding of strata which completes an anticlinal trap for migrating hydrocarbons.

In contrast, the Barons oilfield, located at kilometre 39 in figure 5.13b, is located within nearly-horizontal strata and no structural trap is evident. However, the example of the Claresholm field shows that basement tectonics have contributed to hydrocarbon entrapment in southern Alberta. In addition, the effect of basement tectonics upon stratigraphic and density patterns discussed in this report implies a relationship between basement faulting and stratigraphic traps. This is a possible

explanation in the case of the Barons oil field where no structural trap is evident.

7.5 - Recommendations for Further Study.

Further study of the effects of basement block faulting may be carried out to delineate basement faulting elsewhere in Alberta. Of special interest would be interpretation of Paleozoic and Mesozoic stratigraphy. Investigation may be extended into the disturbed belt of thrust faulting to test the method's applicability in complexly thrust-faulted areas. This additional study may also provide information about the involvement of the basement in the thrust-fault deformation of that area. Studies of this problem have indicated uncertain and conflicting results. Lastly, further study of this method's applicability in areas of hydrocarbon production may indicate its value in exploration where basement-related traps are likely.

BIBLIOGRAPHY

- Bally, A.W., Gordy, P.L., and Stewart, G.A., Structure, Seismic Data and Orogenic Evolution of the Southern Canadian Rocky Mountains. Bulletin of the Canadian Society of Petroleum Geologists, 14(3), pp. 337-381, 1966.
- Bible, J.L., 1962. Terrain Correction Tables for Gravity. Geophysics, Vol. 4, pp. 715-718.
- Borowski, R.A., 1975. Gravity Study in the Mount Eisenhower Area, Banff-Kootenay National Parks. Unpublished M.Sc. Thesis, The University of Calgary.
- Buck, R.J., 1967. Gravity Map Series of the Dominion Observatory - No. 40: Lethbridge-Banff. Department of Energy, Mines and Resources, Canada.
- Burwash, R.A., 1957. Reconnaissance of Subsurface Precambrian of Alberta. Bulletin of the American Association of Petroleum Geologists, 41(1), pp.70-103.
- Davis, T.L., 1979. Seismic-Stratigraphic Facies Models IN Facies Models. Geoscience Canada Publication. Geological Association of Canada.
- Energy, Resources Conservation Board, 1969. Structure Contours on Base of Fish Scales, Area No. 2, Alberta.
- Energy, Resources Conservation Board, 1978. Structure Contours on Paleozoic Surface, Area No. 2, Alberta.
- Garland, G.D., and Burwash, R.A., 1959. Geophysical and Petrological Study of Precambrian of Central Alberta, Canada

- Bulletin of the American Association of Petroleum Geologists, 43(4), pp. 790-806.
- Garland, G.D., Kanasewich, E.R., and Thompson, T.L., 1961. Gravity Measurements over the Southern Rocky Mountain Trench in British Columbia. Journal of Geophysics Research, 66(8), pp. 2495-2505.
- Geiger, K.W., 1967. Bedrock Topography of the Gleichen Map Area, Alberta. Research Council of Alberta Report No. 67-2.
- Hammer, S., 1939. Terrain Corrections for Gravimeter Stations. Geophysics, Vol. 4, pp. 184-194.
- Herbaly, E.L., 1974. Petroleum Geology of the Sweetgrass Arch, Alberta. Bulletin of the American Association of Petroleum Geologists, 58(11), pp. 2227-2244.
- Maxant, J., 1975. Distribution and Regional Variation of Density in the Western Canada Basin. Geophysics, 40(1), p. 56.
- Maxant, J., 1980. Variation of Density with Rocktype, Depth, and Formation in the Western Canada Basin from Density Logs. Geophysics, 45(6), 1061-1076.
- McCrossan, R.G., 1964. Geologic History of Western Canada, Alberta Society of Petroleum Geology.
- Molnar, P., and Tapponier, P., 1978. Active Tectonics of Tibet, Journal of Geophysical Research, Vol. 83, No. 11, pp. 5361-5375.
- Nelson, S.J., 1970. The Face of Time - Geologic History of Western Canada. Alberta Society of Petroleum Geologists.

- Talwani, M., Worzel, J.L., and Landisman, M., 1959. Rapid Computations for Two-Dimensional Bodies with Application to the Mendicino Submarine Fracture Zone. *Journal of Geophysical Research*, 64(1), pp. 40-59.
- Telford, W.M., Geldart, L.P., Sheriff, R.E., and Keys, D.A., 1976. *Applied Geophysics*, Cambridge University Press, 860 pp.
- Trott, B.G., 1981. Gravity Study of the Golden Spike and Westrose South Reefs, Alberta. Unpublished M.Sc. Thesis, University of Calgary.
- Weimer, R.J., 1978. Influence of the Transcontinental Arch on Cretaceous Marine Sedimentation - A Preliminary Report. Energy Resources of the Denver Basin. *Rocky Mountain Association of Geologists*, pp. 211-222.
- White, R.M., 1976. Noise Level in a Mountain Gravity Survey. Unpublished M.Sc. Thesis, University of Calgary.

APPENDIX I - FIELD GRAVITY DATA

CARMANGAY PROFILE

Station Number	Distance(x) (metres)	Station Elevation (metres)	Bouguer Anomaly (G.U.)	Residual Bouguer Anomaly (G.U.)	Theor. Bouguer Anomaly (G.U.)
500	0.0	1036.9	3350	-326	-322.3
501	534.0	1033.0	3355	-321	-319.3
502	1054.1	1029.3	3359	-317	-316.2
503	1545.1	1026.7	3363	-312	-313.6
504	2012.4	1023.4	3367	-308	-310.3
505	2531.3	1023.6	3370	-305	-305.5
506	3029.0	1023.5	3374	-301	-301.3
507	3530.1	1020.1	3377	-297	-295.5
508	4034.8	1017.4	3381	-293	-292.8
509	4519.1	1013.6	3384	-290	-289.2
510	4990.4	1012.8	3387	-287	-287.4
511	5510.3	1017.3	3389	-285	-288.2
512	6016.1	1019.0	3392	-281	-285.4
513	6521.7	1019.2	3391	-282	-281.5
514	6977.6	1022.9	3393	-280	-282.2
515	7498.9	1010.4	3395	-278	-275.0
516	8000.1	1004.7	3398	-274	-272.4
517	8457.1	1003.9	3399	-273	-273.0
519	8953.8	1001.3	3403	-269	-272.7
520	9473.8	1000.6	3403	-269	-275.7
521	9965.5	990.8	3404	-268	-269.6
522	10475.6	988.6	3402	-269	-269.0
523	10958.4	986.4	3402	-269	-268.8
524	11434.2	985.2	3403	-268	-269.4
525	11933.2	983.2	3403	-268	-269.7
526	12406.9	981.4	3404	-267	-270.2
527	12914.1	980.8	3404	-266	-268.9
528	13425.6	976.7	3405	-265	-267.4
529	13894.0	971.2	3405	-265	-266.0
530	14444.4	969.3	3404	-266	-265.9
531	14895.6	964.1	3403	-266	-263.7
532	15413.6	966.9	3402	-267	-266.4
533	15879.9	969.1	3399	-270	-267.1
534	16106.6	962.3	3405	-264	-265.2
535	16298.8	964.2	3404	-265	-267.4
536	16811.3	963.6	3401	-268	-269.3
537	17299.6	961.4	3398	-270	-269.7
538	17832.8	963.9	3396	-272	-271.1
539	18276.9	969.0	3395	-273	-273.8

540	18794.3	970.1	3395	-273	-274.4
541	19281.1	962.9	3397	-270	-270.9
542	19767.4	954.5	3399	-268	-265.8
543	20227.3	953.0	3400	-267	-264.8
544	20745.6	956.7	3399	-268	-263.0
545	21229.3	957.8	3399	-268	-261.5
546	21742.0	958.2	3397	-269	-265.6
547	22222.4	963.0	3398	-268	-267.5
548	22732.8	960.8	3399	-267	-266.8
549	23219.8	955.8	3401	-265	-265.2
550	23708.9	948.2	3404	-262	-263.0
551	24280.7	948.8	3403	-262	-261.3
552	24826.1	955.9	3403	-262	-259.6
553	25294.5	956.2	3404	-261	-258.4
554	25774.9	956.6	3405	-260	-257.6
555	26267.5	952.6	3406	-258	-257.0
556	26776.6	955.2	3407	-257	-256.9
557	27406.2	952.4	3408	-256	-256.5
558	27915.6	956.3	3409	-255	-255.0
559	28416.1	956.9	3409	-254	-254.2
560	29068.0	953.7	3409	-254	-253.3
561	29570.9	953.1	3410	-253	-251.8
562	30080.0	953.0	3412	-251	-250.2
563	30554.2	946.6	3413	-250	-248.7
564	31048.1	946.5	3415	-247	-247.0
565	31538.5	946.6	3414	-248	-245.3
566	32033.9	947.6	3414	-248	-243.3
567	32499.9	947.3	3416	-246	-241.0
568	33010.1	947.4	3418	-243	-237.2
569	33487.9	945.1	3422	-239	-234.7
570	34036.6	944.4	3426	-235	-232.2
571	34510.4	944.6	3431	-230	-230.3
572	35020.3	941.7	3433	-228	-228.6
573	35485.1	941.8	3435	-225	-227.3
574	35927.4	944.4	3435	-225	-226.2
575	36438.3	944.4	3436	-224	-225.8
576	36951.4	945.8	3436	-224	-225.2
577	37406.8	945.1	3436	-223	-224.9
578	37940.6	945.8	3436	-223	-225.9
579	38442.0	945.3	3434	-225	-230.1
580	38958.3	945.3	3432	-227	-236.2
581	39460.9	938.6	3432	-227	-234.0
582	39993.8	936.5	3433	-225	-229.6
583	40582.1	941.0	3436	-222	-224.2
584	41113.0	941.4	3439	-219	-220.8
585	41824.7	949.3	3442	-216	-217.8
586	42286.0	948.9	3444	-213	-216.0
587	42746.7	951.8	3445	-212	-214.6
588	43307.6	955.1	3446	-211	-213.1

589	43777.9	958.0	3447	-211	-213.1
590	44266.3	959.1	3450	-206	-210.2
591	44784.5	966.1	3448	-208	-206.5
592	45316.3	982.9	3449	-207	-196.0
593	45759.2	1005.9	3448	-208	-199.2
594	46408.0	1025.2	3451	-205	-205.5
595	46977.2	1021.5	3452	-203	-203.2
596	47678.2	1022.7	3454	-201	-203.9
597	48250.3	1010.4	3455	-200	-296.6
598	48766.8	1013.6	3456	-198	-201.7
599	49430.2	1013.9	3458	-196	-198.9
600	49938.8	1011.0	3458	-195	-196.6
601	50533.1	986.9	3459	-195	-194.0
602	51054.0	980.4	3461	-192	-191.8
603	51642.4	972.9	3462	-191	-189.3
604	52220.0	966.7	3466	-187	-186.6
605	52663.0	954.9	3469	-184	-181.5
606	53144.3	952.3	3472	-181	-181.5
607	53675.7	948.8	3473	-179	-180.3
608	54218.2	950.9	3474	-178	-179.3
609	54688.3	951.6	3474	-178	-178.6
610	55359.5	952.4	3474	-178	-177.5
611	55891.4	954.6	3474	-177	-176.7
612	56406.4	949.4	3475	-176	-179.0
613	56897.8	957.3	3475	-176	-174.8
614	57469.3	957.5	3476	-175	-173.3
615	57951.2	950.6	3477	-173	-173.4
616	58462.8	949.9	3478	-172	-173.9
617	59104.1	939.9	3479	-171	-172.7
618	59626.1	935.5	3481	-169	-170.3
619	60179.3	923.9	3483	-166	-166.1
620	60655.3	926.8	3484	-165	-164.0
621	61098.1	924.1	3485	-164	-162.7
622	61609.1	919.8	3486	-163	-161.3
623	62099.6	913.9	3488	-161	-160.1
624	62587.8	904.8	3489	-159	-158.9
625	63183.4	906.8	3491	-157	-159.2
626	63441.6	894.5	3494	-154	-156.4

CLARESHOLM PROFILE

100	0.0	1042.7	3399	-303	-302.5
101	254.9	1040.1	3401	-301	-300.4
102	503.7	1038.0	3402	-300	-298.6
103	751.3	1037.6	3404	-298	-297.7
104	997.1	1036.1	3405	-297	-296.1
105	1240.8	1034.6	3406	-296	-294.3
106	1500.9	1034.3	3407	-294	-292.9

107	1766.0	1035.9	3409	-292	-292.3
108	2022.7	1036.0	3410	-291	-290.7
109	2221.0	1034.6	3411	-290	-289.7
110	2492.6	1034.4	3412	-289	-288.3
111	2714.0	1030.6	3414	-287	-286.6
112	3003.1	1028.3	3416	-285	-284.7
113	3236.0	1027.5	3417	-284	-283.8
114	3481.2	1025.0	3418	-283	-281.9
115	3745.9	1024.0	3419	-282	-281.0
116	3981.3	1022.7	3420	-281	-279.9
117	4210.8	1022.5	3422	-279	-279.5
118	4470.5	1022.8	3423	-277	-279.3
119	4727.2	1021.0	3424	-276	-278.0
120	4957.6	1020.5	3425	-275	-277.4
121	5200.1	1020.7	3426	-274	-277.3
122	5448.7	1020.4	3427	-273	-276.3
123	5682.1	1022.3	3427	-273	-275.5
124	5938.5	1021.7	3428	-272	-274.5
125	6193.0	1020.8	3429	-271	-273.6
126	6443.1	1018.3	3430	-270	-272.7
127	6703.5	1018.4	3431	-269	-271.5
128	6970.0	1017.8	3432	-268	-270.4
129	7170.8	1015.4	3432	-268	-269.7
130	7410.1	1011.2	3433	-266	-268.8
131	7650.3	1009.7	3433	-265	-268.0
132	7917.4	1004.6	3435	-264	-265.1
133	8175.9	1002.0	3436	-263	-263.7
134	8421.0	1002.1	3435	-264	-264.0
135	8697.9	1001.0	3435	-264	-263.6
136	8935.9	1002.6	3435	-264	-264.9
137	9161.7	1000.8	3436	-263	-264.1
138	9405.6	1000.4	3436	-263	-264.0
139	9427.8	1000.6	3435	-264	-263.9
140	9645.5	1001.2	3434	-265	-263.5
141	9900.9	1005.3	3432	-267	-263.0
142	10099.3	1007.2	3435	-264	-262.7
143	10383.1	1010.6	3436	-262	-262.2
144	10634.5	1016.4	3438	-260	-261.7
145	10861.4	1014.7	3437	-261	-261.4
146	11112.6	1011.3	3438	-260	-261.0
147	11345.3	1006.9	3438	-260	-260.7
148	11631.0	1001.3	3439	-259	-260.3
149	11790.3	997.6	3439	-259	-260.1
150	12023.2	994.6	3439	-259	-259.9
151	12283.6	992.4	3439	-259	-259.7
152	12535.5	988.9	3440	-258	-259.6
153	12760.6	985.4	3440	-258	-259.6
154	13003.8	983.3	3439	-259	-259.6
155	13265.5	979.0	3439	-258	-259.8
156	13507.4	977.2	3438	-259	-259.4

157	13720.1	975.5	3438	-259	-259.0
158	13936.9	973.5	3436	-261	-258.5
159	14222.0	972.0	3436	-261	-259.1
160	14469.1	969.8	3435	-262	-259.6
161	14671.3	969.7	3435	-262	-261.0
162	14912.6	970.7	3434	-263	-263.2
163	15175.1	971.1	3433	-264	-264.2
164	15375.4	970.6	3432	-265	-264.5
165	15625.2	968.0	3432	-265	-264.3
166	15851.8	966.7	3432	-265	-264.0
167	16111.5	966.8	3433	-264	-264.1
168	16346.1	967.4	3433	-263	-264.3
169	16569.8	966.7	3433	-263	-264.3
170	16826.1	966.9	3432	-264	-264.4
171	17104.2	965.9	3432	-264	-264.7
172	17294.8	964.7	3431	-265	-265.0
173	17559.6	965.9	3431	-265	-267.5
174	17786.0	964.4	3430	-266	-267.9
175	18040.1	962.9	3429	-267	-268.0
176	18303.9	965.6	3429	-267	-269.9
177	18522.0	965.4	3427	-269	-270.1
178	18763.5	968.4	3428	-268	-272.1
179	19029.0	959.3	3428	-268	-267.1
180	19218.6	959.5	3429	-266	-267.0
181	19448.5	959.7	3427	-268	-266.9
182	19717.4	973.6	3425	-270	-273.2
183	20062.3	968.6	3425	-270	-272.2
185	20408.5	962.5	3426	-269	-268.6
186	20773.9	973.5	3456	-239	-273.3
187	21130.1	973.7	3424	-271	-273.8
188	21389.5	972.9	3425	-270	-273.3
189	21619.2	965.5	3426	-269	-271.6
190	21860.9	965.5	3428	-267	-271.1
191	22119.4	967.7	3428	-266	-271.3
192	22319.4	963.7	3429	-265	-269.0
193	22583.5	965.3	3429	-265	-269.4
194	22839.2	971.6	3429	-265	-269.1
195	23055.6	969.8	3427	-267	-268.5
196	23336.6	975.1	3428	-268	-267.7
197	23544.9	974.6	3425	-269	-267.2
198	23854.4	973.8	3426	-268	-266.6
199	24123.9	971.9	3427	-267	-266.3
200	24367.6	966.5	3427	-267	-266.6
201	24598.0	965.7	3427	-267	-268.0
202	24849.3	967.0	3426	-268	-269.2
203	25085.8	969.3	3426	-267	-269.3
204	25322.8	964.5	3425	-268	-269.0
205	25555.9	961.8	3426	-267	-268.4
206	25793.6	961.2	3427	-266	-267.6
207	26051.5	961.7	3427	-266	-267.1
208	26295.8	961.0	3426	-267	-265.9

209	26540.5	962.2	3426	-267	-265.9
210	26761.1	959.9	3427	-266	-265.0
211	27014.8	958.9	3428	-265	-264.1
212	27258.0	959.2	3428	-265	-264.1
213	27495.4	961.6	3428	-265	-264.7
214	27745.0	962.2	3429	-264	-265.7
215	27998.1	966.5	3430	-262	-265.2
216	28228.8	969.1	3430	-262	-264.5
217	28430.3	971.3	3431	-261	-263.8
218	28621.9	968.9	3431	-261	-263.1
219	28906.4	967.2	3432	-260	-262.0
220	29130.0	962.8	3434	-258	-261.2
221	29390.6	959.8	3434	-258	-260.9
222	29616.3	953.7	3435	-257	-260.5
223	29885.4	959.6	3435	-257	-260.1
224	30124.7	960.3	3435	-257	-259.8
225	30329.2	960.1	3435	-257	-259.5
226	30593.2	959.6	3435	-257	-259.2
227	30845.9	959.6	3435	-256	-258.9
228	31058.3	958.8	3434	-257	-258.7
229	31300.6	957.9	3433	-258	-258.5
230	31531.7	956.4	3432	-259	-257.9
231	31785.7	955.9	3432	-259	-257.5
232	32032.0	954.0	3431	-260	-257.2
233	32262.9	953.1	3431	-260	-257.0
234	32511.7	952.5	3431	-260	-257.1
235	32750.9	952.3	3432	-259	-257.3
236	32970.4	951.8	3433	-258	-258.0
237	33217.8	951.2	3434	-257	-259.3
238	33439.6	950.0	3434	-257	-259.6
239	33689.0	948.9	3435	-256	-259.5
240	33940.3	948.9	3434	-256	-259.2
241	34100.5	949.3	3435	-255	-258.9
242	34321.9	946.5	3434	-256	-258.4
243	34562.3	944.4	3433	-257	-257.6
244	34815.3	943.8	3428	-262	-257.4
245	35036.2	944.0	3426	-264	-259.5
246	35202.7	942.8	3425	-265	-260.1
247	35306.7	946.6	3428	-262	-262.8
248	35475.4	942.9	3429	-261	-261.1
249	35724.3	942.3	3430	-260	-261.0
250	35946.8	942.0	3430	-260	-260.2
251	36193.2	941.9	3430	-260	-258.9
252	36441.6	942.8	3431	-259	-257.9
253	36680.2	945.0	3431	-259	-256.5
254	36911.2	949.7	3432	-257	-256.6
255	37146.4	948.0	3433	-256	-254.4
256	37400.2	948.1	3435	-254	-253.3
257	37643.2	947.6	3437	-252	-251.8

258	37890.6	947.6	3439	-250	-250.6
259	38114.2	948.3	3439	-250	-249.9
260	38373.9	949.8	3439	-250	-249.4
261	38603.9	951.6	3439	-250	-248.5
262	38828.4	953.0	3440	-249	-247.4
263	39038.9	955.5	3440	-249	-247.1
264	39231.0	956.9	3441	-248	-246.2
265	39481.7	959.0	3442	-247	-246.0
266	39710.3	961.8	3443	-245	-246.4
267	39959.9	964.4	3445	-243	-246.2
268	40220.8	966.9	3446	-242	-245.6
269	40433.2	970.3	3447	-241	-244.9
270	40670.8	973.9	3448	-240	-244.0
272	41143.4	979.6	3448	-240	-241.4
273	41376.1	982.9	3449	-239	-240.1
274	41637.5	985.0	3450	-238	-239.0
275	41883.9	991.0	3450	-238	-239.4
276	42093.5	995.4	3444	-244	-238.2
277	42341.0	1000.0	3443	-245	-236.9
278	42585.0	1009.5	3442	-246	-235.8
279	42827.7	1019.9	3448	-239	-234.8
280	43099.3	1034.8	3447	-240	-234.4
281	43365.4	1036.1	3447	-240	-234.2
282	43623.9	1035.0	3448	-239	-234.0
283	43872.8	1037.1	3448	-239	-233.9
284	44136.4	1041.5	3448	-239	-233.8
285	44351.6	1041.5	3448	-239	-233.7
286	44832.4	1036.4	3448	-239	-233.6
287	44832.4	1036.4	3448	-239	-233.5
288	45063.2	1039.1	3449	-238	-233.6
289	45316.2	1038.3	3450	-235	-233.5
290	45578.8	1034.7	3451	-235	-233.5
291	45805.0	1032.6	3451	-235	-233.5
292	46048.2	1031.5	3453	-233	-233.6
293	46274.7	1026.8	3453	-233	-233.6
294	46505.7	1023.9	3454	-232	-233.6
295	46757.9	1021.8	3455	-231	-233.6
296	46982.5	1021.3	3456	-230	-233.7
297	47236.5	1021.9	3456	-230	-232.7
298	47464.7	1020.3	3456	-230	-231.8
299	47700.7	1018.0	3457	-229	-230.9
300	47940.3	1014.6	3457	-229	-230.0
301	48188.7	1010.7	3458	-228	-229.1
302	48457.9	1006.7	3460	-226	-228.0
303	48689.9	1002.8	3461	-224	-227.2
304	48927.6	999.6	3462	-223	-226.3
305	49166.6	997.9	3463	-222	-225.3
306	49400.0	998.2	3463	-222	-224.5
307	49640.3	996.5	3464	-221	-223.5

308	49865.0	996.5	3464	-220	-223.5
309	50132.6	977.9	3468	-217	-217.7
310	50376.4	973.1	3470	-215	-215.2
311	50620.0	967.6	3471	-214	-212.4
312	50850.3	967.3	3472	-213	-211.8
313	51094.6	966.3	3472	-213	-210.9
314	51331.7	965.7	3474	-211	-210.1
315	51569.3	963.6	3475	-209	-208.7
316	51785.2	963.4	3476	-208	-208.1
317	52033.1	962.0	3476	-208	-206.9
318	52285.8	961.3	3477	-207	-206.6
319	52500.1	961.6	3478	-206	-207.9
320	52744.5	959.8	3478	-206	-207.1
321	52995.0	960.9	3479	-205	-208.7
322	53240.5	960.4	3479	-205	-208.2
323	53482.8	959.2	3479	-205	-207.0
324	53730.7	959.9	3479	-205	-206.5
325	53976.6	957.2	3480	-204	-203.2
326	54205.7	957.7	3480	-204	-200.8
327	54430.5	960.4	3480	-203	-200.6
327 $\frac{1}{2}$	54664.9	963.0	3480	-203	-200.6
328	54921.6	966.5	3480	-203	-201.4
329	55162.5	970.0	3481	-202	-200.7
330	55402.4	966.8	3482	-201	-200.1
331	56666.9	960.3	3485	-198	-190.9
333	56158.4	942.7	3487	-196	-193.8
334	56393.7	937.9	3490	-193	-192.6
335	56615.7	930.2	3491	-192	-191.3
336	56864.2	924.9	3492	-191	-189.8
337	57109.4	919.8	3494	-189	-188.2
338	57349.8	910.9	3495	-187	-184.3
339	57568.9	910.1	3497	-185	-185.1
340	57825.1	905.1	3498	-184	-183.5
341	58074.5	903.2	3499	-183	-182.3
342	58317.4	900.5	3500	-182	-181.1
343	58558.8	899.7	3500	-182	-179.9
344	58796.1	900.1	3500	-182	-178.7
345	59029.2	895.8	3501	-181	-177.6
346	59284.6	891.3	3502	-180	-176.3
347	59495.7	891.6	3506	-176	-175.3
348	59760.4	884.7	3507	-175	-174.0
349	60017.4	887.2	3509	-173	-172.8
350	60242.8	879.7	3507	-174	-171.7
351	60470.1	881.4	3509	-172	-170.7
352	60732.8	872.5	3510	-171	-169.6
353	60979.3	871.0	3511	-170	-168.4
354	61218.8	867.7	3513	-168	-167.9
355	61452.9	864.5	3514	-167	-167.3
356	61685.6	864.6	3515	-166	-166.6

BARONS PROFILE

801	0.0	1016.6	3470	-315	-317.0
802	496.9	1015.9	3472	-312	-312.1
803	988.9	1021.4	3474	-309	-308.1
804	1471.3	1024.2	3476	-306	-304.7
805	1947.5	1027.1	3478	-303	-301.9
806	2414.7	1029.4	3481	-299	-299.6
807	2893.6	1029.9	3483	-297	-297.3
808	3405.2	1028.7	3485	-294	-295.0
809	3878.4	1026.1	3486	-292	-292.7
810	4370.7	1023.6	3489	-288	-289.8
811	4832.2	1017.9	3491	-285	-285.2
812	5334.8	1016.9	3494	-281	-278.4
813	5810.8	1016.3	3495	-279	-278.1
814	6280.6	1018.2	3496	-277	-277.9
815	6734.9	1016.7	3497	-275	-276.5
816	7233.7	1013.1	3498	-273	-274.1
817	7723.5	1007.3	3499	-271	-271.9
818	8196.3	1005.0	3499	-270	-269.9
819	8686.9	1003.9	3499	-270	-268.1
820	9163.1	1005.3	3499	-269	-266.8
821	9642.3	1005.1	3498	-269	-266.7
822	10146.7	997.2	3497	-269	-270.7
823	10618.2	993.7	3496	-269	-271.1
824	11097.5	992.7	3494	-270	-272.4
825	11865.3	989.8	3491	-271	-274.7
826	12382.3	987.1	3488	-273	-275.1
827	12874.1	982.8	3486	-275	-276.5
828	13321.6	980.1	3484	-276	-277.5
829	13852.8	976.5	3482	-277	-277.6
830	14303.7	972.8	3479	-279	-277.5
831	14787.3	970.6	3477	-280	-277.7
832	15308.5	971.3	3476	-280	-278.5
833	15745.5	969.4	3475	-280	-279.6
834	16214.7	968.9	3472	-282	-281.5
835	16722.1	965.1	3468	-285	-286.4
836	17234.3	963.8	3464	-288	-288.7
837	17697.6	963.1	3462	-289	-289.3
838	18159.1	960.0	3461	-290	-289.4
839	18654.9	960.2	3460	-290	-289.1
840	19124.1	958.1	3459	-290	-288.6
841	19624.2	958.0	3459	-289	-288.0
842	20090.8	960.6	3458	-289	-287.5
843	20611.2	967.7	3458	-288	-287.6
844	21055.0	962.0	3458	-287	-290.5
845	21553.7	963.9	3456	-288	-291.8
846	22058.9	970.0	3456	-287	-289.3
847	22520.2	964.7	3455	-287	-287.4

848	22975.8	965.3	3457	-284	-285.3
849	23473.4	955.4	3458	-282	-282.4
850	23951.0	953.5	3459	-281	-279.5
851	24510.5	952.3	3458	-280	-277.0
852	24935.0	956.8	3457	-281	-278.4
853	25429.8	957.4	3457	-280	-277.4
854	25918.7	958.0	3459	-277	-276.2
855	26395.4	957.1	3460	-275	-274.7
856	26890.6	957.9	3460	-274	-276.0
857	27367.3	958.5	3459	-274	-276.9
858	27830.4	956.8	3459	-273	-277.0
859	28335.2	955.9	3458	-273	-276.7
860	28810.5	955.8	3456	-274	-276.3
861	29172.5	955.1	3454	-276	-279.1
862	29590.2	960.8	3447	-282	-278.8
863	30075.2	956.5	3447	-281	-278.1
864	30585.7	957.4	3448	-279	-273.7
865	31081.2	957.5	3455	-271	-271.4
866	31539.9	957.3	3456	-269	-270.4
867	32029.5	957.6	3456	-268	-270.4
868	32489.9	956.6	3456	-267	-268.5
869	32994.5	956.2	3457	-265	-266.0
870	33470.1	957.1	3458	-263	-263.7
871	33954.7	958.5	3458	-263	-261.2
872	34456.6	964.2	3460	-260	-258.7
873	34899.8	963.5	3461	-258	-256.7
874	35409.6	969.9	3463	-255	-254.7
875	35947.6	984.1	3464	-253	-252.7
876	36473.1	980.6	3466	-250	-251.0
877	36952.4	972.8	3468	-247	-246.1
878	37433.0	971.3	3469	-245	-242.5
879	37937.9	972.8	3471	-242	-240.7
880	38410.8	974.7	3472	-240	-239.6
881	38907.9	980.2	3473	-238	-238.8
882	39412.0	973.6	3473	-237	-234.7
883	39856.6	969.6	3474	-235	-229.3
884	40352.0	975.2	3475	-233	-228.2
885	40838.9	996.6	3475	-232	-235.1
886	41280.5	1008.1	3474	-233	-233.1
887	41773.5	1022.0	3474	-232	-230.8
888	42271.0	1022.6	3474	-231	-228.4
889	42735.7	1014.4	3476	-228	-226.1
890	43214.4	1011.8	3477	-226	-223.6
891	43705.4	1016.5	3478	-224	-221.4
892	44234.5	1009.2	3479	-222	-219.4
893	44661.0	1006.2	3479	-221	-219.2
894	45143.5	1006.4	3480	-219	-219.1
895	45664.3	999.5	3481	-217	-217.4
896	46122.8	996.6	3481	-216	-215.8
897	46609.9	992.6	3480	-217	-214.1

898	47064.5	988.8	3481	-215	-212.6
899	47582.6	987.7	3483	-212	-210.8
900	48050.1	985.4	3485	-209	-209.2
901	48525.8	981.1	3487	-206	-207.6
902	49011.6	978.2	3488	-204	-205.9
903	49478.4	972.7	3489	-202	-203.7
904	49975.3	967.8	3490	-200	-200.6
905	50489.4	971.7	3490	-199	-200.4
906	50918.4	964.1	3491	-197	-198.5
907	51408.0	967.9	3494	-193	-208.2
908	51880.6	954.7	3496	-191	-190.1
909	52407.5	939.8	3499	-187	-185.5
910	52852.2	929.6	3500	-185	-183.8
911	53341.2	922.2	3502	-182	-181.2
912	53843.9	914.6	3505	-178	-177.2
913	54343.6	908.0	3507	-175	-175.7
914	54795.0	903.4	3509	-172	-174.1
915	55293.0	901.3	3509	-171	-171.8
916	55765.4	901.4	3509	-170	-169.3
917	56217.7	896.7	3511	-167	-166.6
918	56701.8	888.4	3514	-163	-163.7
919	57203.4	884.1	3517	-159	-160.4
920	57680.8	880.2	3519	-157	-157.4
921	58150.4	879.2	3522	-153	-153.9
922	58652.3	874.4	3524	-150	-148.3
923	59141.9	873.6	3527	-146	-144.9
924	59616.6	872.3	3529	-143	-142.1
925	60094.8	870.3	3531	-140	-139.5
926	60566.7	869.9	3533	-137	-137.4
927	61118.7	867.1	3535	-134	-135.2